APPENDIX - A : Device Drawing

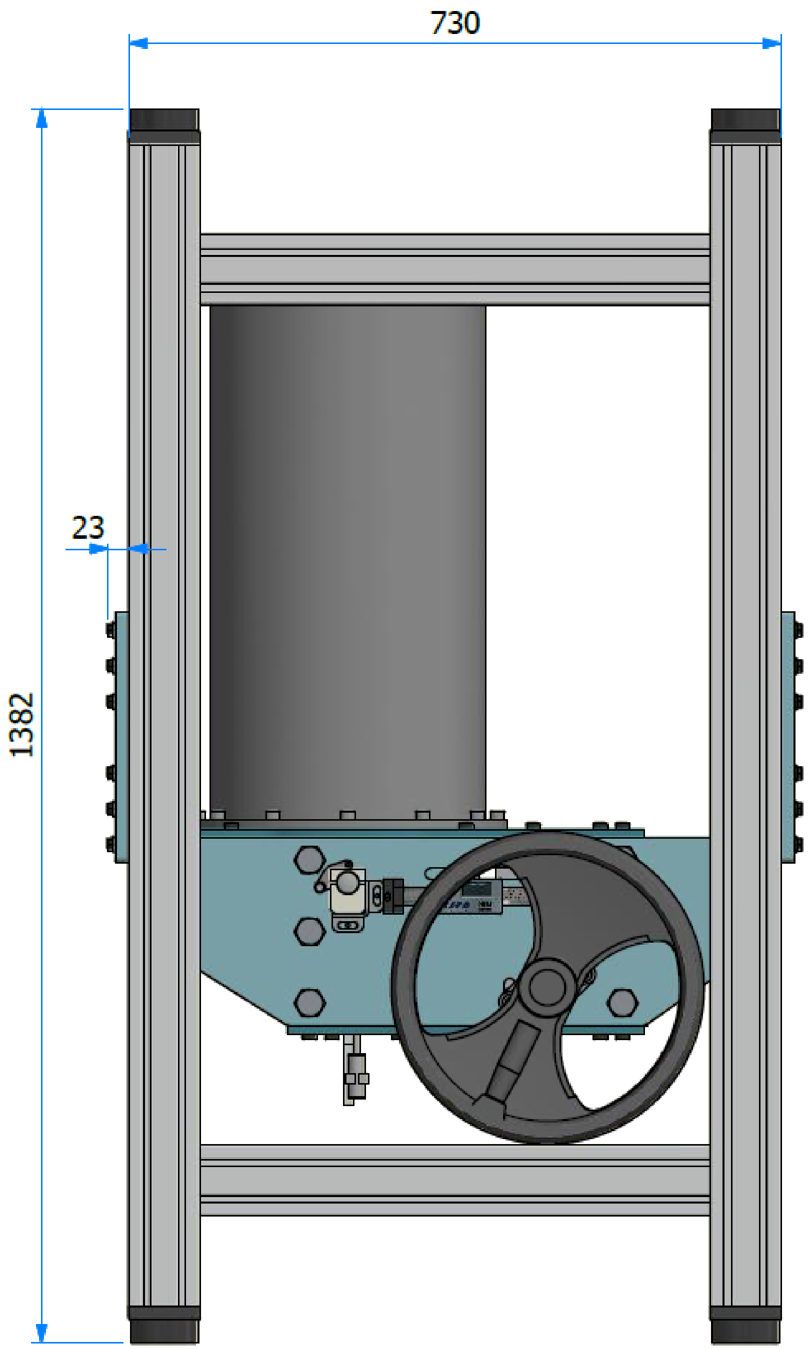

Appendix A-1 Test Equipment Technical Drawing (Side View A)

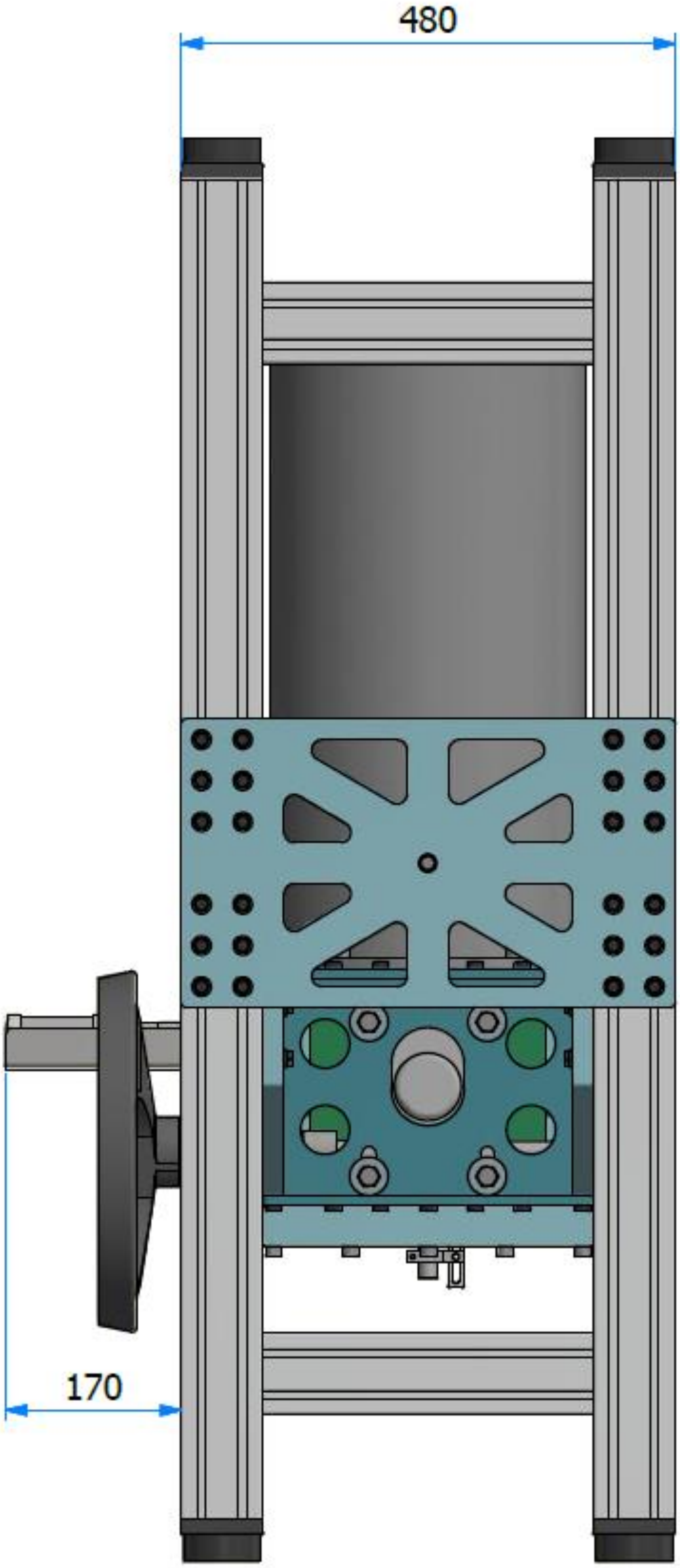

Appendix A-2 Test Equipment Technical Drawing (Side View B)

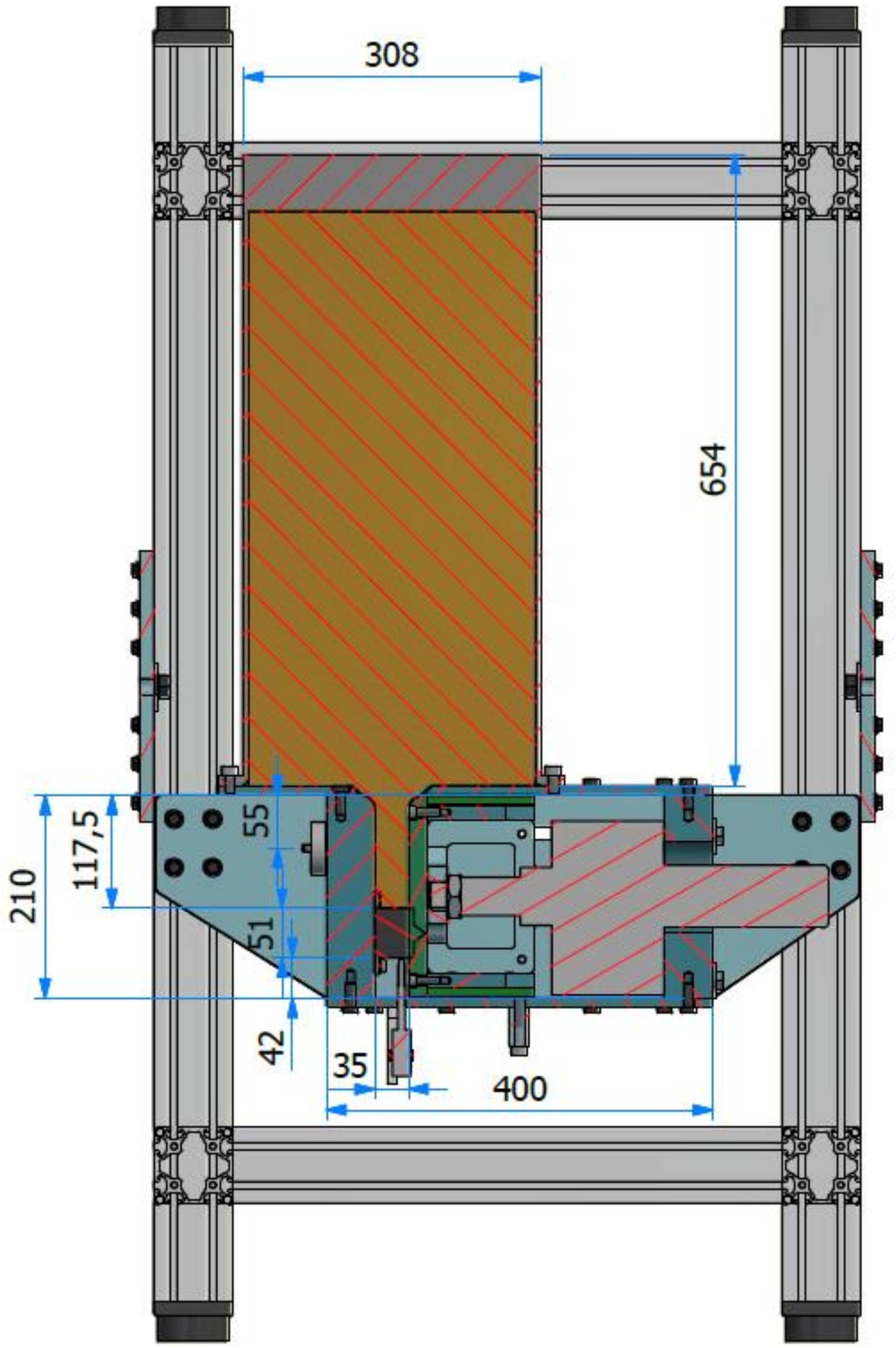

Appendix A-3 Test Equipment Technical Drawing (Cross Section A)

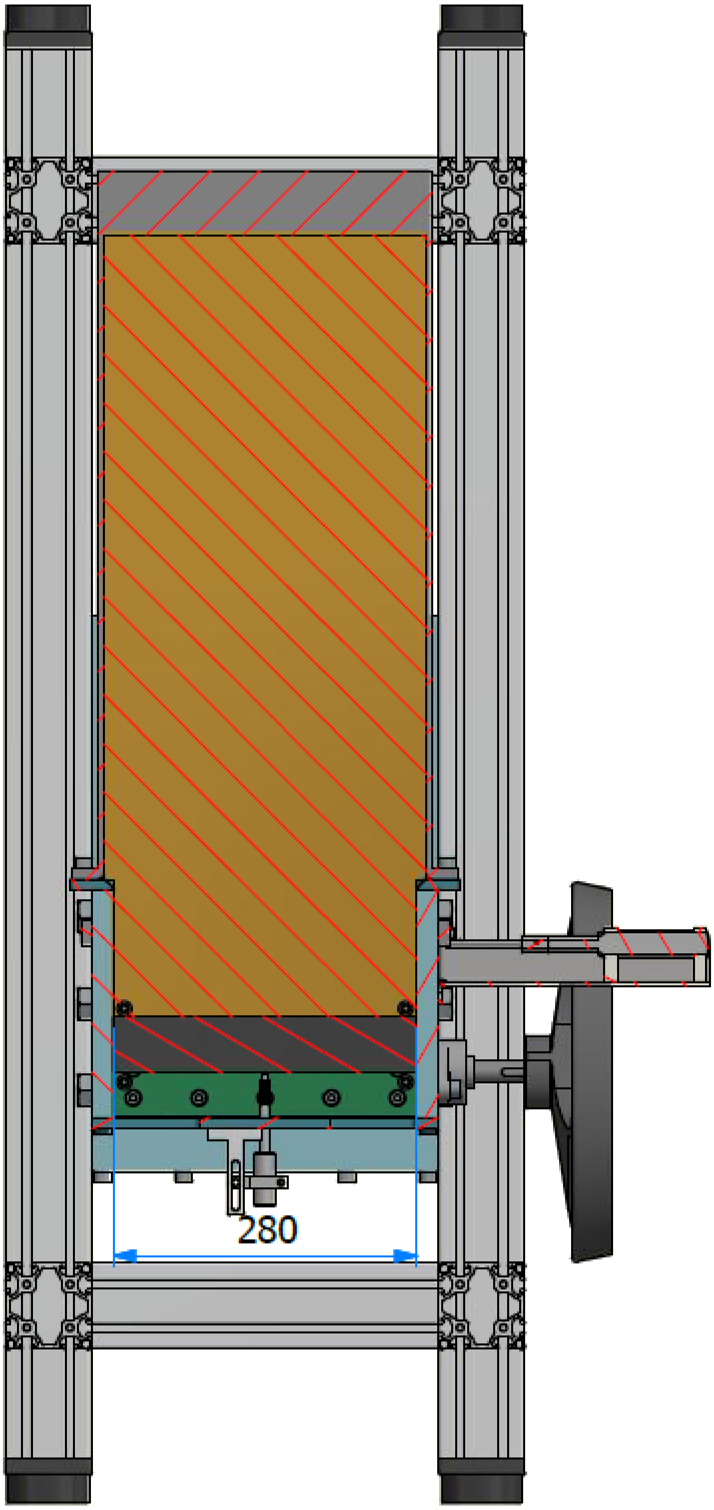

Appendix A-4 Test Equipment Technical Drawing (Cross Section B)

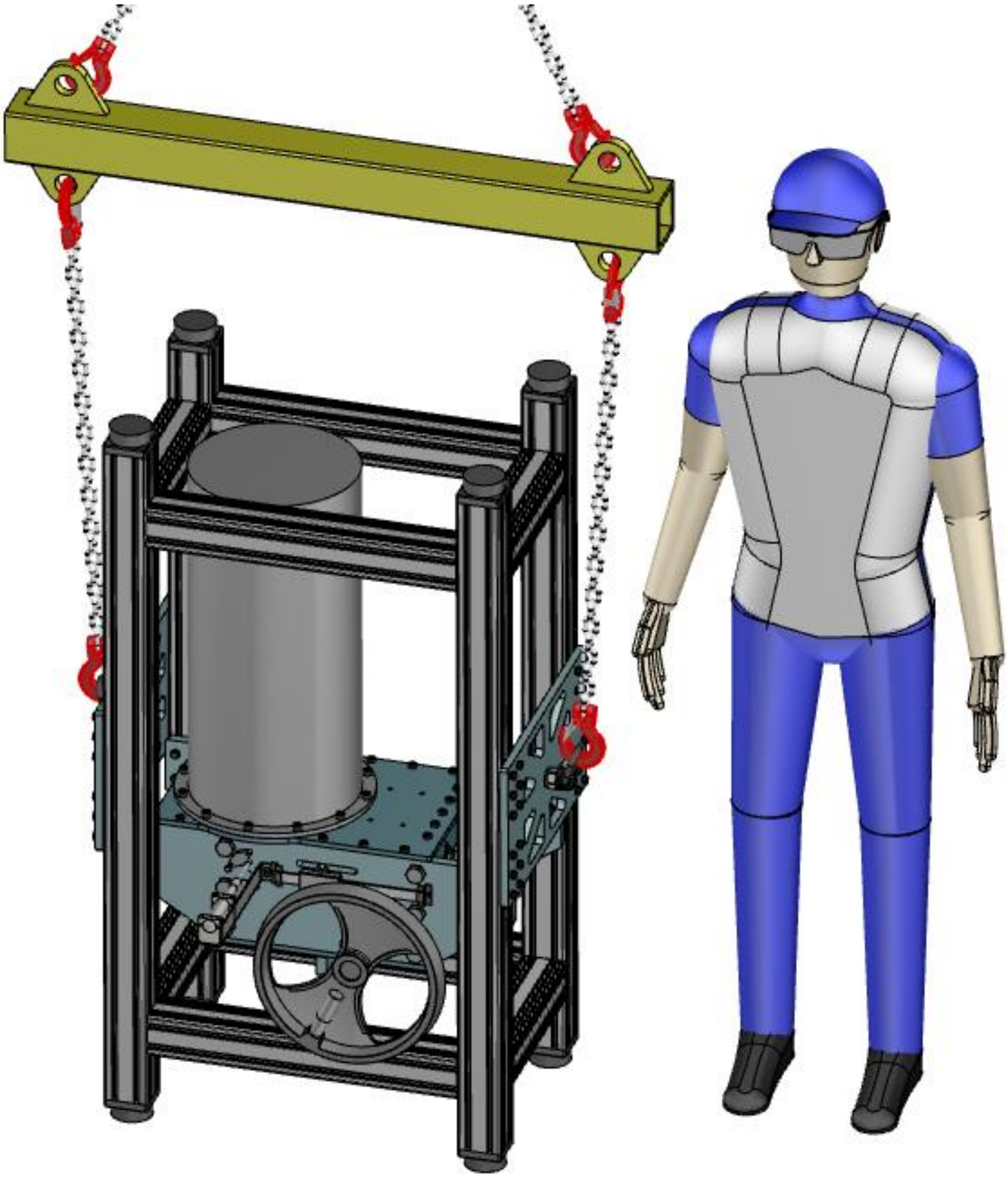

Appendix A-5 Test Equipment Technical Drawing (3D View)

Appendix A-6 Test Equipment 3D Render

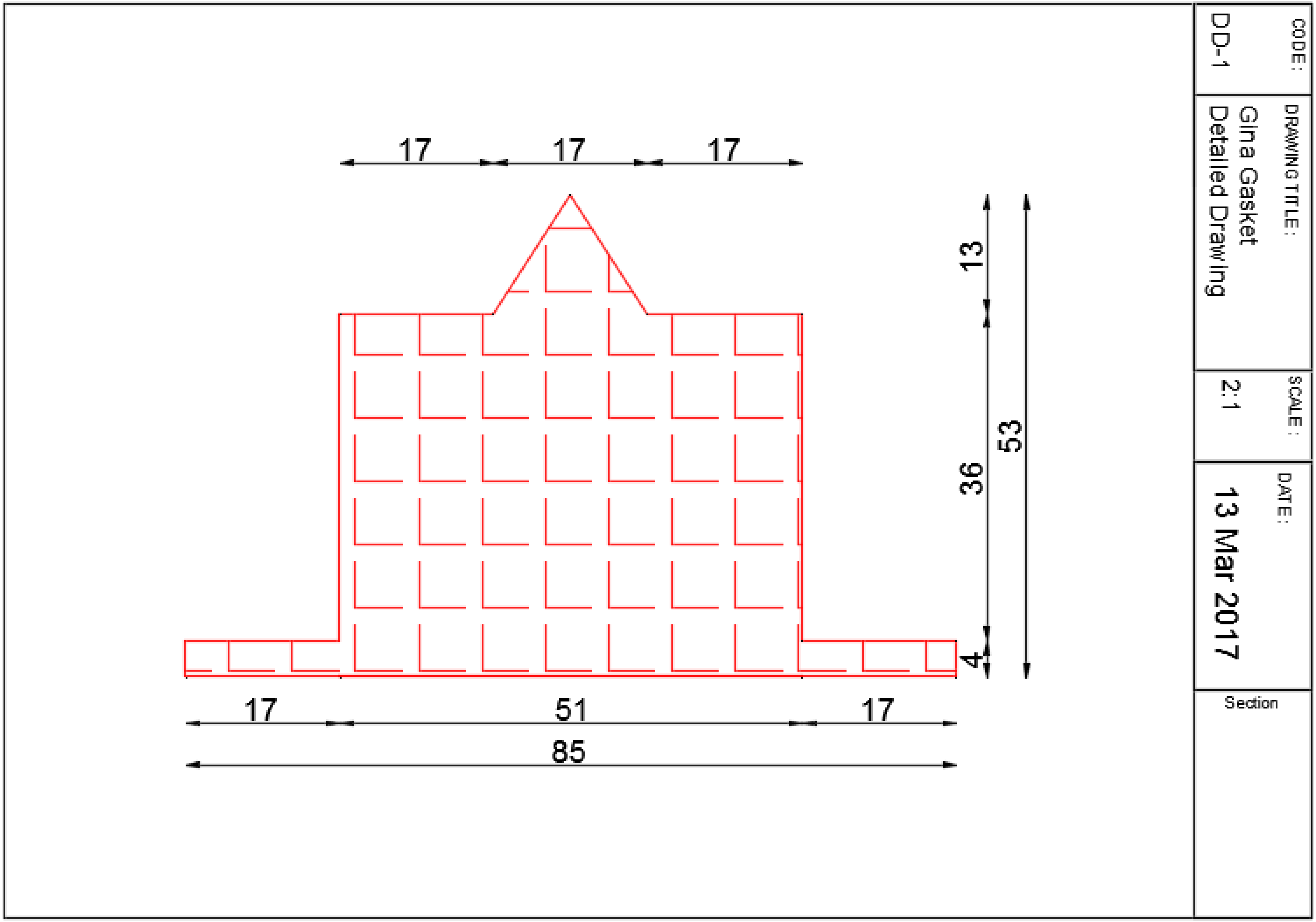

Appendix A-7 Test Equipment Technical Drawing (Model Gina Gasket)

APPENDIX - B : FIELD SAND TEST RESULTS

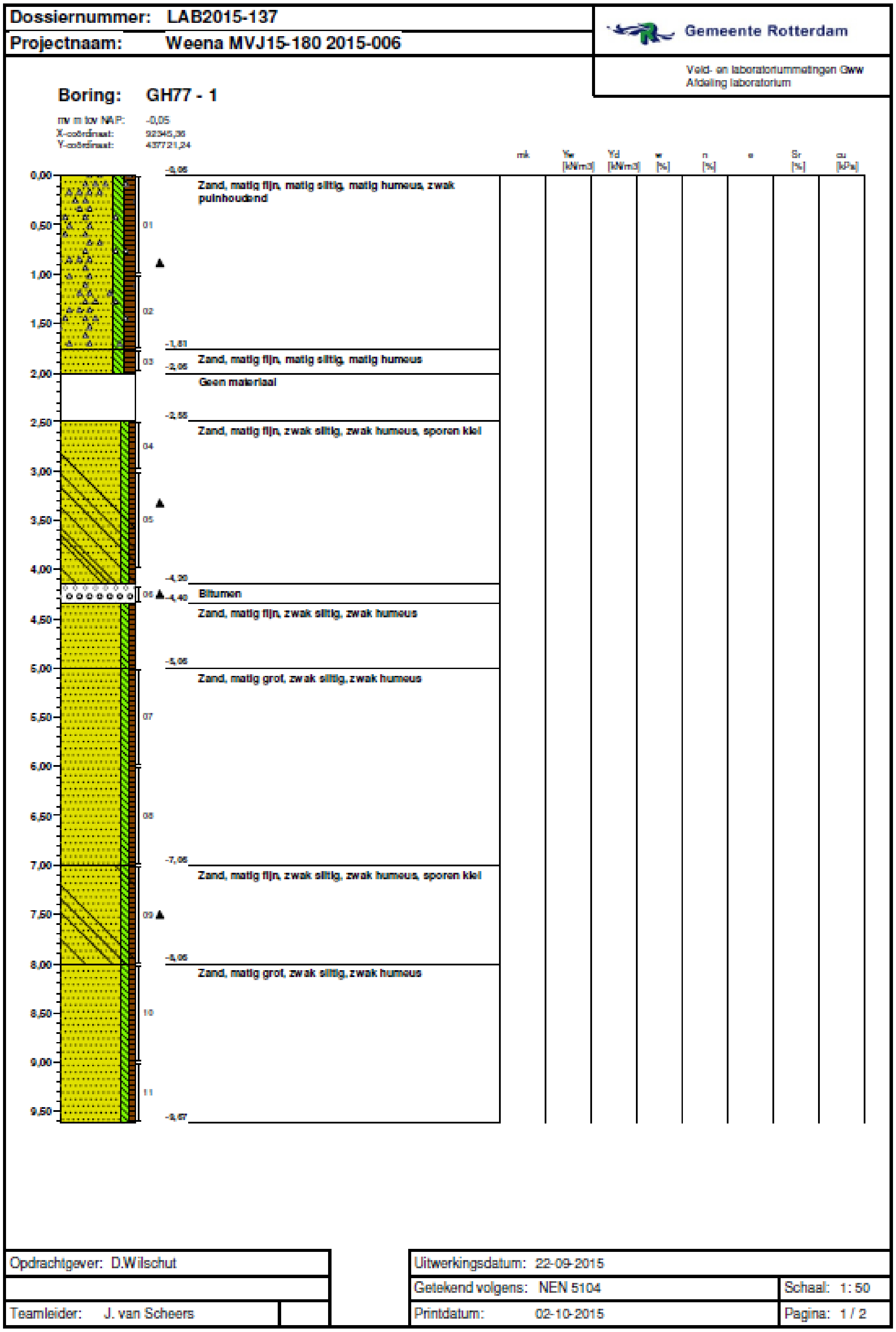

Appendix B-1 Borehole GH-77

Dossiernummer:	LAB2015-137
Projectnaam:	Weena MVJ15-180 2015-006

Gemeente Rotterdam

Veld- en laboratoriummetingen Gww
Afdeling laboratorium

Boring: GH78 - 1

mv m tov NAP: -0,053
X-coördinaat: 92360,77
Y-coördinaat: 437726,17

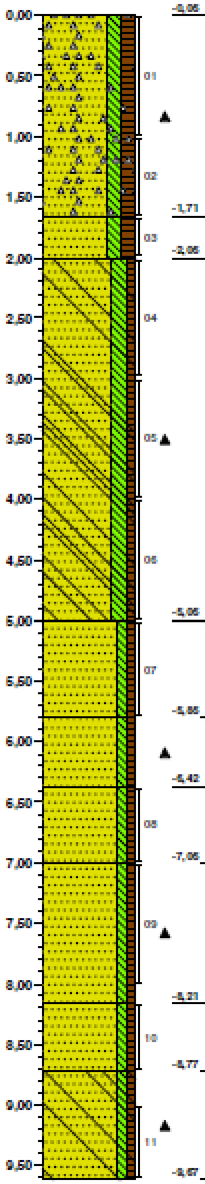

NAP	Omschrijving	mk	Yw [kN/m3]	Yd [kN/m3]	w [%]	n [%]	e	Sr [%]	cu [kPa]
-0,06	Zand, matig fijn, matig siltig, matig humeus, zwak puinhoudend								
-1,71	Zand, matig fijn, matig siltig, matig humeus								
-2,06	Zand, matig fijn, matig siltig, zwak humeus, sporen klei								
-5,06	Zand, matig grof, zwak siltig, zwak humeus								
-5,85	Zand, matig grof, zwak siltig, zwak humeus, resten hout								
-6,42	Zand, matig grof, zwak siltig, zwak humeus								
-7,06	Zand, matig grof, zwak siltig, zwak humeus, sporen hout								
-8,21	Zand, matig grof, zwak siltig, zwak humeus								
-8,77	Zand, matig grof, zwak siltig, zwak humeus, sporen klei								
-9,67									

Opdrachtgever: D.Wilschut	Uitwerkingsdatum: 22-09-2015		
	Getekend volgens: NEN 5104	Schaal: 1: 50	
Teamleider: J. van Scheers	Printdatum: 02-10-2015	Pagina: 1 / 2	

Appendix B-2 Borehole GH-78

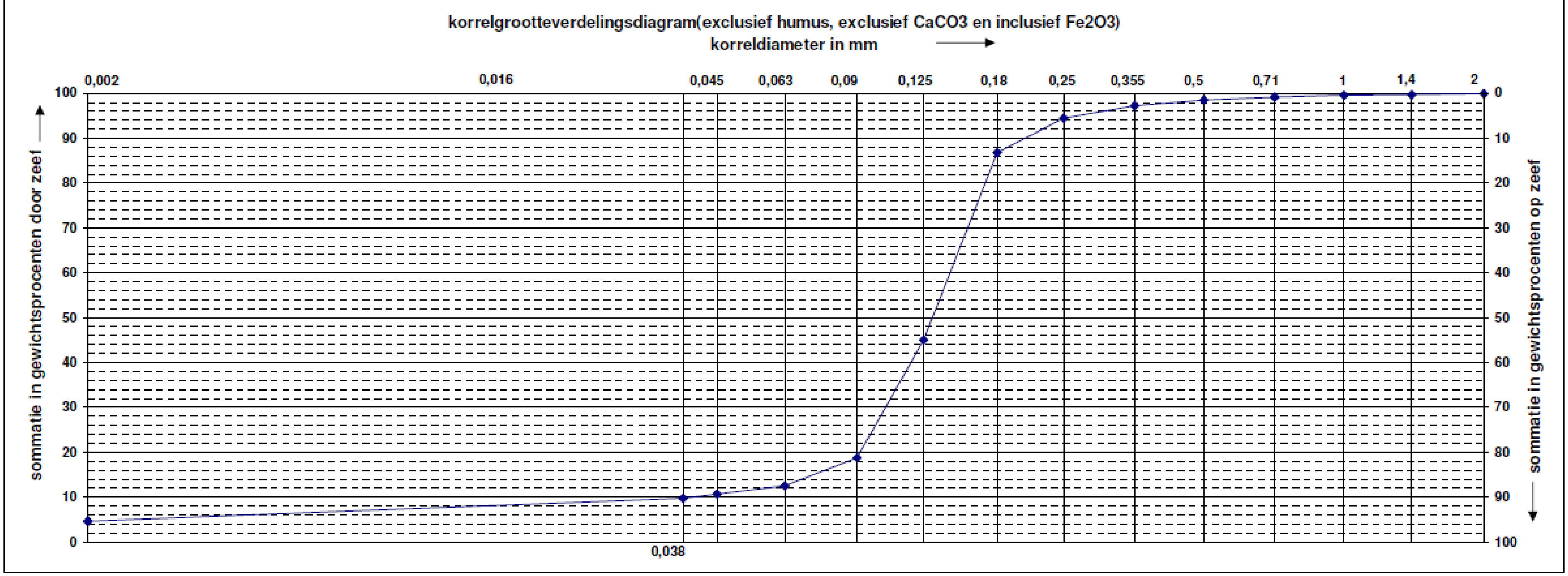

samenstelling monster (inclusief humus, CaCO3 en Fe2O3)

identificatie monster	grind >2 mm %	zand 0.063-2mm %	silt 0.002-0.063mm %	lutum <0.002 mm %	humus %	CaCO3 %	D50 mm	M50 (0.063-2mm) mm	D60/D10 (0.063-2mm)	grondsoort volgens NEN5104
3,0-4,0m-mv	0,1	81,4	7,4	4,3	0,9	5,9	0,131	0,138	1,60	Z(138)s2, h1, g1 ,Ca3

Tabel uitgedrukt in massapercentages van de stoofdroge grond

opdrachtgever: D.Wilschut	monsterklasse : 3	datum: 23-9-2015	boringnummer: GH77
laborant: E.Drinkwaard	projectleider:	mapnr.: 2015-137	hoogteligging: mv tov NAP: -0,05m

GEMEENTE ROTTERDAM
INGENIEURSBUREAU

Veld- en Laboratoriummetingen Gww

project: Weena MVJ15180 Dossier 2015-006

KORRELGROOTTEVERDELING

Appendix B-3 Grain Size Distribution GH77 Depth 3.0 m – 4.0 m

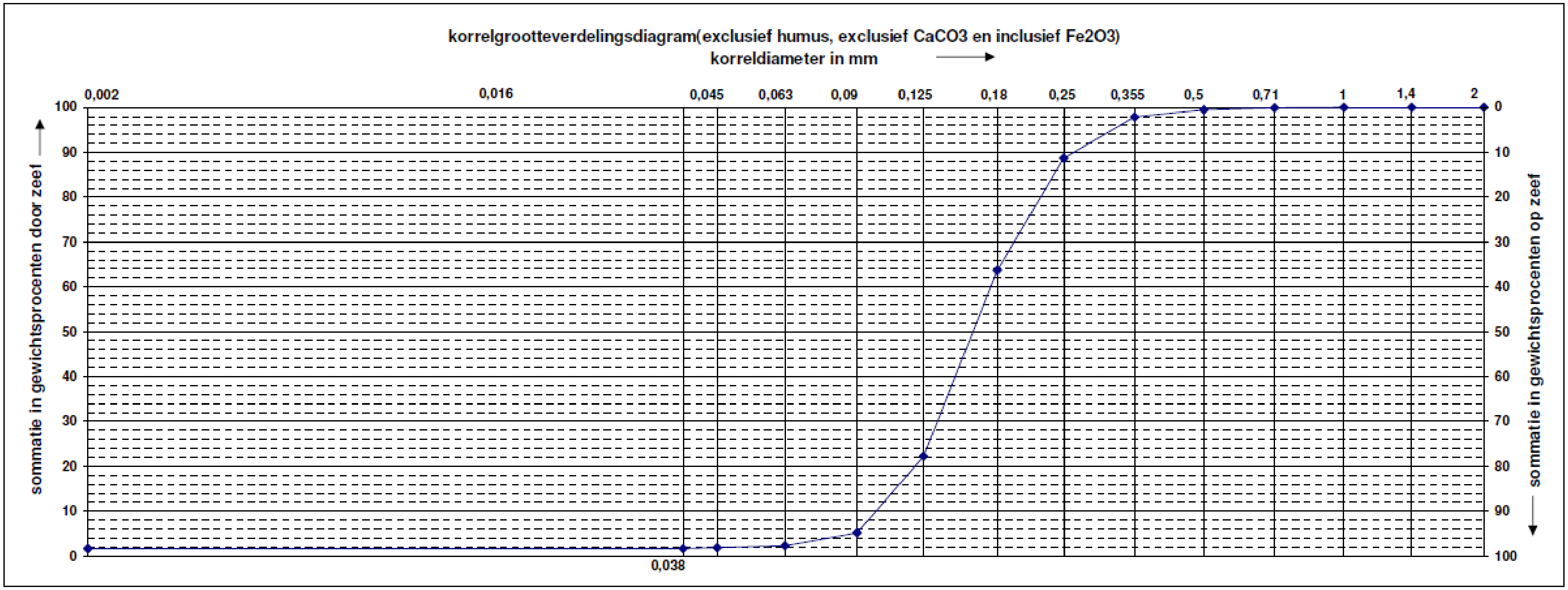

samenstelling monster (inclusief humus, CaCO3 en Fe2O3)

identificatie monster	grind >2 mm %	zand 0.063-2mm %	silt 0.002-0.063mm %	lutum <0.002 mm %	humus %	CaCO3 %	D50 mm	M50 (0.063-2mm) mm	D60/D10 (0.063-2mm)	grondsoort volgens NEN5104
5,0-6,0m-mv	0,0	93,2	0,6	1,6	0,3	4,3	0,160	0,161	1,71	Z(161)s1, h1, g1 ,Ca3

Tabel uitgedrukt in massapercentages van de stoofdroge grond

opdrachtgever: D.Wilschut	monsterklasse : 3	datum: 23-9-2015	boringnummer: GH77
laborant: E.Drinkwaard	projectleider:	mapnr.: 2015-137	hoogteligging: mv tov NAP: -0,05m

GEMEENTE ROTTERDAM
INGENIEURSBUREAU

Veld- en Laboratoriummetingen Gww

project: **Weena MVJ15180 Dossier 2015-006**

KORRELGROOTTEVERDELING

Appendix B-4 Grain Size Distribution GH77 Depth 5.0 m – 6.0 m

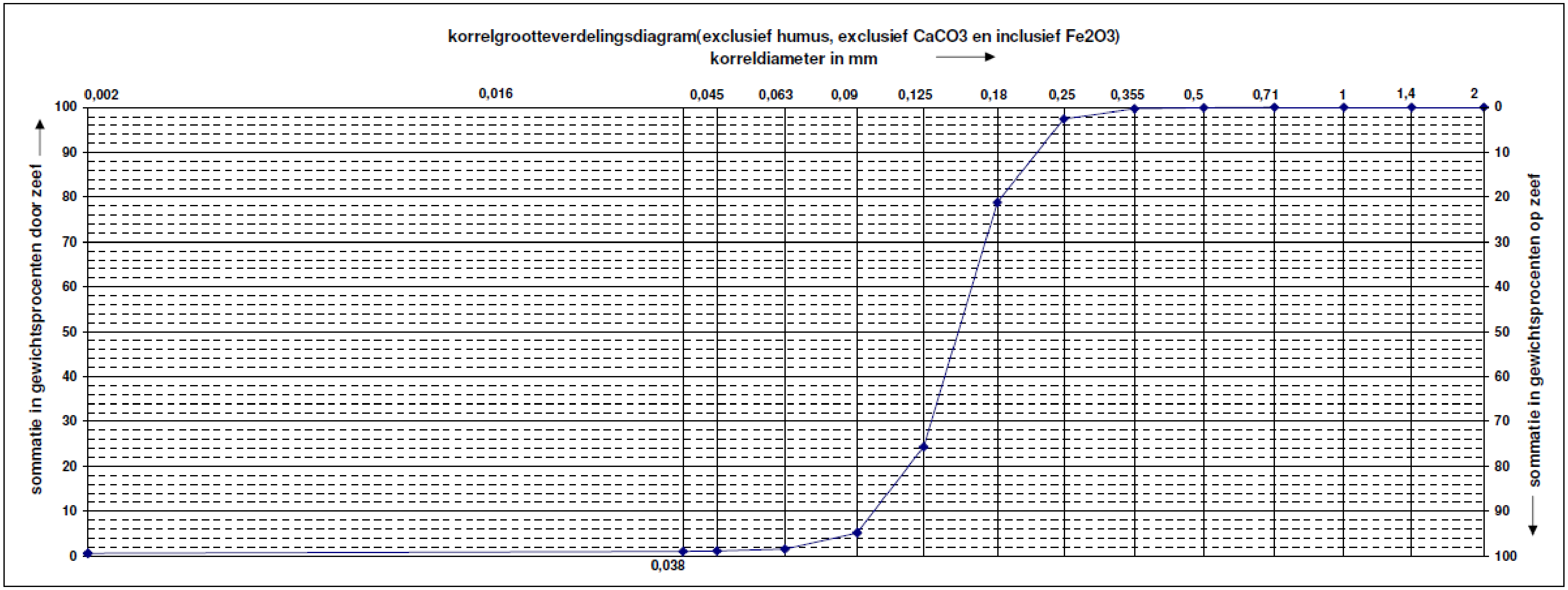

samenstelling monster (inclusief humus, CaCO3 en Fe2O3)

identificatie monster	grind >2 mm %	zand 0.063-2mm %	silt 0.002-0.063mm %	lutum <0.002 mm %	humus %	CaCO3 %	D50 mm	M50 (0.063-2mm) mm	D60/D10 (0.063-2mm)	grondsoort volgens NEN5104
7,0-8,0m-mv	0,0	94,0	0,9	0,6	0,3	4,2	0,148	0,149	1,59	Z(149)s1, h1 ,Ca3

Tabel uitgedrukt in massapercentages van de stoofdroge grond

opdrachtgever: D.Wilschut	monsterklasse :	3	datum:	23-9-2015	boringnummer:	GH77	
laborant: E.Drinkwaard	projectleider:		mapnr.:	2015-137	hoogteligging: mv	tov NAP:	-0,05m
GEMEENTE ROTTERDAM INGENIEURSBUREAU Veld- en Laboratoriummetingen Gww		project:	Weena MVJ15180 Dossier 2015-006				
			KORRELGROOTTEVERDELING				

Appendix B-5 Grain Size Distribution GH77 Depth 7.0 m – 8.0 m

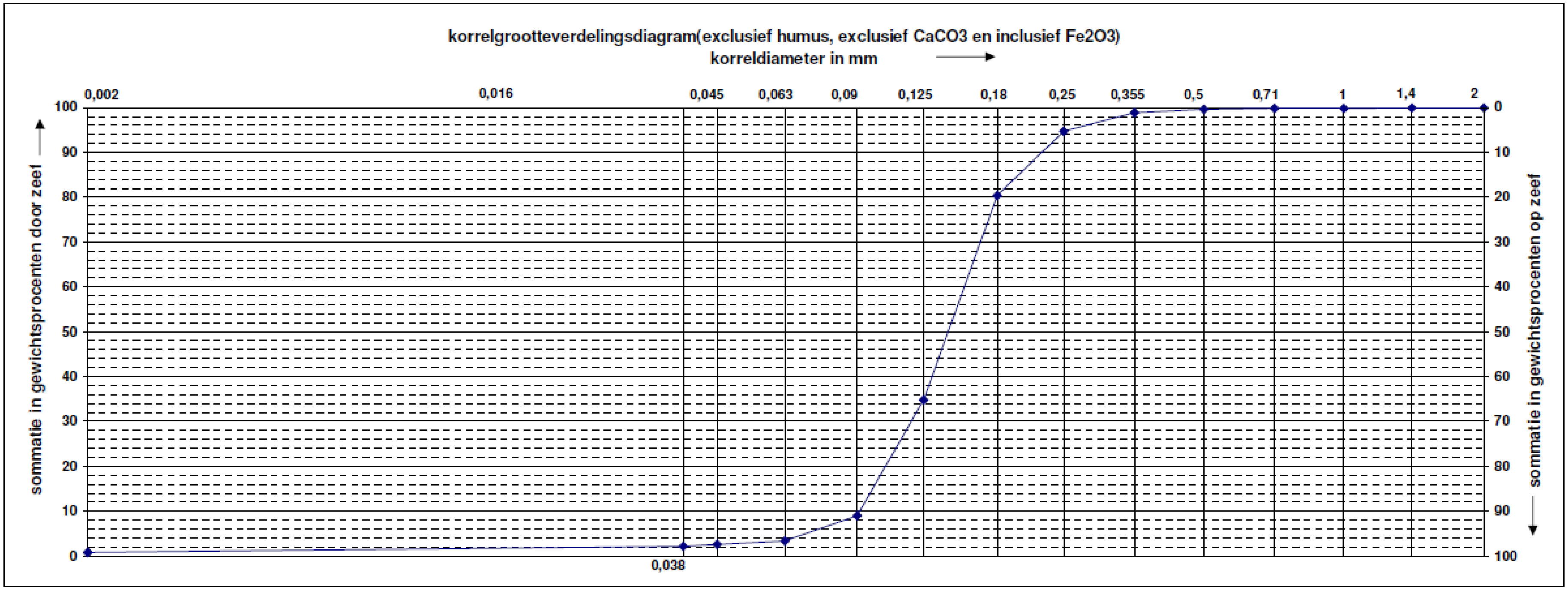

samenstelling monster (inclusief humus, $CaCO_3$ en Fe_2O_3)

identificatie monster	grind >2 mm %	zand 0.063-2mm %	silt 0.002-0.063mm %	lutum <0.002 mm %	humus %	$CaCO_3$ %	D50 mm	M50 (0.063-2mm) mm	D60/D10 (0.063-2mm)	grondsoort volgens NEN5104
4,0-5,0m-mv	0,1	91,3	2,4	0,8	0,4	5,0	0,141	0,143	1,63	Z(143)s1, h1, g1 ,Ca3

Tabel uitgedrukt in massapercentages van de stoofdroge grond

opdrachtgever: D.Wilschut	monsterklasse : 3	datum: 23-9-2015	boringnummer: GH78
laborant: E.Drinkwaard	projectleider:	mapnr.: 2015-137	hoogteligging: mv tov NAP: -0,05m

GEMEENTE ROTTERDAM
INGENIEURSBUREAU

Veld- en Laboratoriummetingen Gww

project: **Weena MVJ15180 Dossier 2015-006**

KORRELGROOTTEVERDELING

Appendix B-6 Grain Size Distribution GH78 Depth 3.0 m – 4.0 m

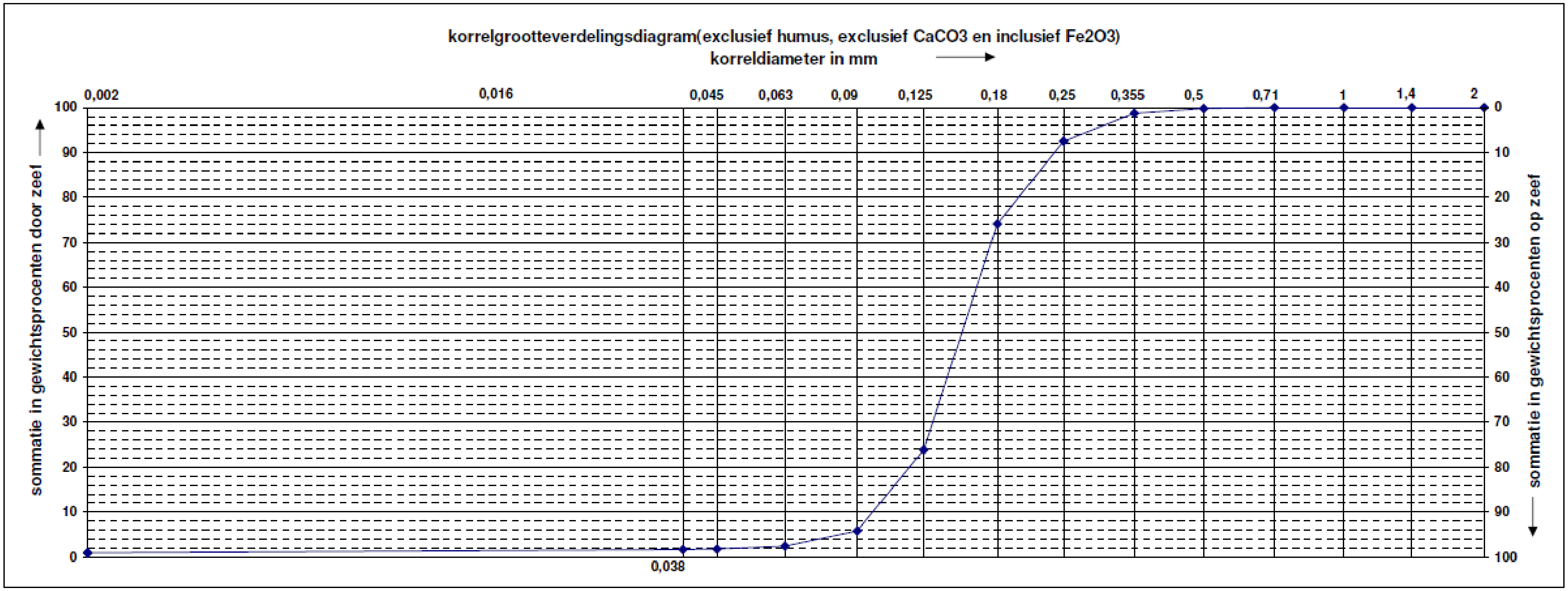

samenstelling monster (inclusief humus, CaCO3 en Fe2O3)

identificatie monster	grind >2 mm %	zand 0.063-2mm %	silt 0.002-0.063mm %	lutum <0.002 mm %	humus %	CaCO3 %	D50 mm	M50 (0.063-2mm) mm	D60/D10 (0.063-2mm)	grondsoort volgens NEN5104
6,37-7,0m-mv	0,0	92,3	1,4	0,9	0,3	5,1	0,151	0,152	1,62	Z(152)s1, h1, g1 ,Ca3

Tabel uitgedrukt in massapercentages van de stoofdroge grond

opdrachtgever:	D.Wilschut	monsterklasse :	3	datum:	23-9-2015	boringnummer:	GH78
laborant:	E.Drinkwaard	projectleider:		mapnr.:	2015-137	hoogteligging: mv tov NAP:	-0,05m

GEMEENTE ROTTERDAM
INGENIEURSBUREAU

Veld- en Laboratoriummetingen Gww

project: **Weena MVJ15180 Dossier 2015-006**

KORRELGROOTTEVERDELING

5

Appendix B-7 Grain Size Distribution GH78 Depth 6.37 m – 7.0 m

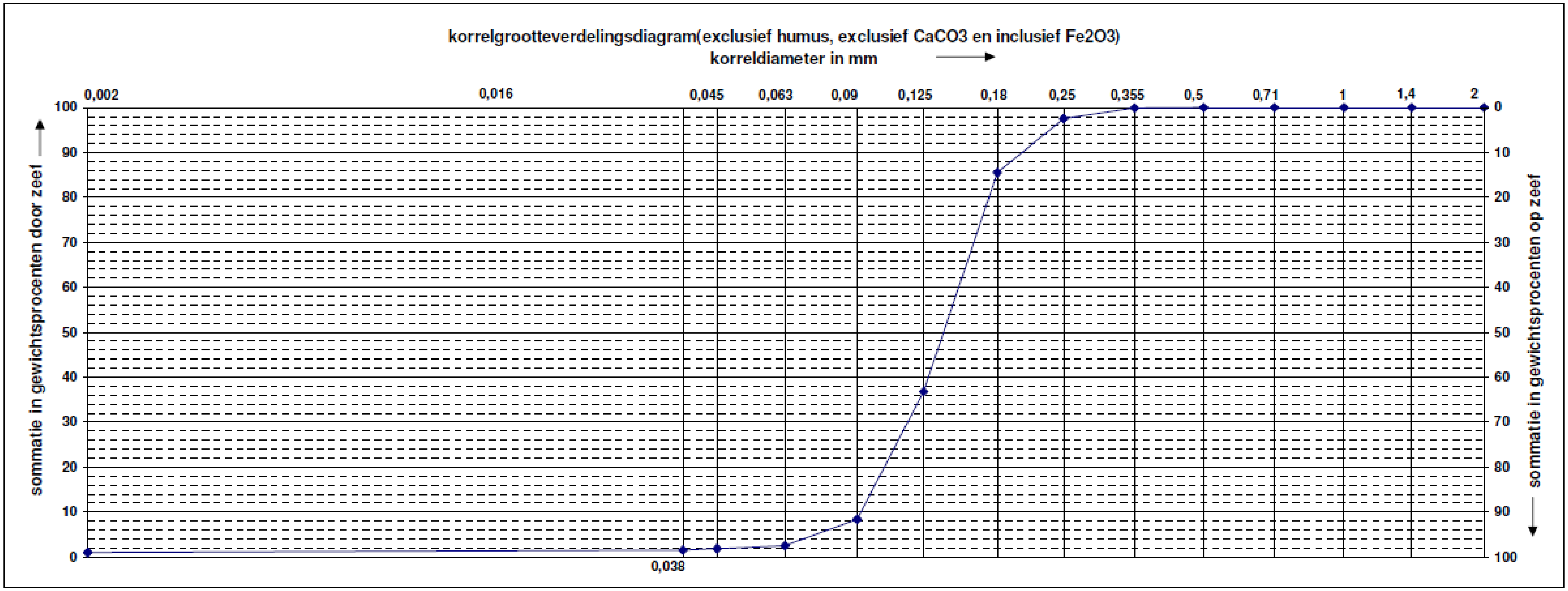

samenstelling monster (inclusief humus, CaCO3 en Fe2O3)

identificatie monster	grind >2 mm %	zand 0.063-2mm %	silt 0.002-0.063mm %	lutum <0.002 mm %	humus %	CaCO3 %	D50 mm	M50 (0.063-2mm) mm	D60/D10 (0.063-2mm)	grondsoort volgens NEN5104
8,0-9,0m-mv	0,0	92,0	1,5	1,0	0,5	5,0	0,138	0,139	1,59	Z(139)s1, h1, g1 ,Ca3

Tabel uitgedrukt in massapercentages van de stoofdroge grond

opdrachtgever: D.Wilschut	monsterklasse :	3	datum:	23-9-2015	boringnummer:	GH78
laborant: E.Drinkwaard	projectleider:		mapnr.:	2015-137	hoogteligging: mv tov NAP:	-0,05m

GEMEENTE ROTTERDAM
INGENIEURSBUREAU

Veld- en Laboratoriummetingen Gww

project: Weena MVJ15180 Dossier 2015-006

KORRELGROOTTEVERDELING

Appendix B-8 Grain Size Distribution GH78 Depth 8.0 m – 9.0 m

APPENDIX - C : Plaxis Output

C.1.Horizontal Soil Stresses

M3-10

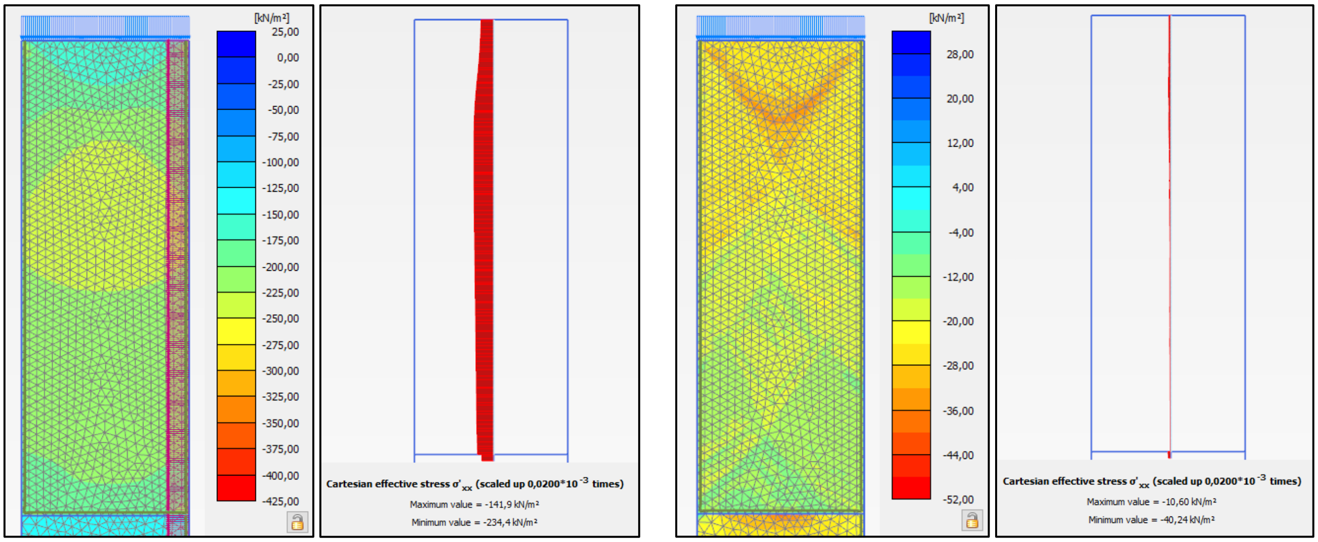

Appendix C-1 M3-10 Horizontal Soil Stresses (left) Loading Stage, (right) Unloading Stage

M3-25

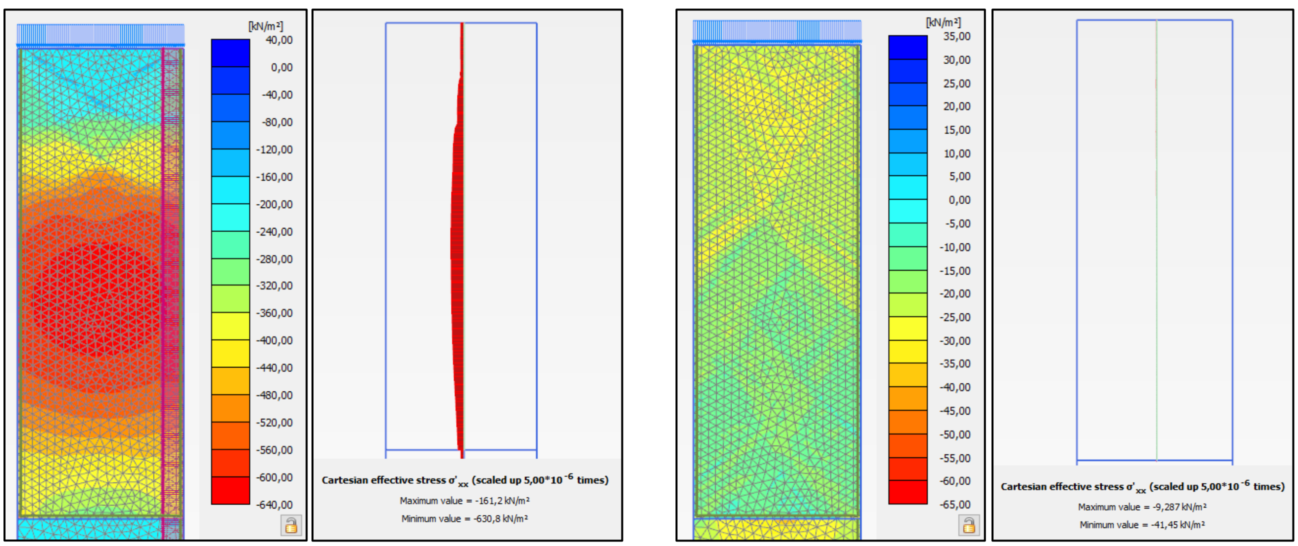

Appendix C-2 M3-25 Horizontal Soil Stresses (left) Loading Stage, (right) Unloading Stage

M3-50

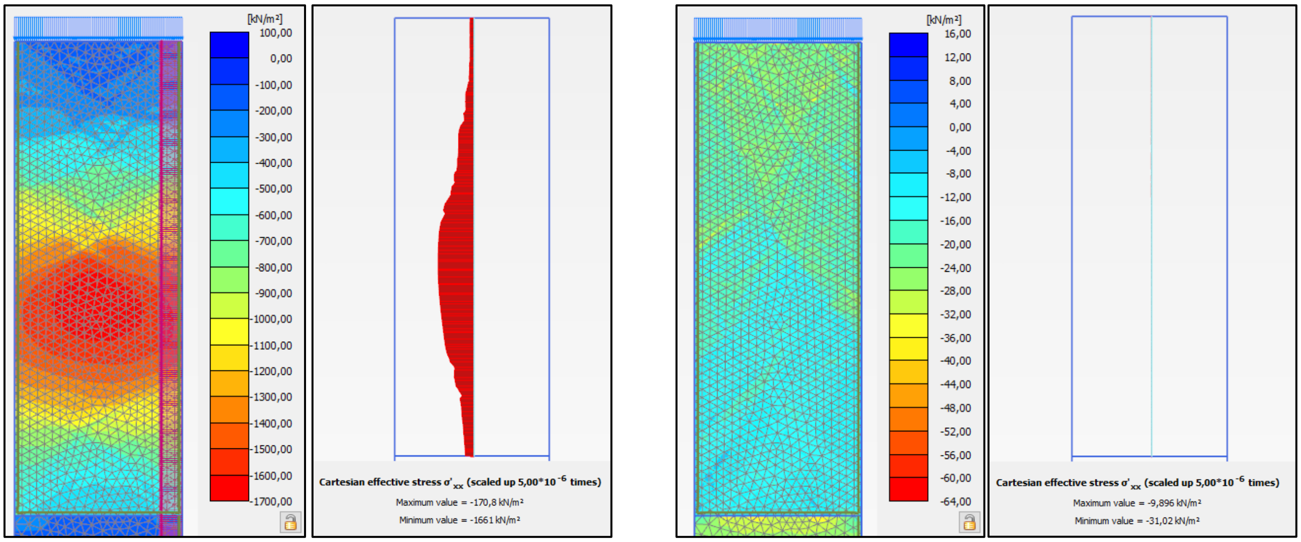

Appendix C-3 M3-50 Horizontal Soil Stresses (left) Loading Stage, (right) Unloading Stage

M3-100

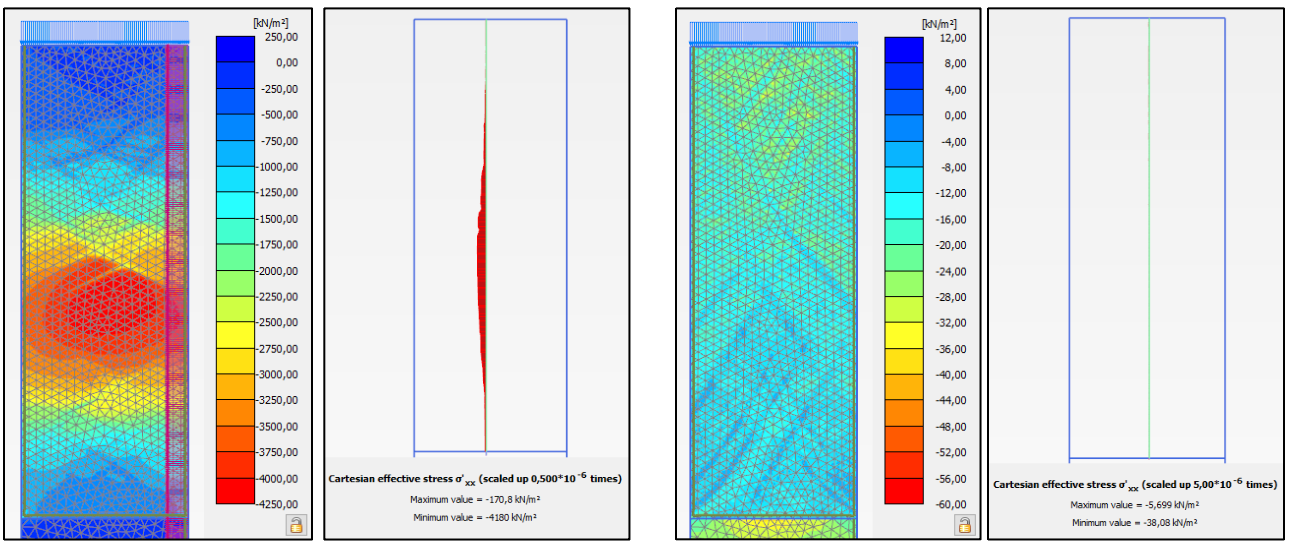

Appendix C-4 M3-100 Horizontal Soil Stresses (left) Loading Stage, (right) Unloading Stage

M3-150

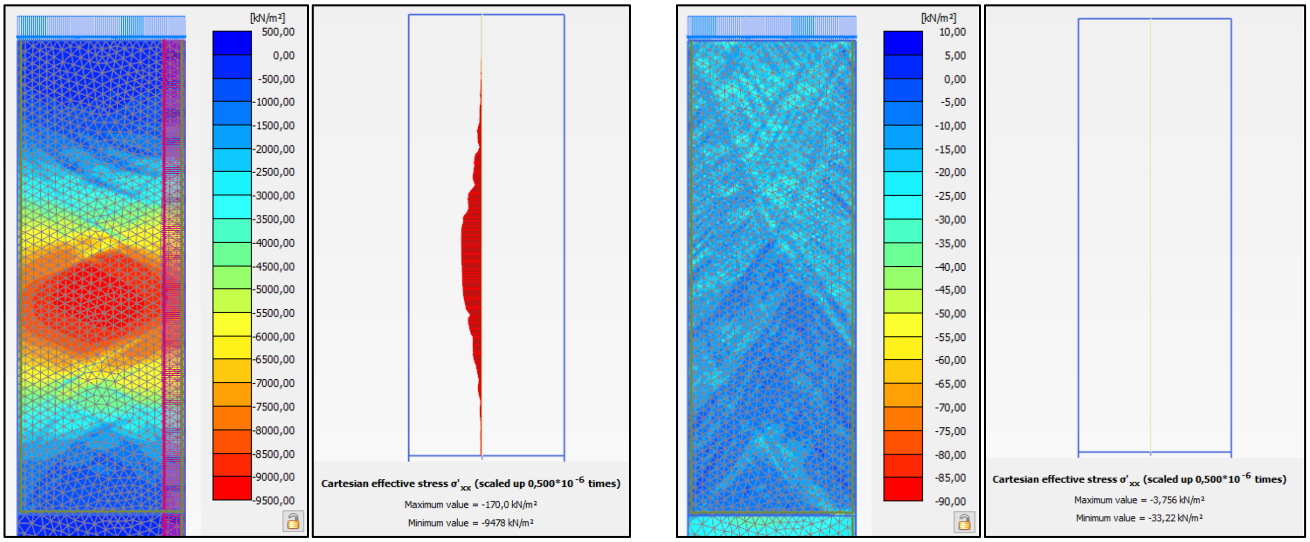

Appendix C-5 M3-150 Horizontal Soil Stresses (left) Loading Stage, (right) Unloading Stage

C.2. Vertical Soil Stresses

M3-10

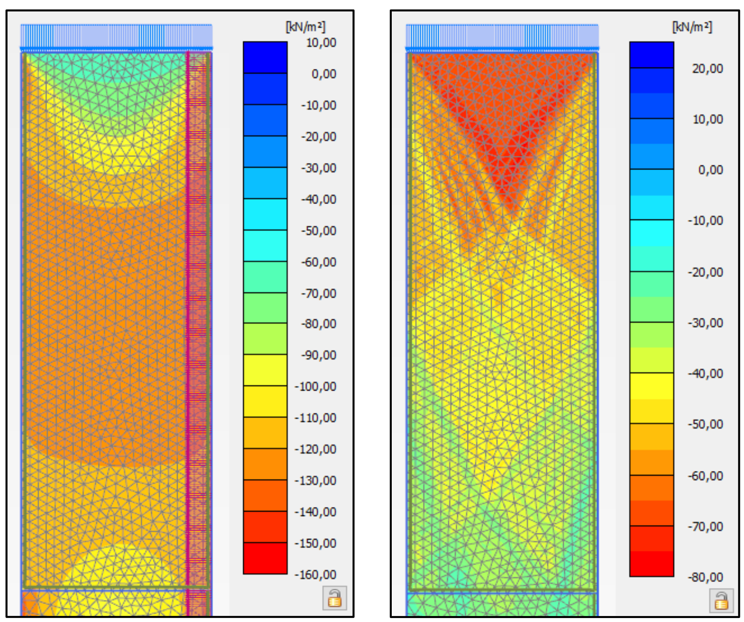

Appendix C-6 M3-10 Vertical Soil Stresses (left) Loading Stage, (right) Unloading Stage

M3-25

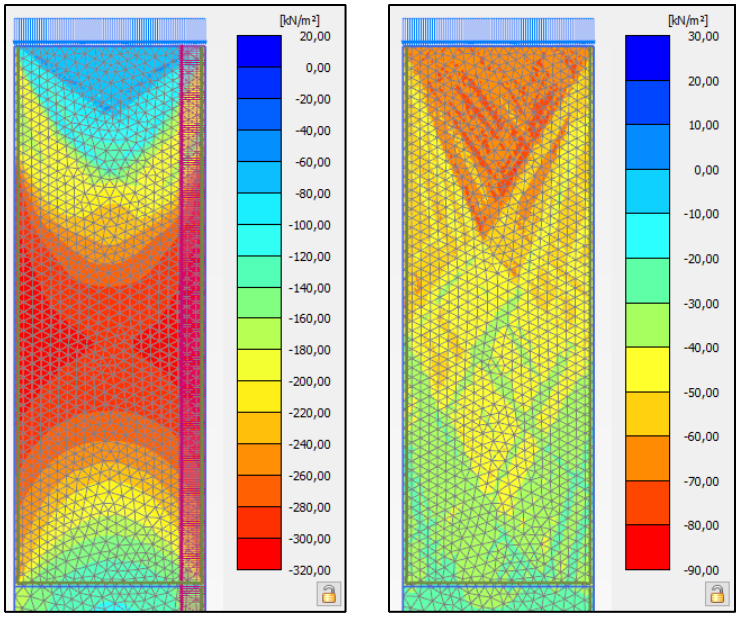

Appendix C-7 M3-25 Vertical Soil Stresses (left) Loading Stage, (right) Unloading Stage

M3-50

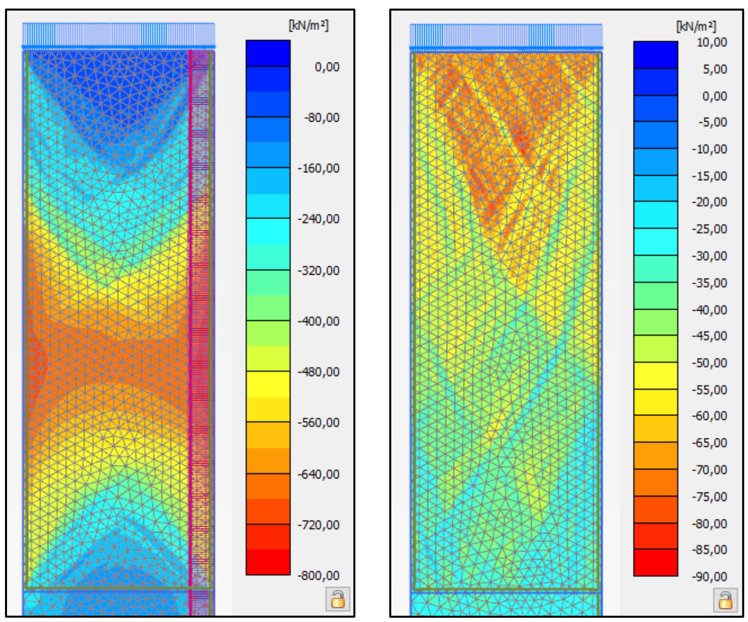

Appendix C-8 M3-50 Vertical Soil Stresses (left) Loading Stage, (right) Unloading Stage

M3-100

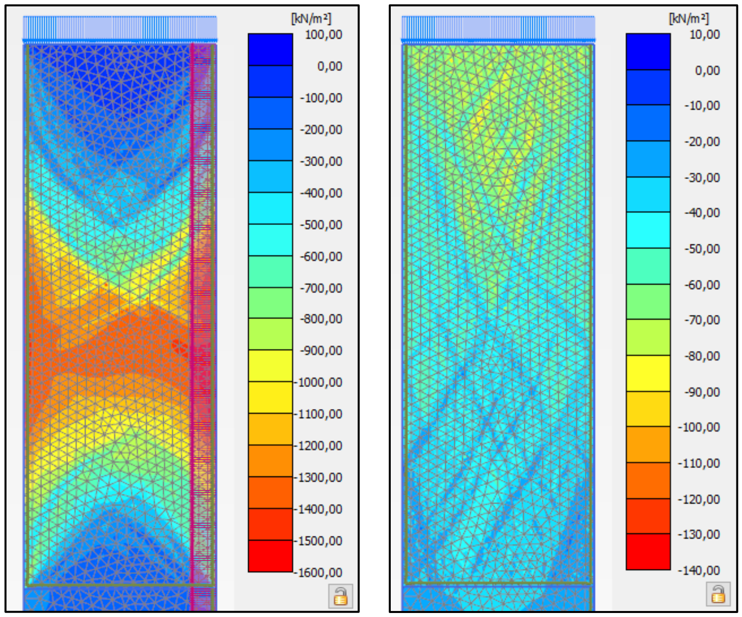

Appendix C-9 M3-100 Vertical Soil Stresses (left) Loading Stage, (right) Unloading Stage

M3-150

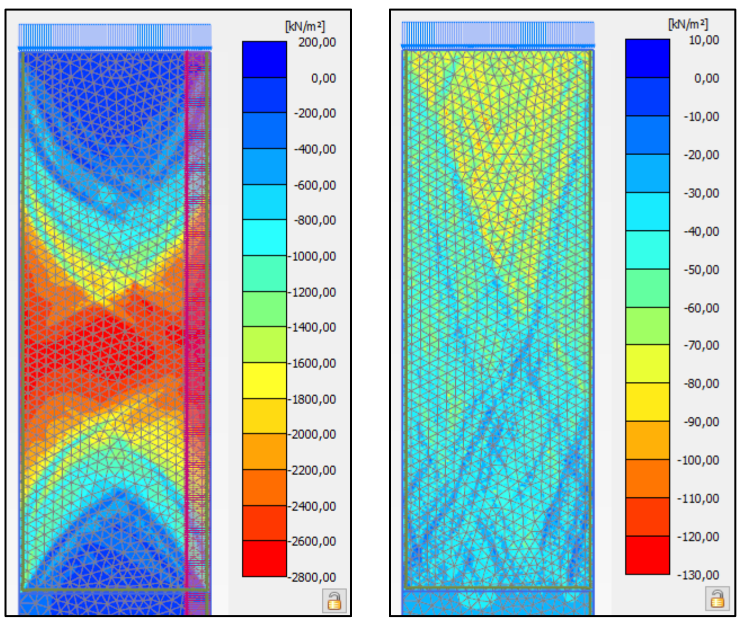

Appendix C-10 M3-150 Vertical Soil Stresses (left) Loading Stage, (right) Unloading Stage

C.3. Plastic Points

Loading Stage

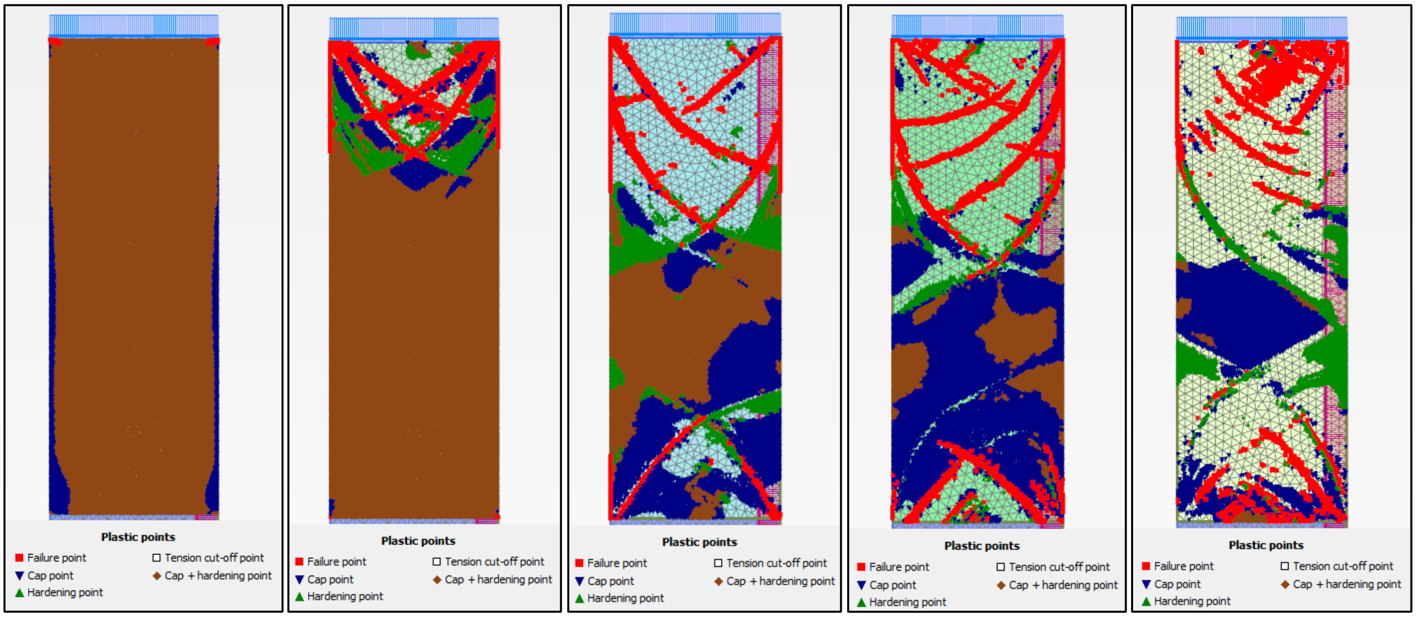

Appendix C-11 Loading Stage Plastic Points (left to right) M3-10, M3-25, M3-50, M3-100, M3-150

Unloading Stage

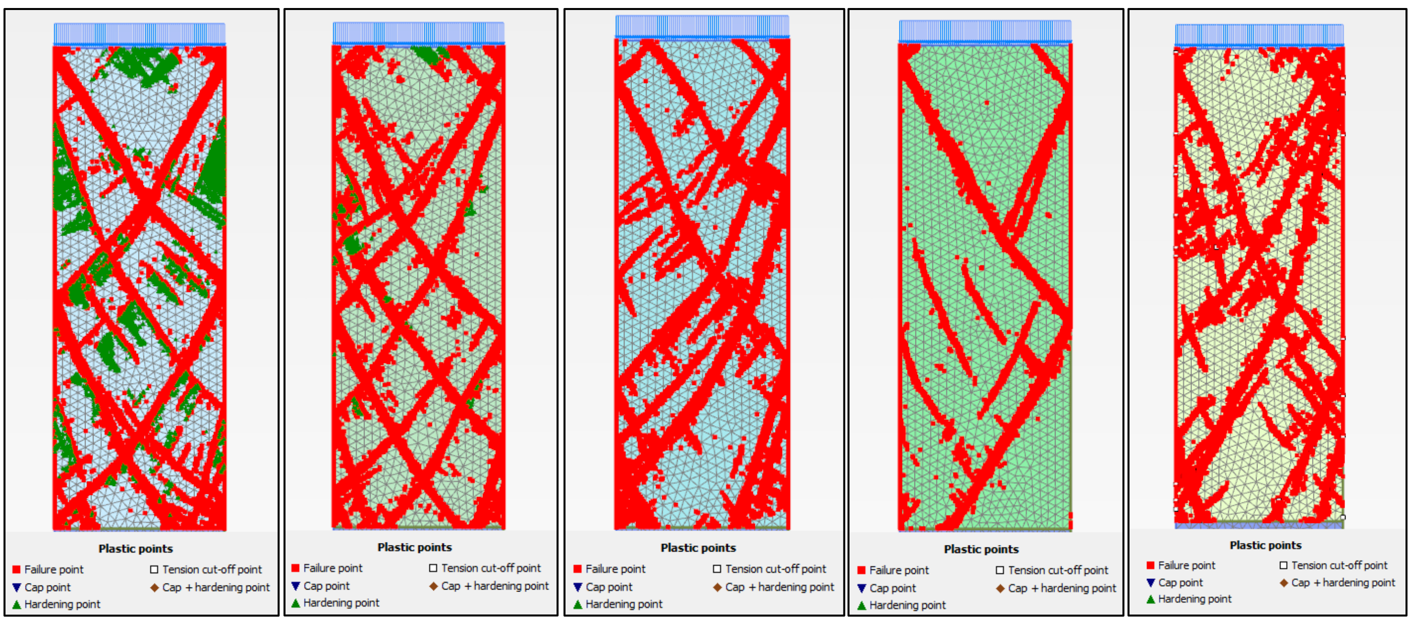

Appendix C-12 Unloading Stage Plastic Points (left to right) M3-10, M3-25, M3-50, M3-100, M3-150

C.4. Gasket Deflection

Loading Stage

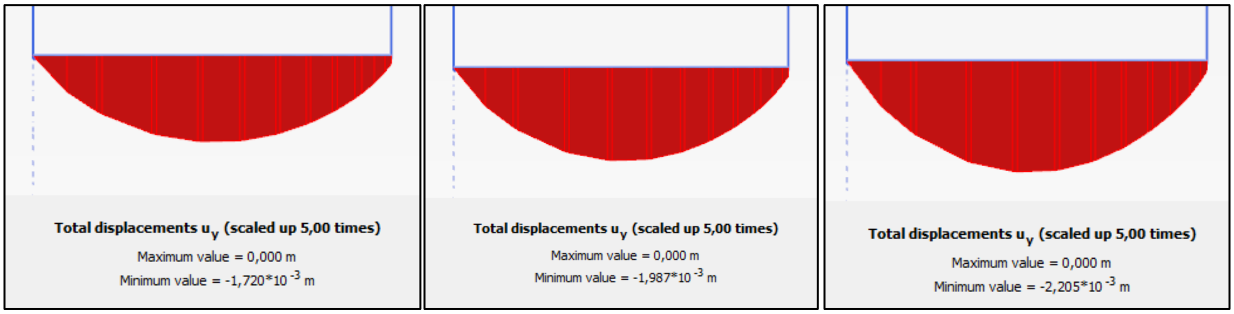

Appendix C-13 Loading Stage Gasket Deflection (left to right) M3-10, M3-25, M3-50

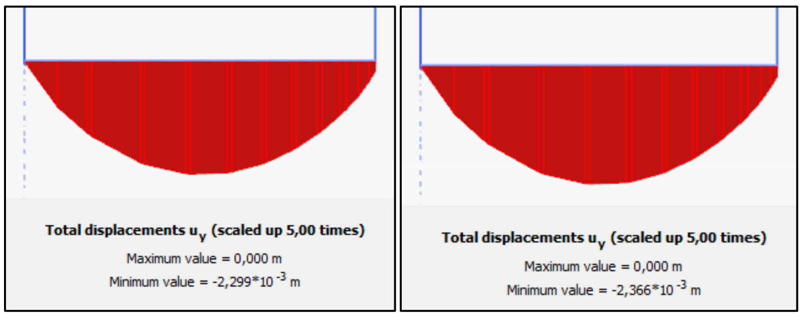

Appendix C-14 Loading Stage Gasket Deflection (left) M3-100, (right) M3-150

Unloading Stage

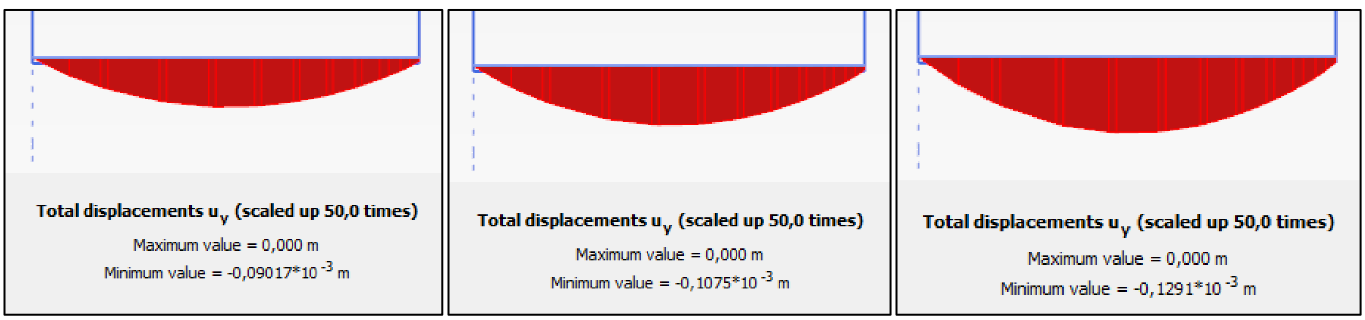

Appendix C-15 Unloading Stage Gasket Deflection (left to right) M3-10, M3-25, M3-50

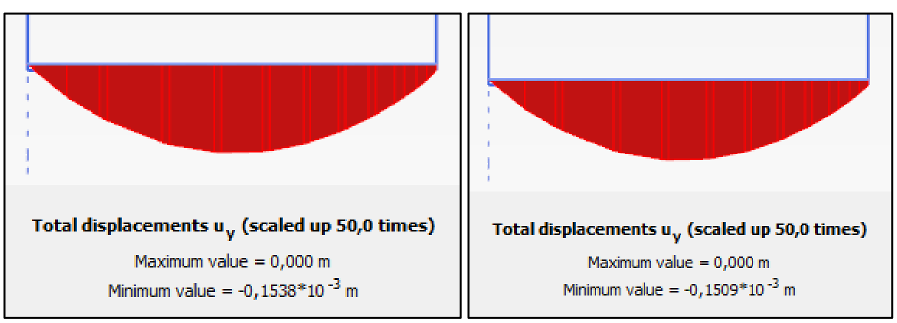

Appendix C-16 Unloading Stage Gasket Deflection (left) M3-100, (right) M3-150

C.5. Sand Top Deflection

Loading Stage

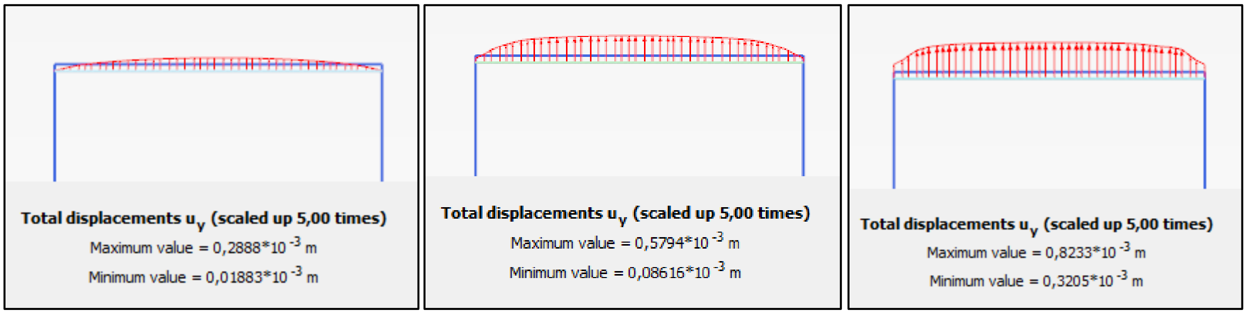

Appendix C-17 Loading Stage Sand Top Deflection (left to right) M3-10, M3-25, M3-50

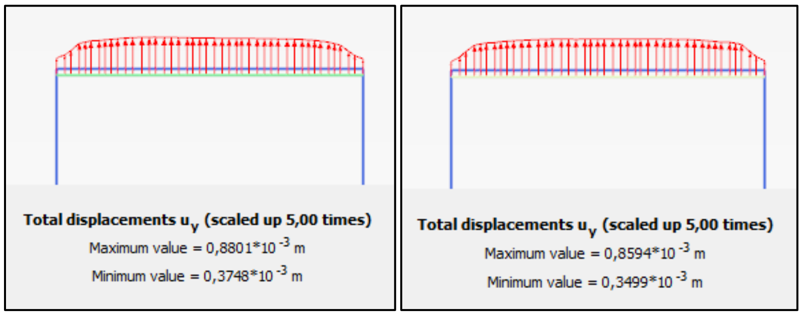

Appendix C-18 Loading Stage Top Deflection (left) M3-100, (right) M3-150

Unloading Stage

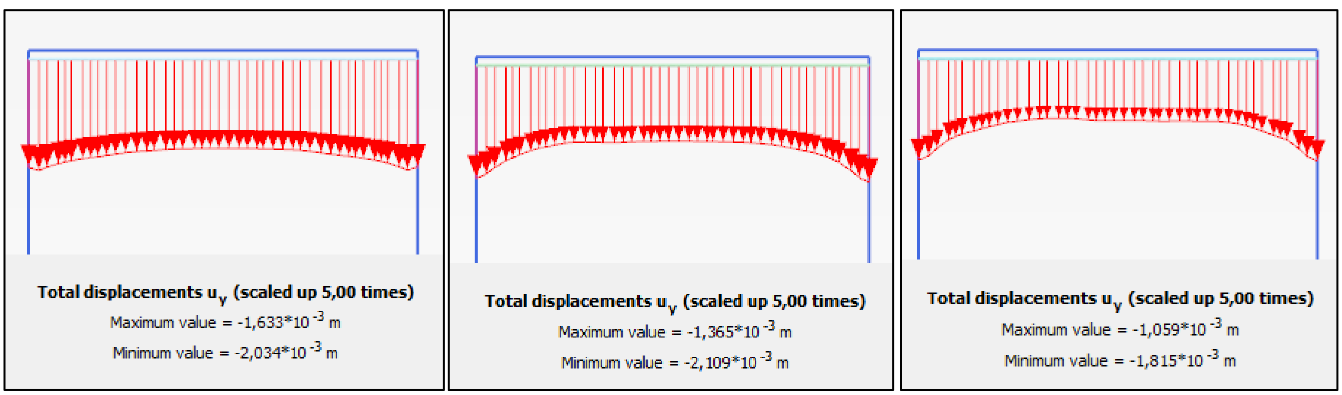

Appendix C-19 Unloading Stage Sand Top Deflection (left to right) M3-10, M3-25, M3-50

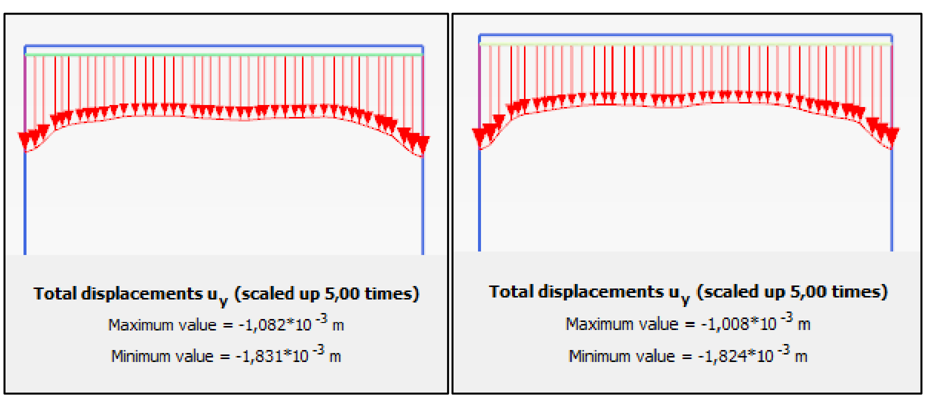

Appendix C-20 Unloading Stage Top Deflection (left) M3-100, (right) M3-150

APPENDIX - D : Laboratory Experiment Results

D.1. Gina Gasket Vertical Deflection Measurements

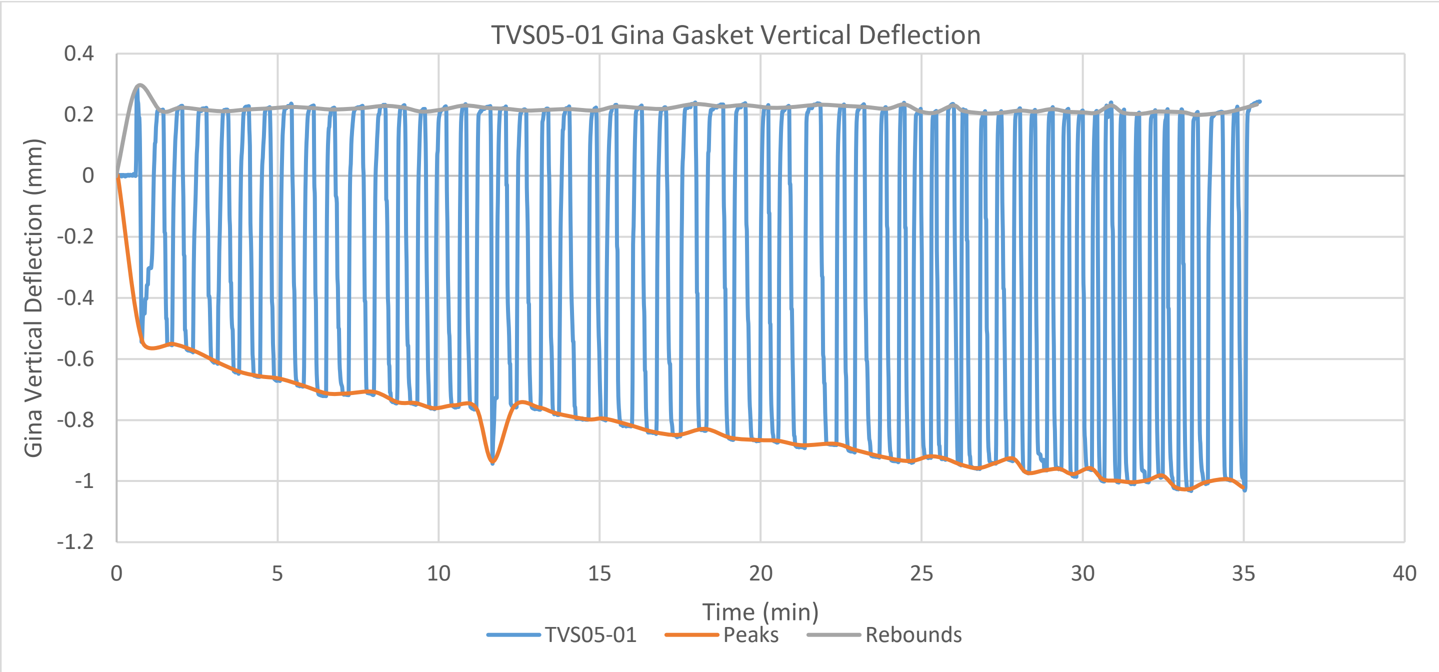

Appendix D-1 TVS05-01 Gina Gasket Vertical Deflection over Time

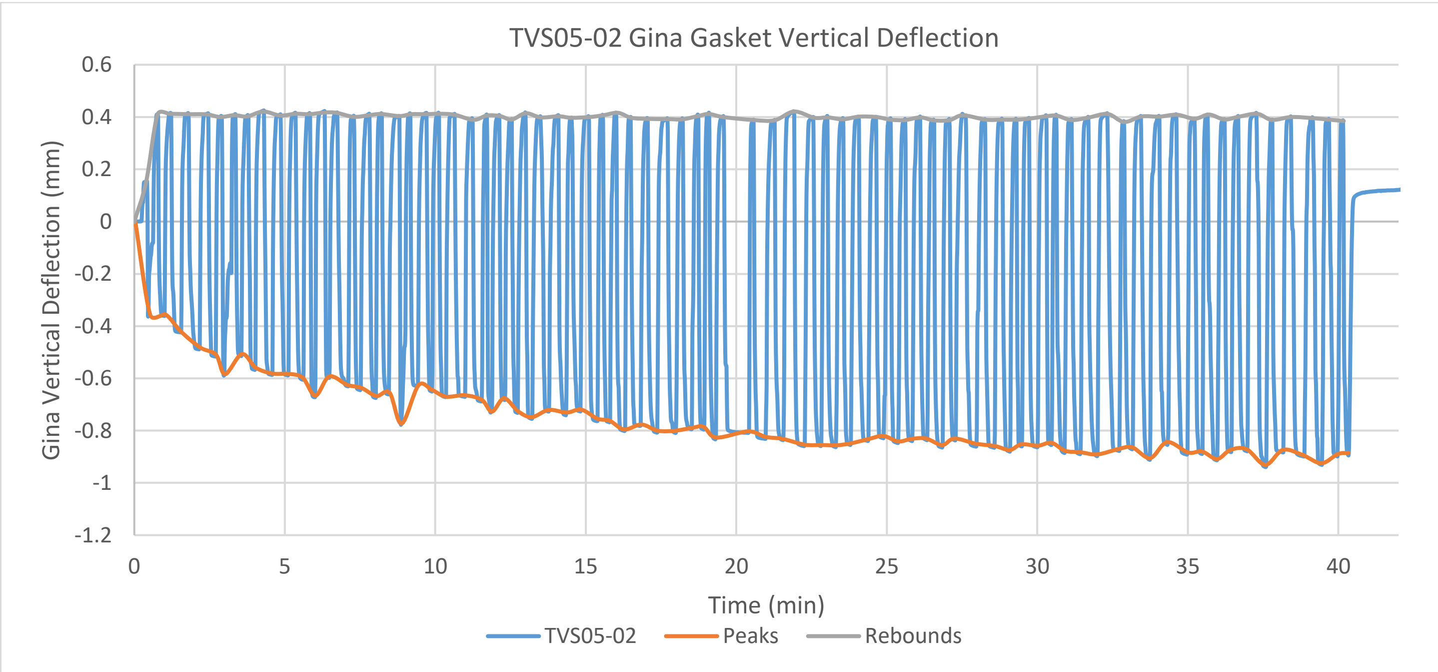

Appendix D-2 TVS05-02 Gina Gasket Vertical Deflection over Time

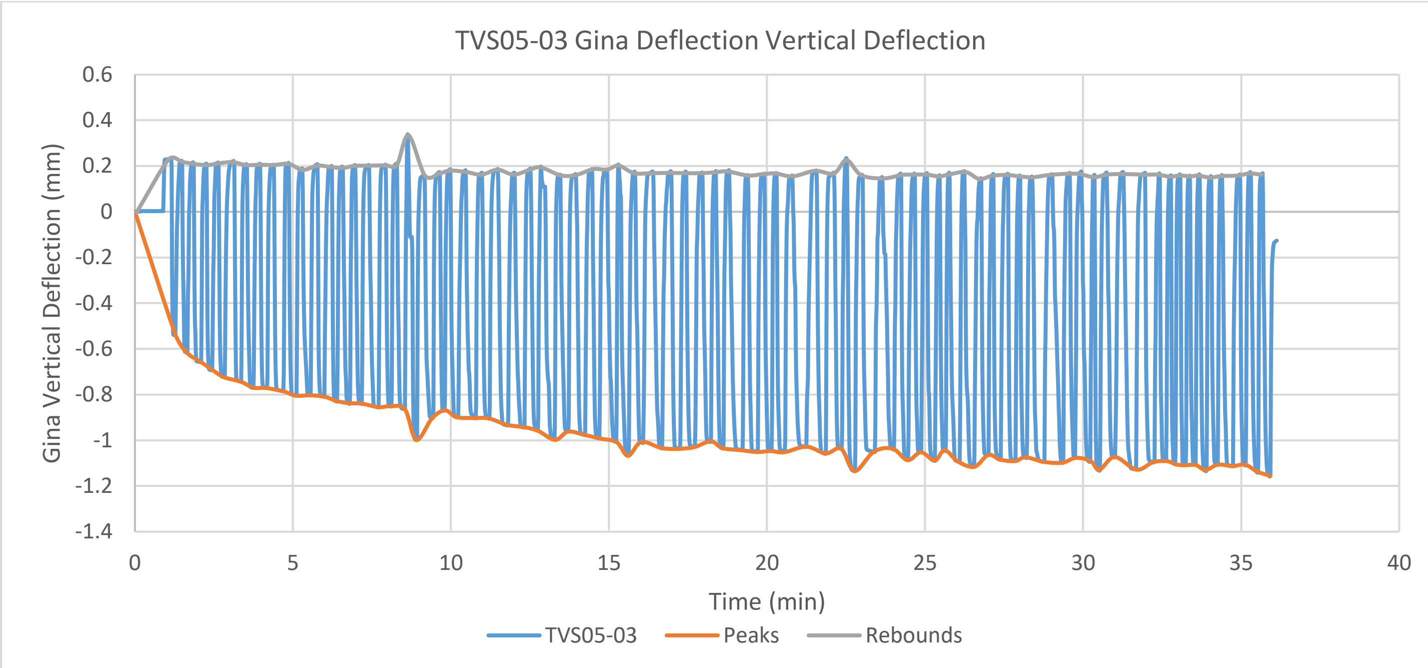

Appendix D-3 TVS05-03 Gina Gasket Vertical Deflection over Time

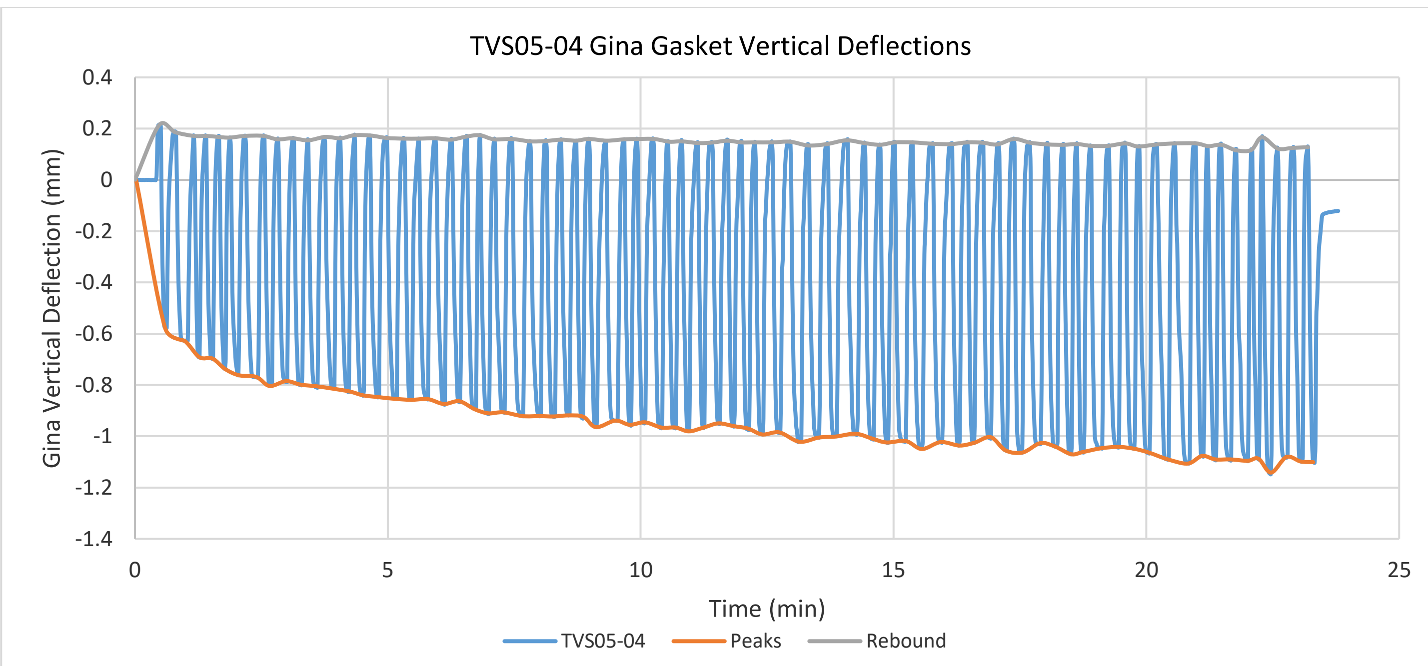

Appendix D-4 TVS05-04 Gina Gasket Vertical Deflection over Time

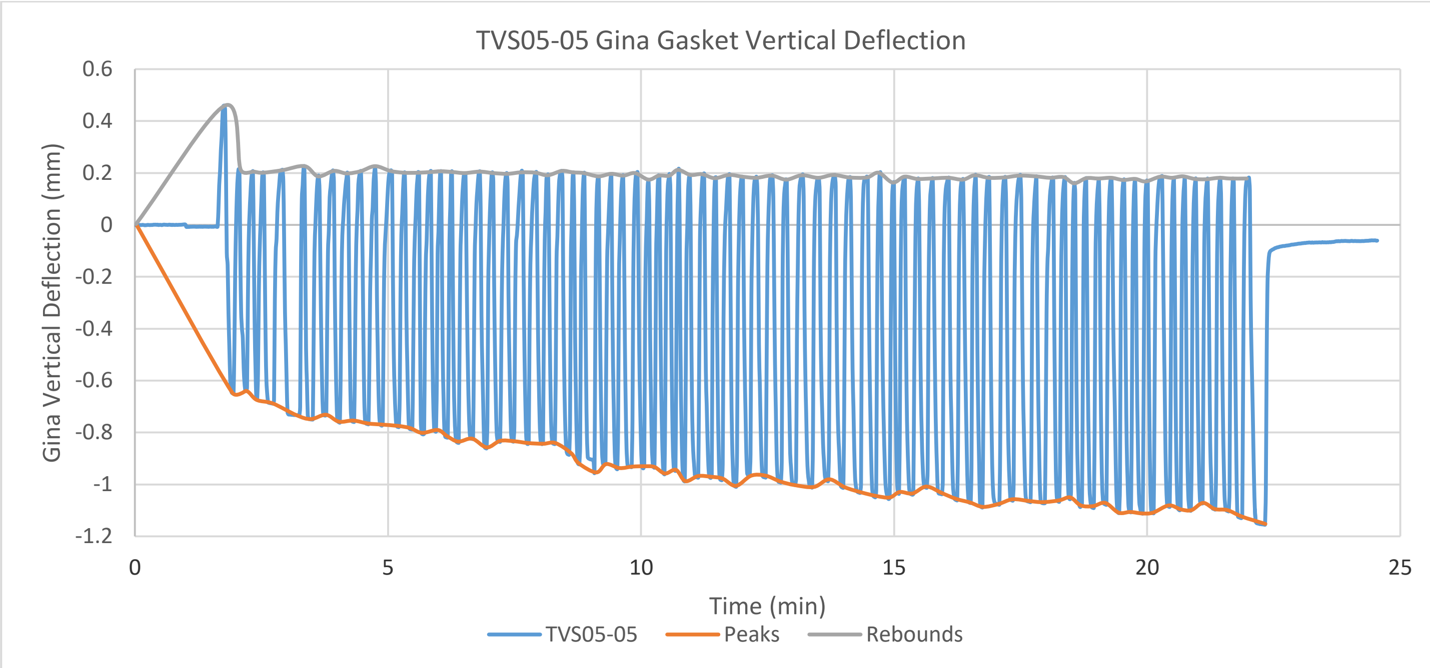

Appendix D-5 TVS05-05 Gina Gasket Vertical Deflection over Time

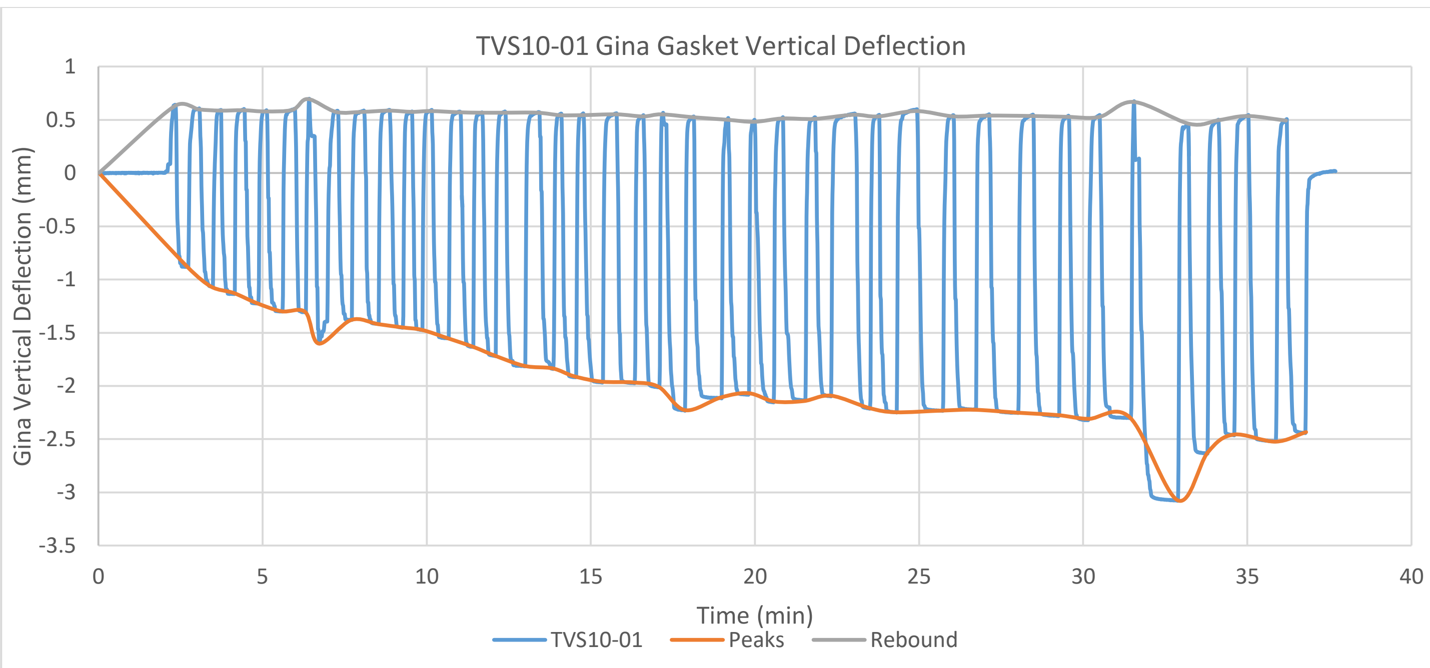

Appendix D-6 TVS10-01 Gina Gasket Vertical Deflection over Time

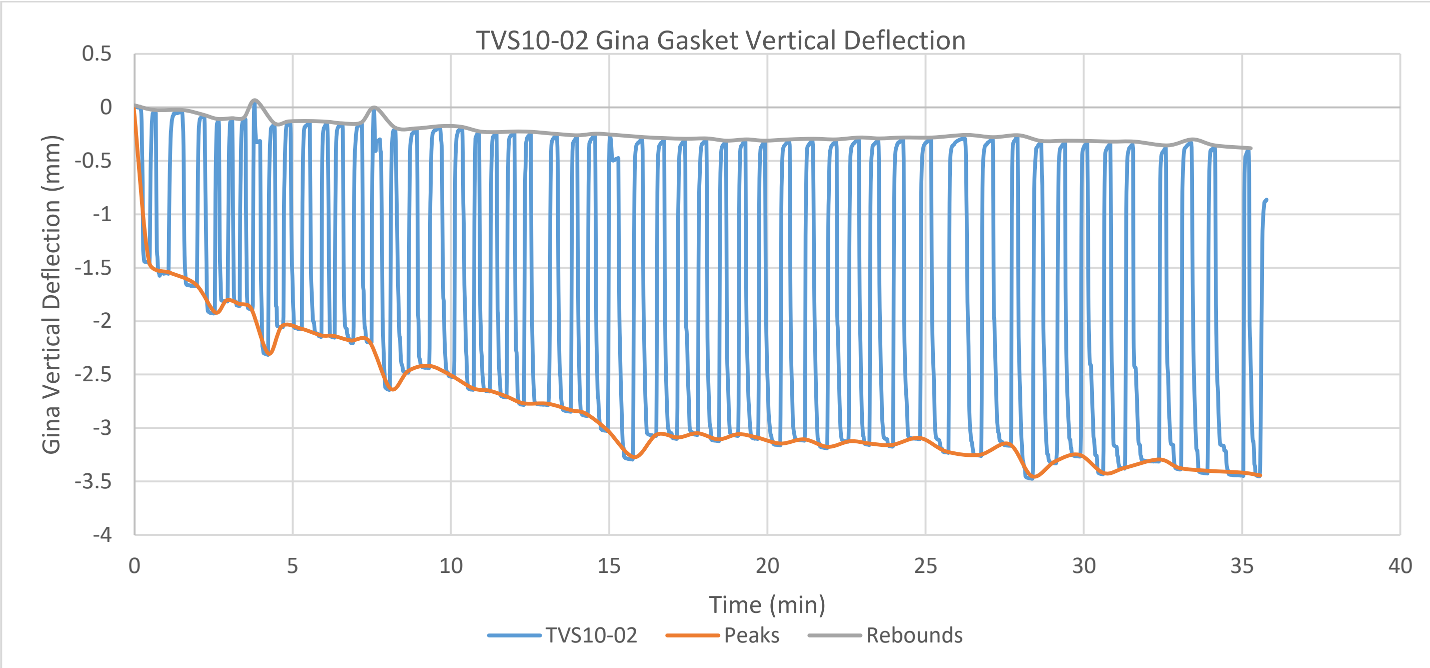

Appendix D-7 TVS10-02 Gina Gasket Vertical Deflection over Time

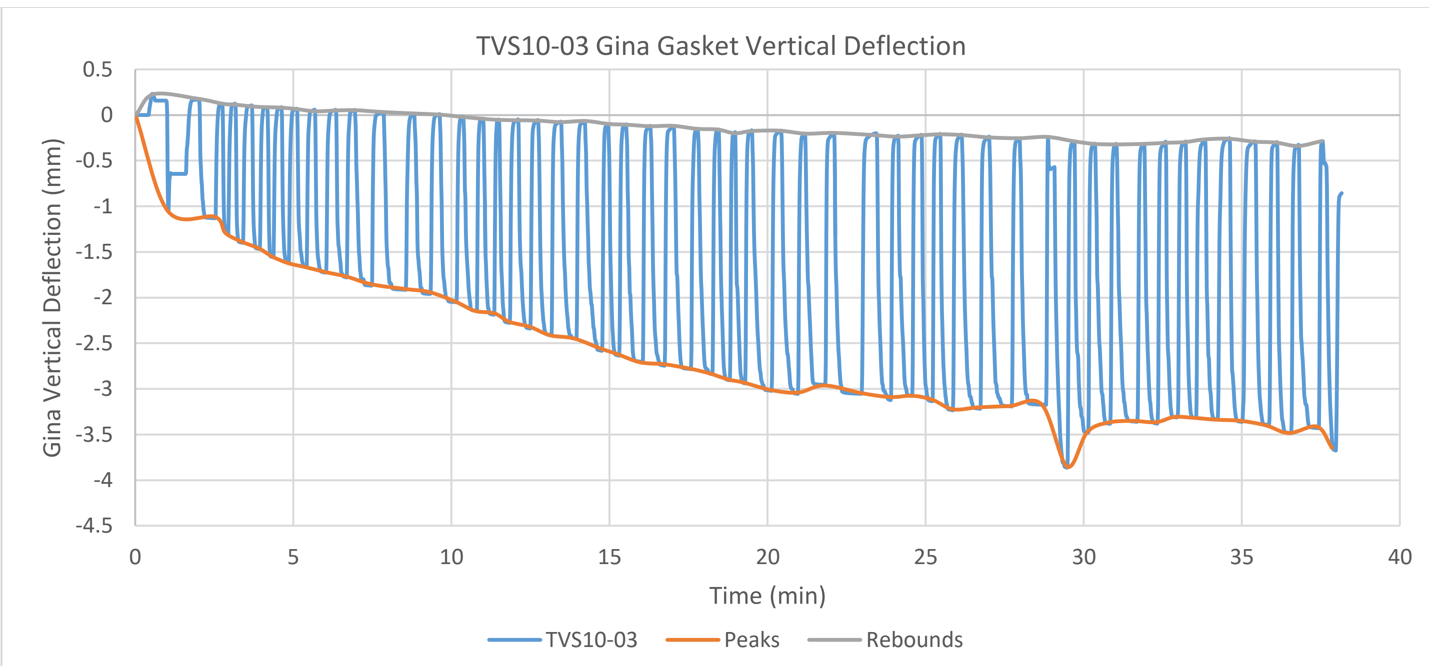

Appendix D-8 TVS10-03 Gina Gasket Vertical Deflection over Time

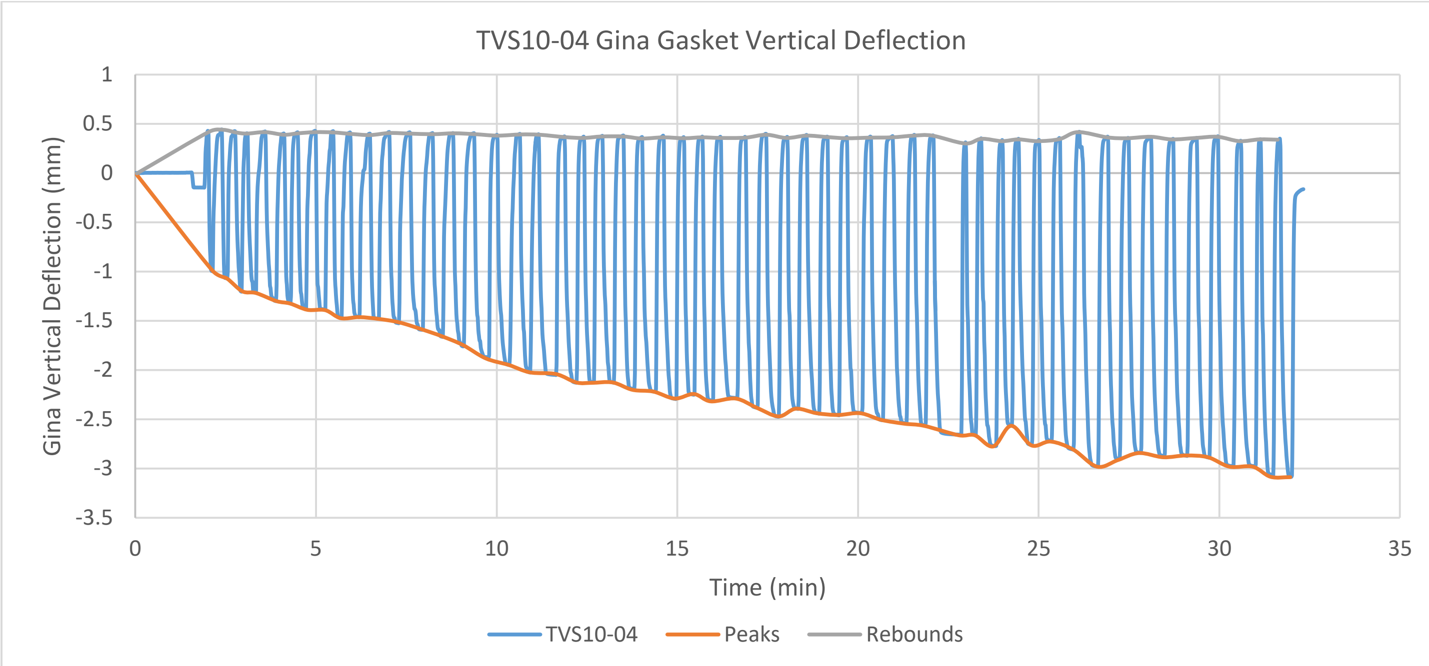

Appendix D-9 TVS10-04 Gina Gasket Vertical Deflection over Time

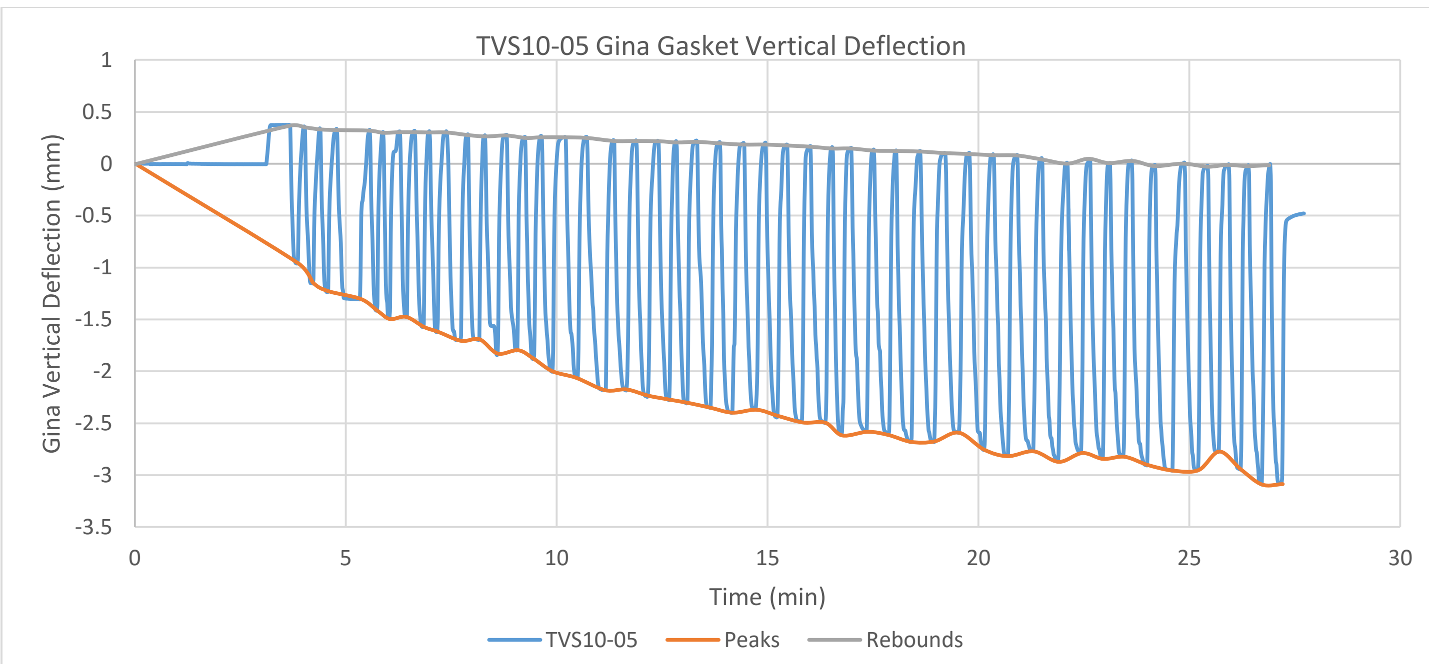

Appendix D-10 TVS10-05 Gina Gasket Vertical Deflection over Time

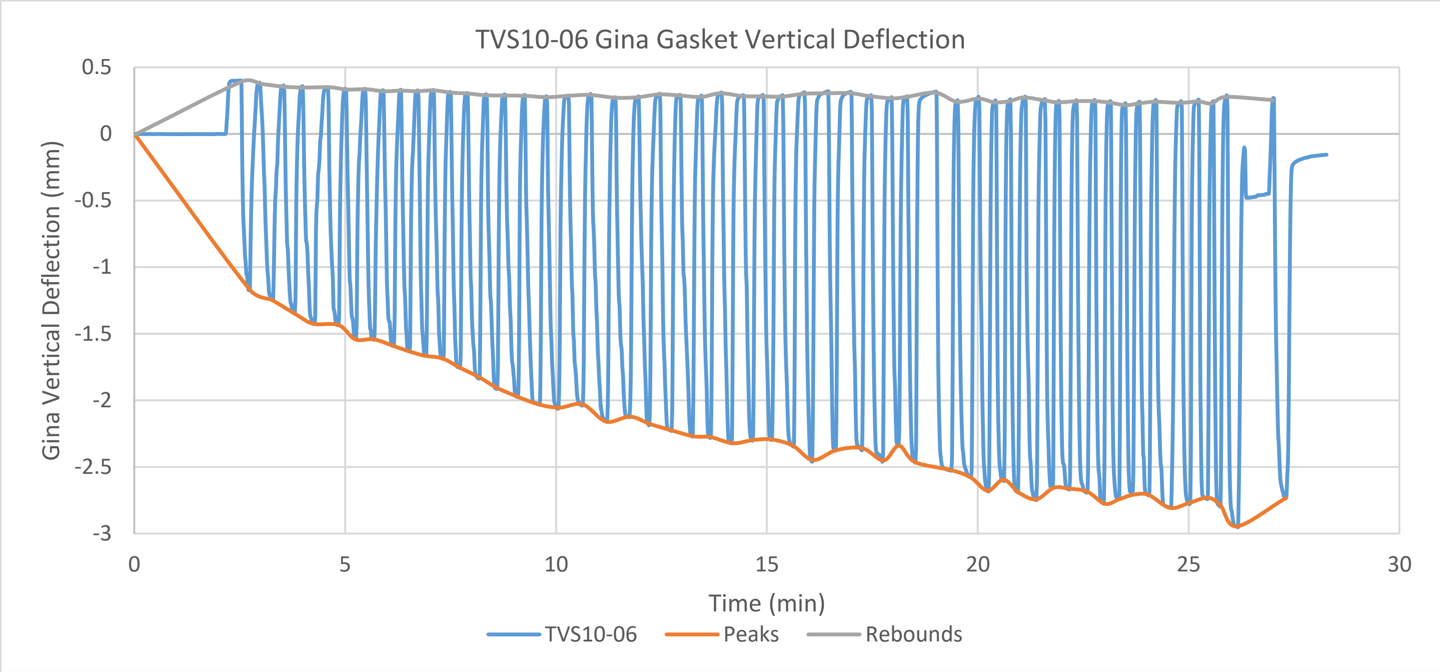

Appendix D-11 TVS10-06 Gina Gasket Vertical Deflection over Time

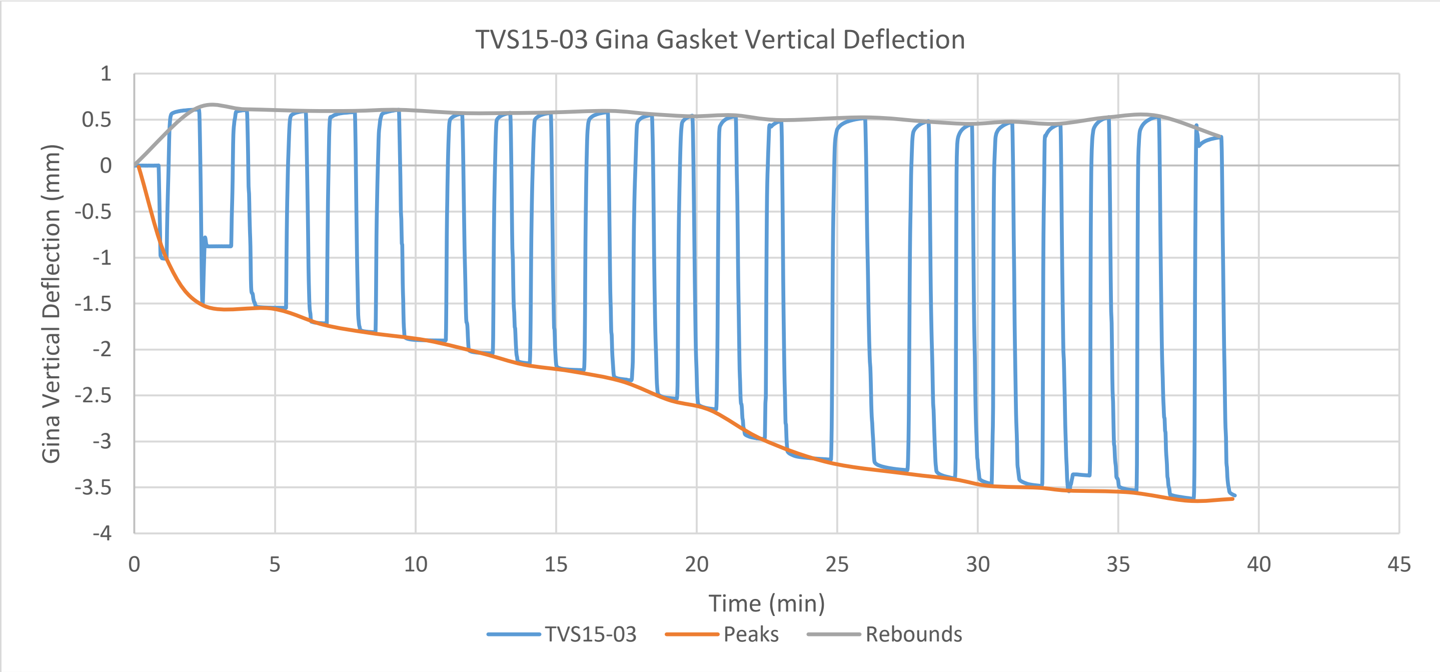

Appendix D-12 TVS15-03 Gina Gasket Vertical Deflection over Time

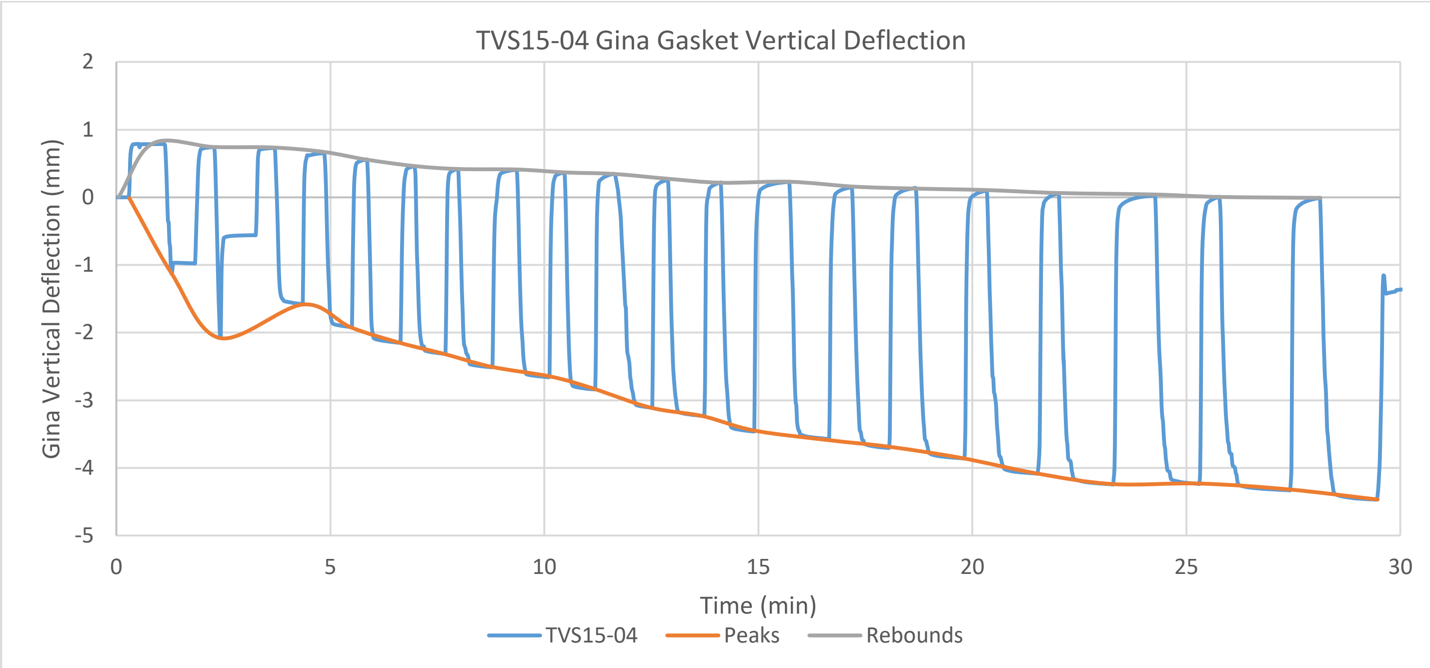

Appendix D-13 TVS15-04 Gina Gasket Vertical Deflection over Time

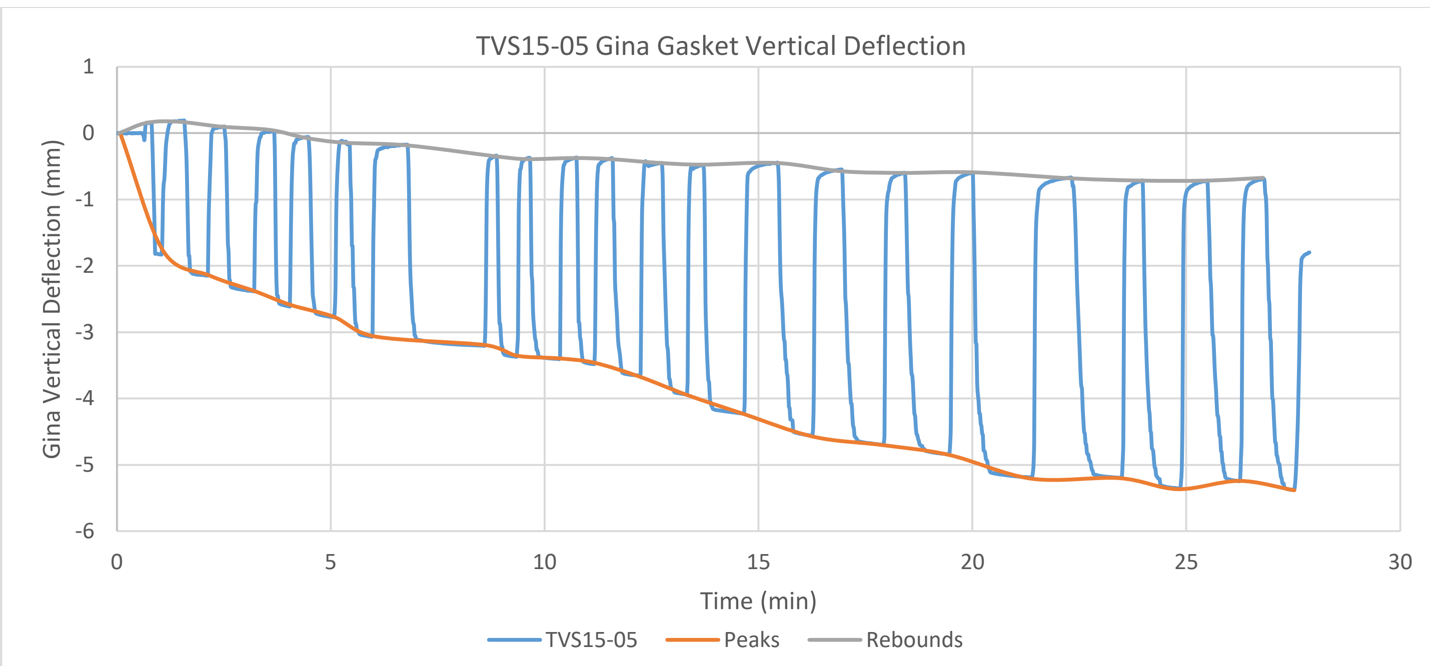

Appendix D-14 TVS15-05 Gina Gasket Vertical Deflection over Time

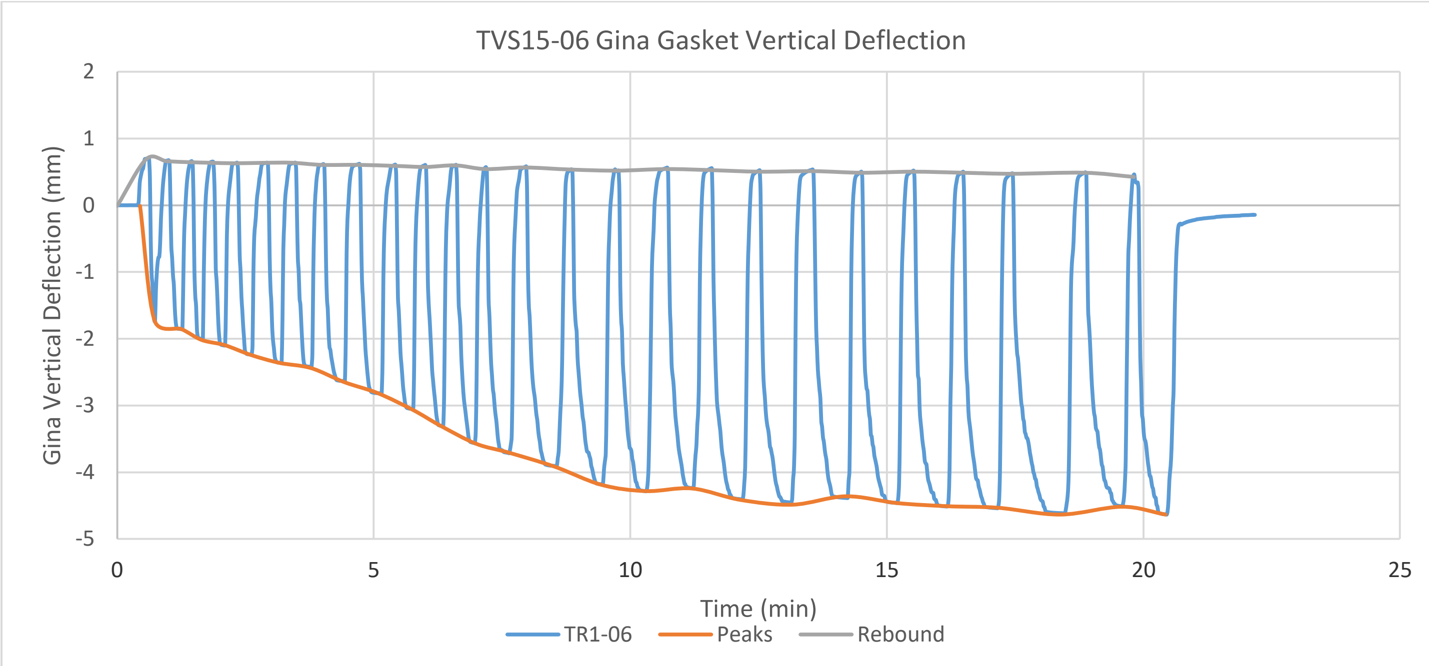

Appendix D-15 TVS15-06 Gina Gasket Vertical Deflection over Time

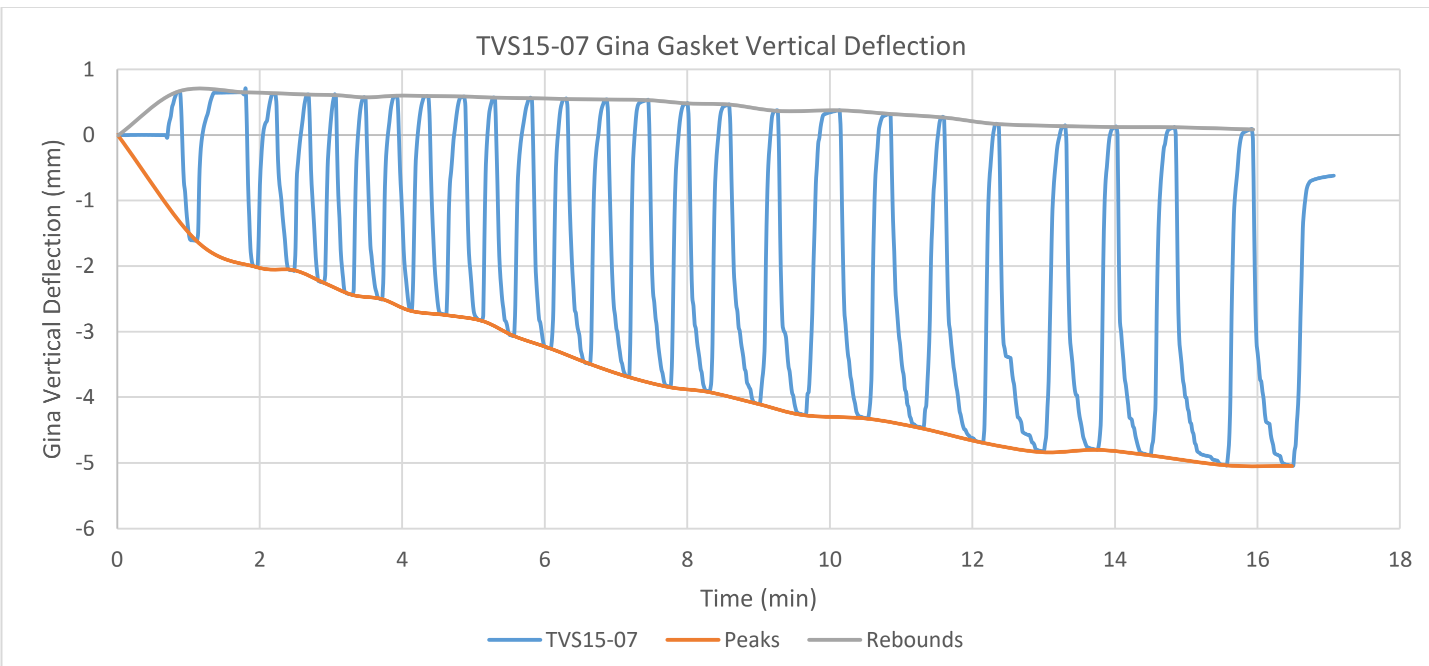

Appendix D-16 TVS15-07 Gina Gasket Vertical Deflection over Time

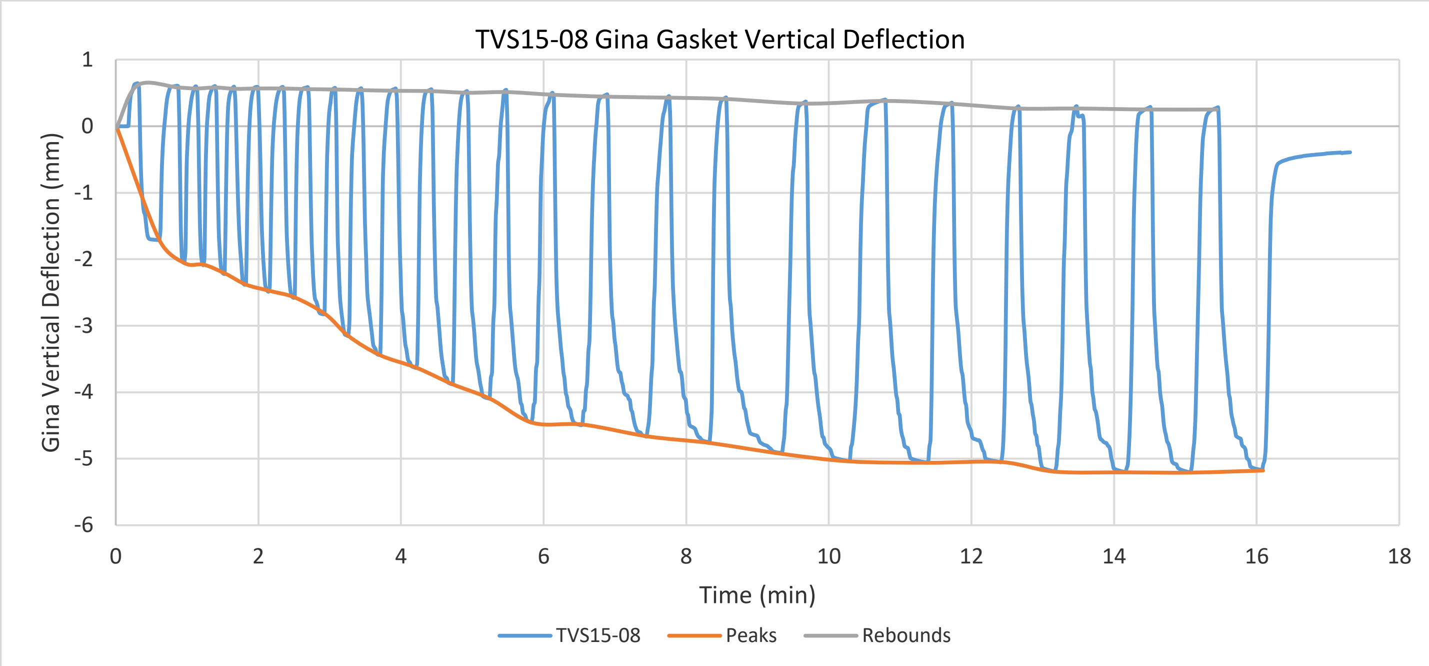

Appendix D-17 TVS15-08 Gina Gasket Vertical Deflection over Time

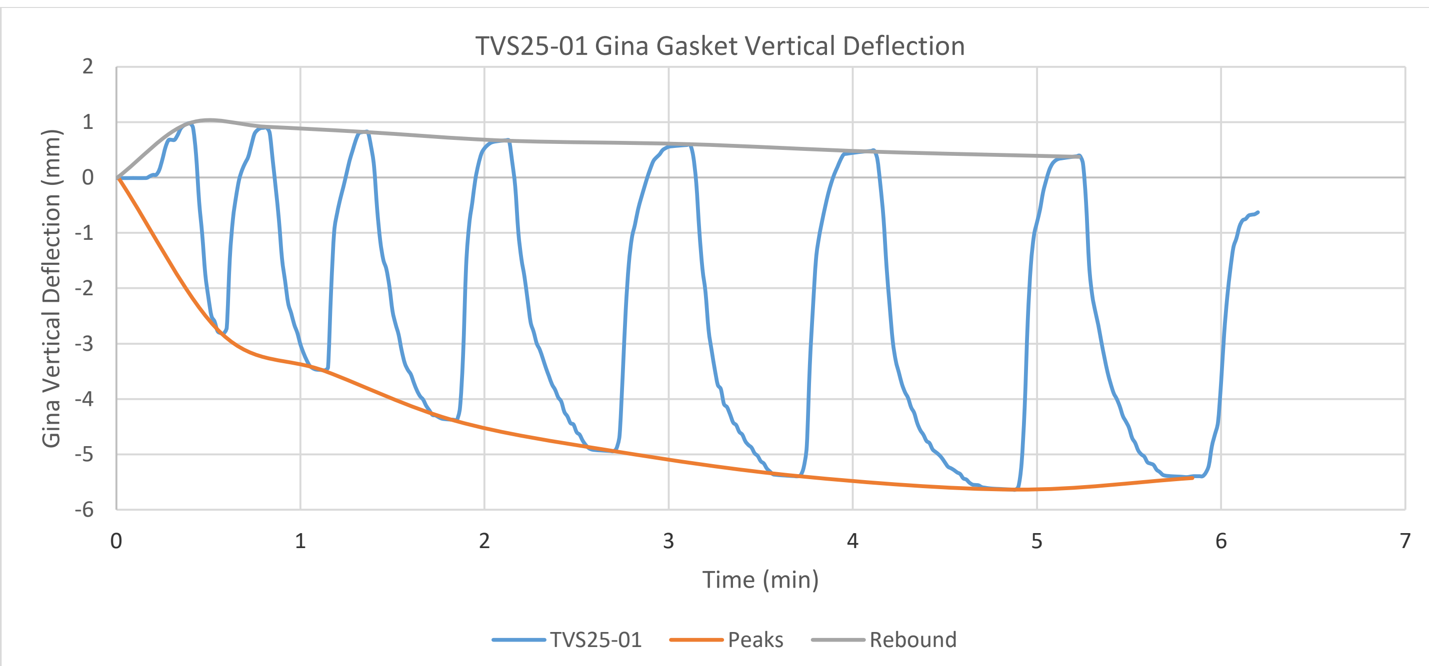

Appendix D-18 TVS25-08 Gina Gasket Vertical Deflection over Time

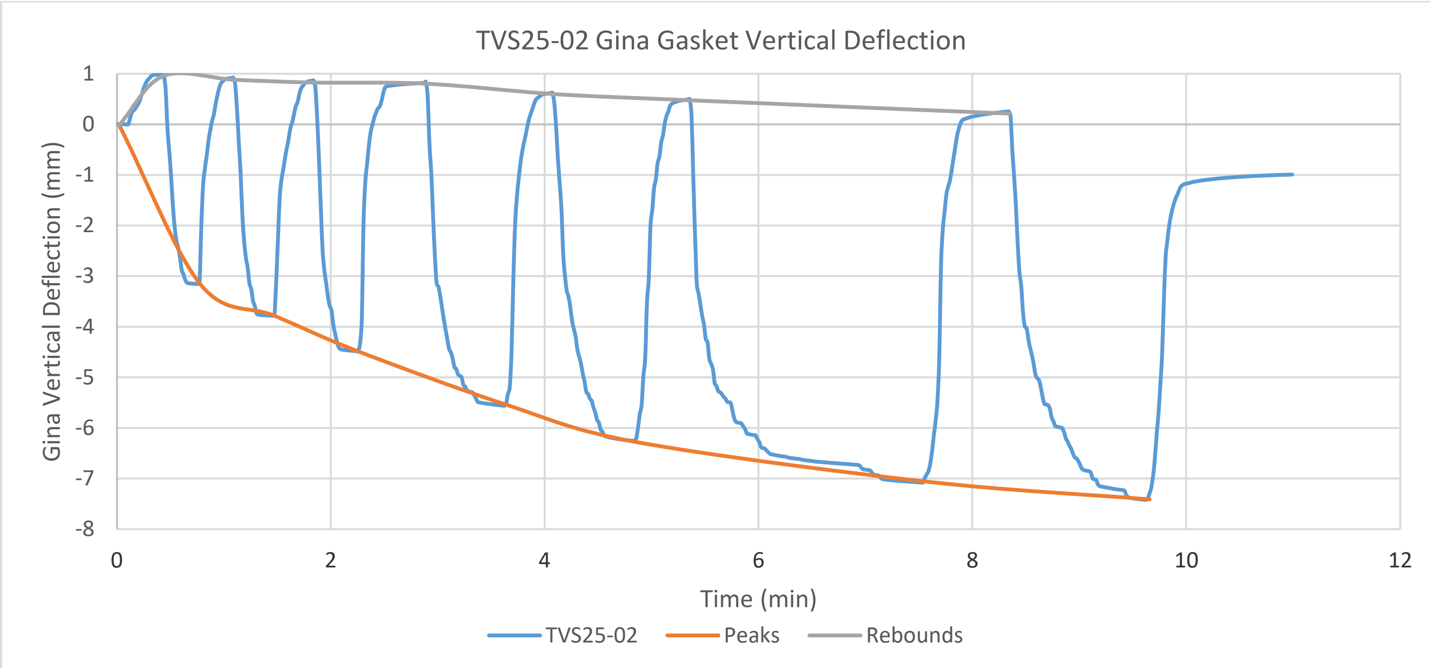

Appendix D-19 TVS-02 Gina Gasket Vertical Deflection over Time

D.2. Stress Measurements

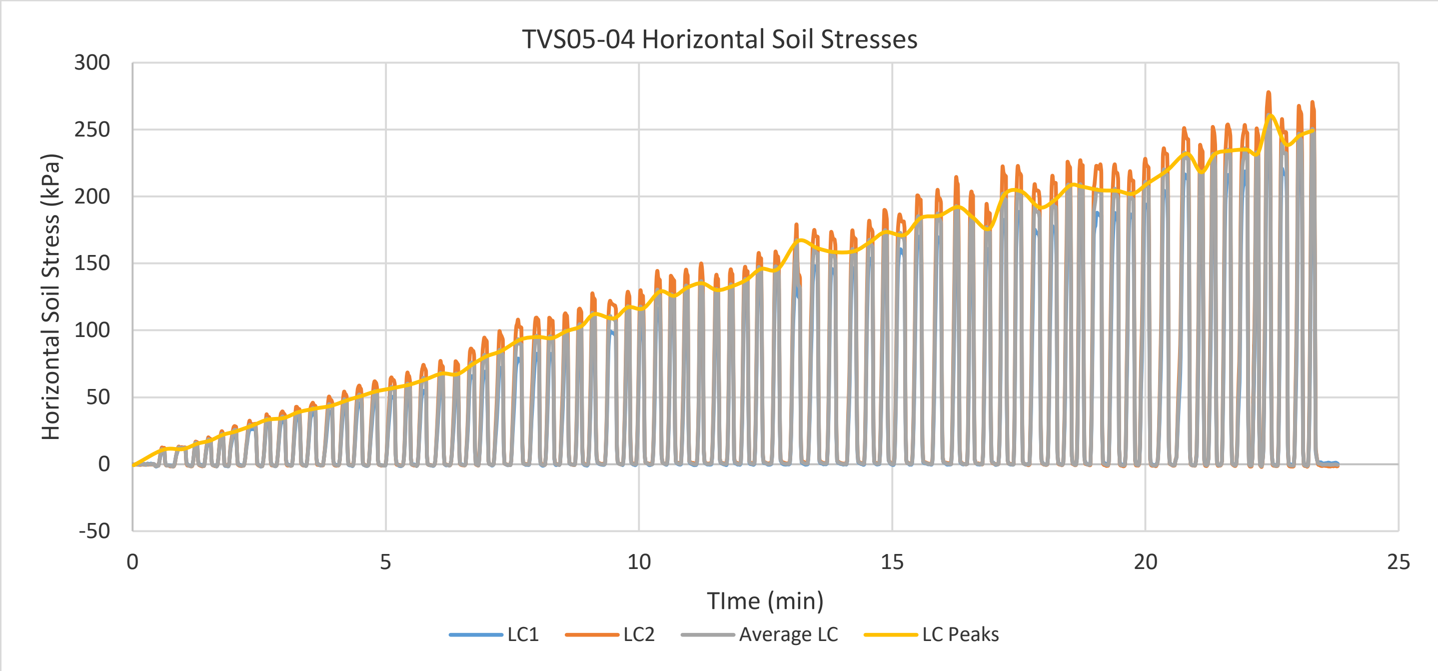

Appendix D-20 TV05-04 Horizontal Soil Stresses over Time

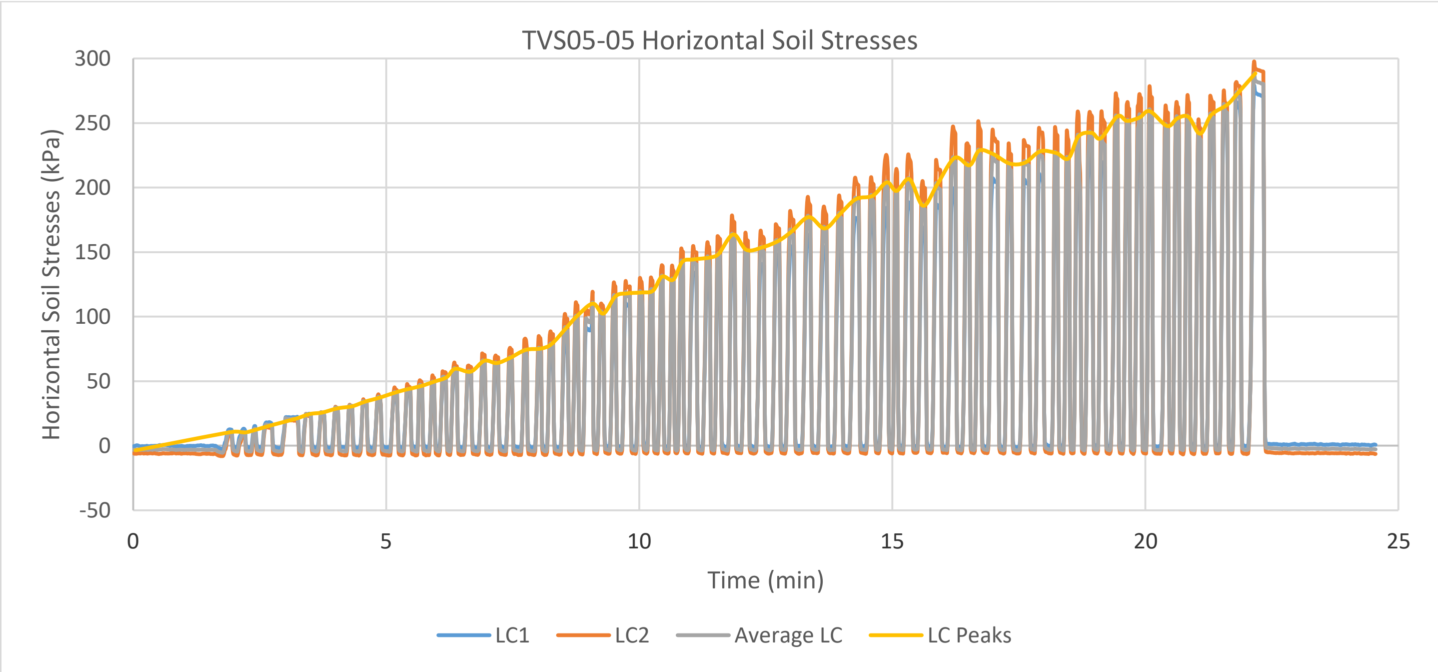

Appendix D-21 TV05-05 Horizontal Soil Stresses over Time

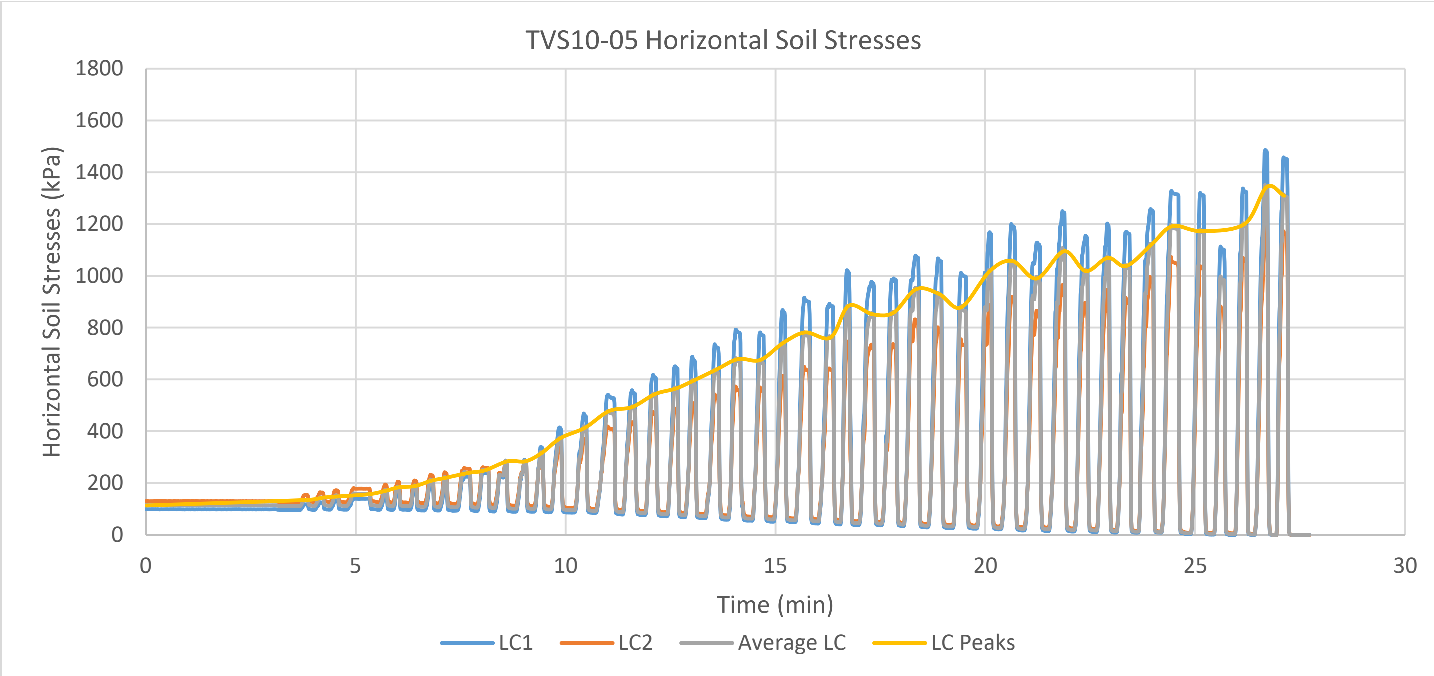

Appendix D-22 TVS10-05 Horizontal Soil Stresses over Time

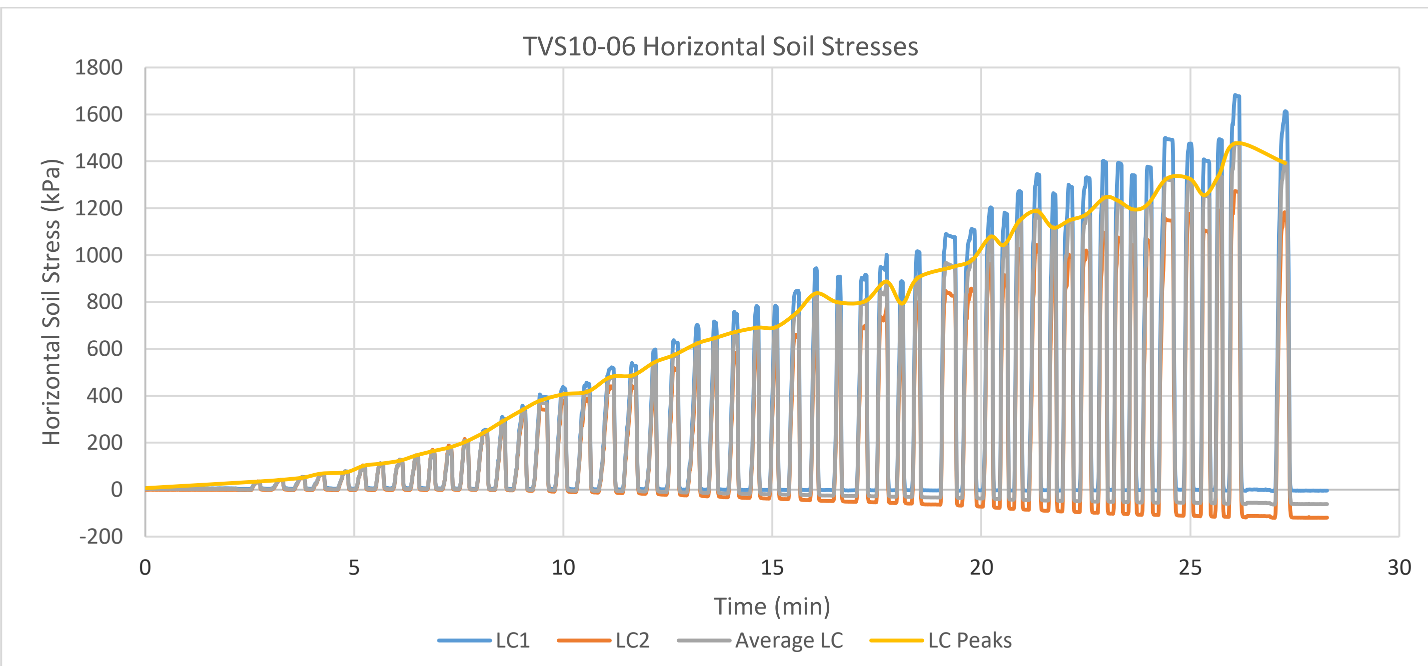

Appendix D-23 TVS10-06 Horizontal Soil Stresses over Time

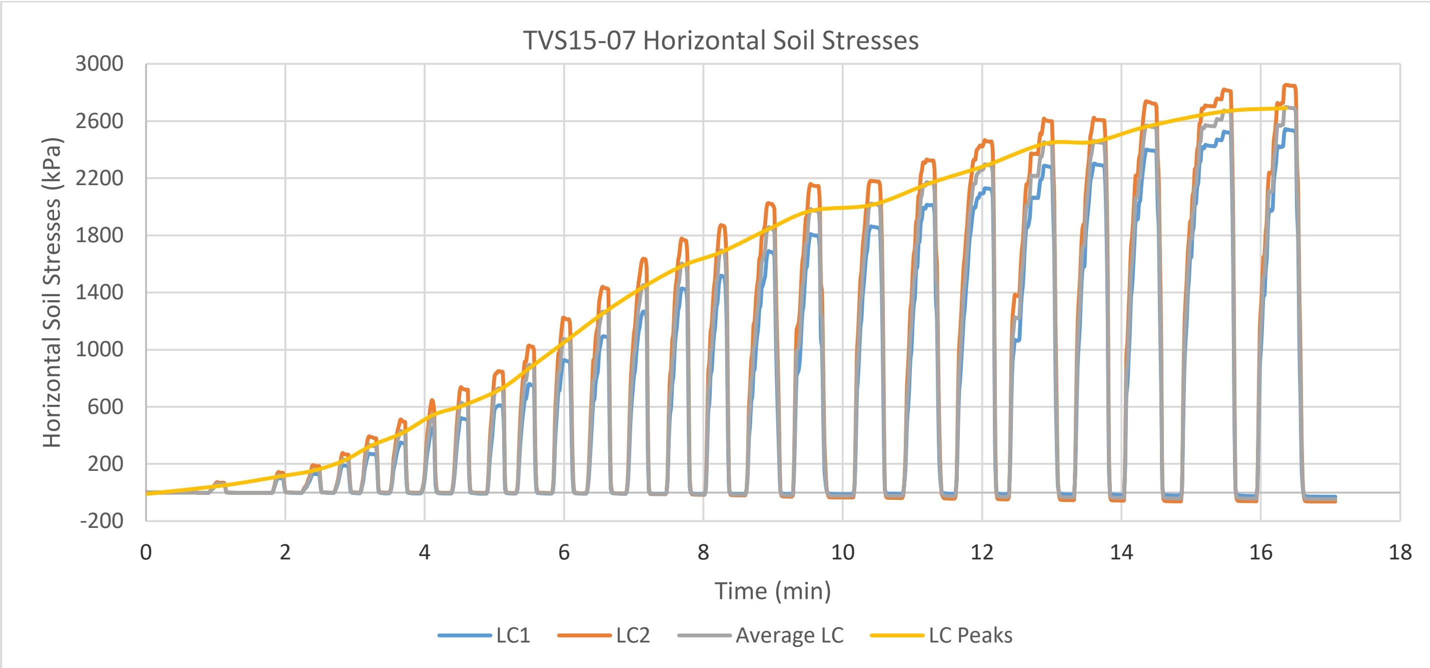

Appendix D-24 TVS15-07 Horizontal Soil Stresses over Time

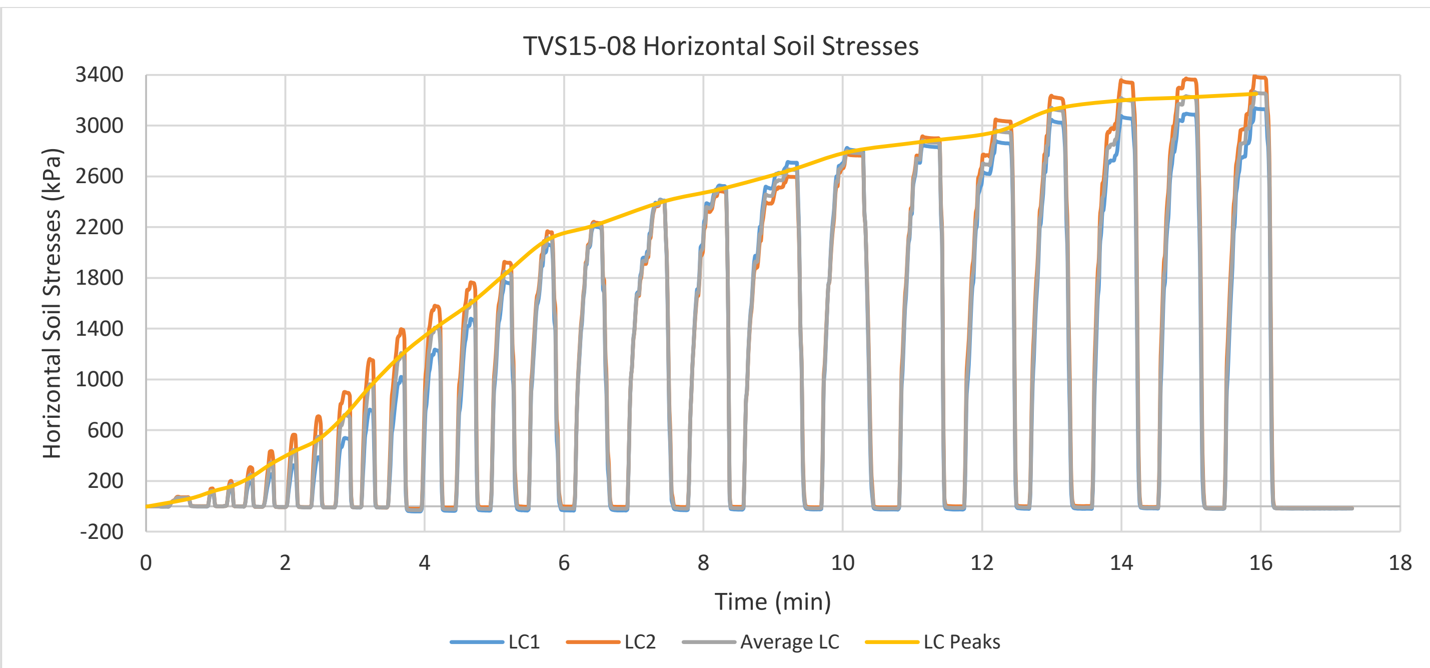

Appendix D-25 TVS15-08 Horizontal Soil Stresses over Time

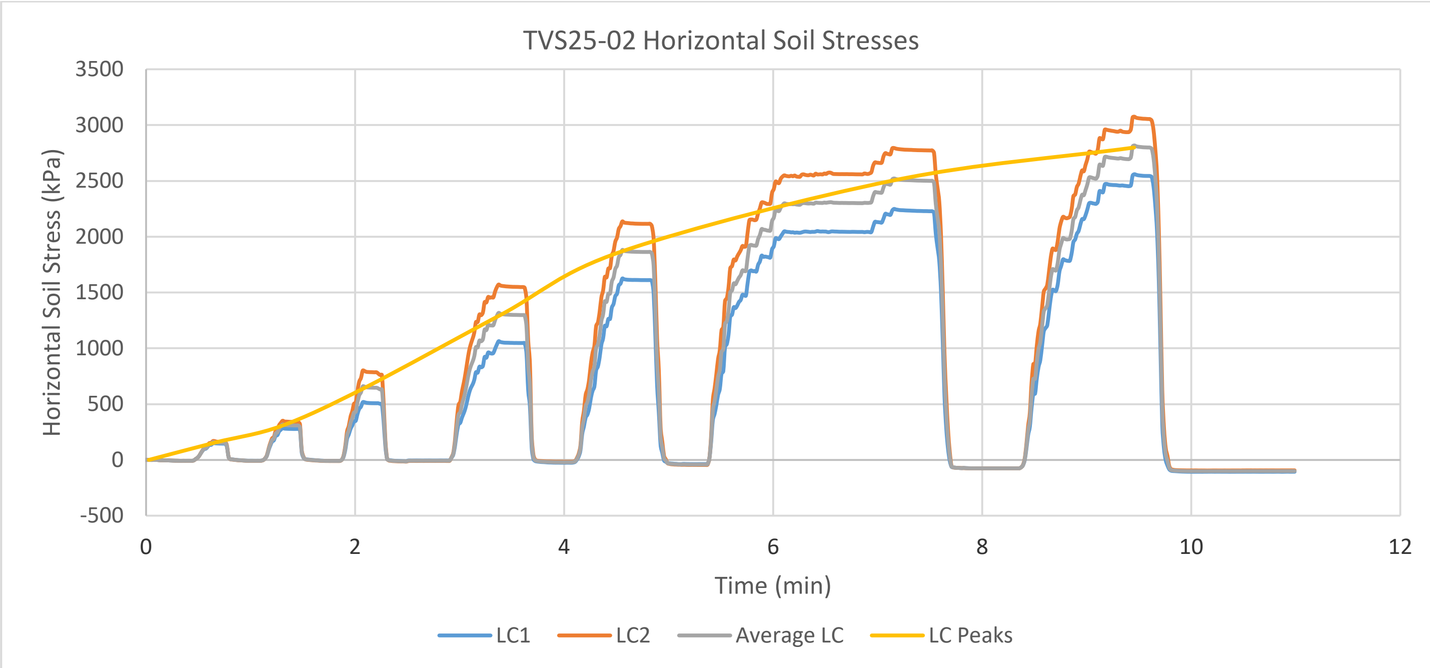

Appendix D-26 TVS25-02 Horizontal Soil Stresses over Time

D.3. Control Test

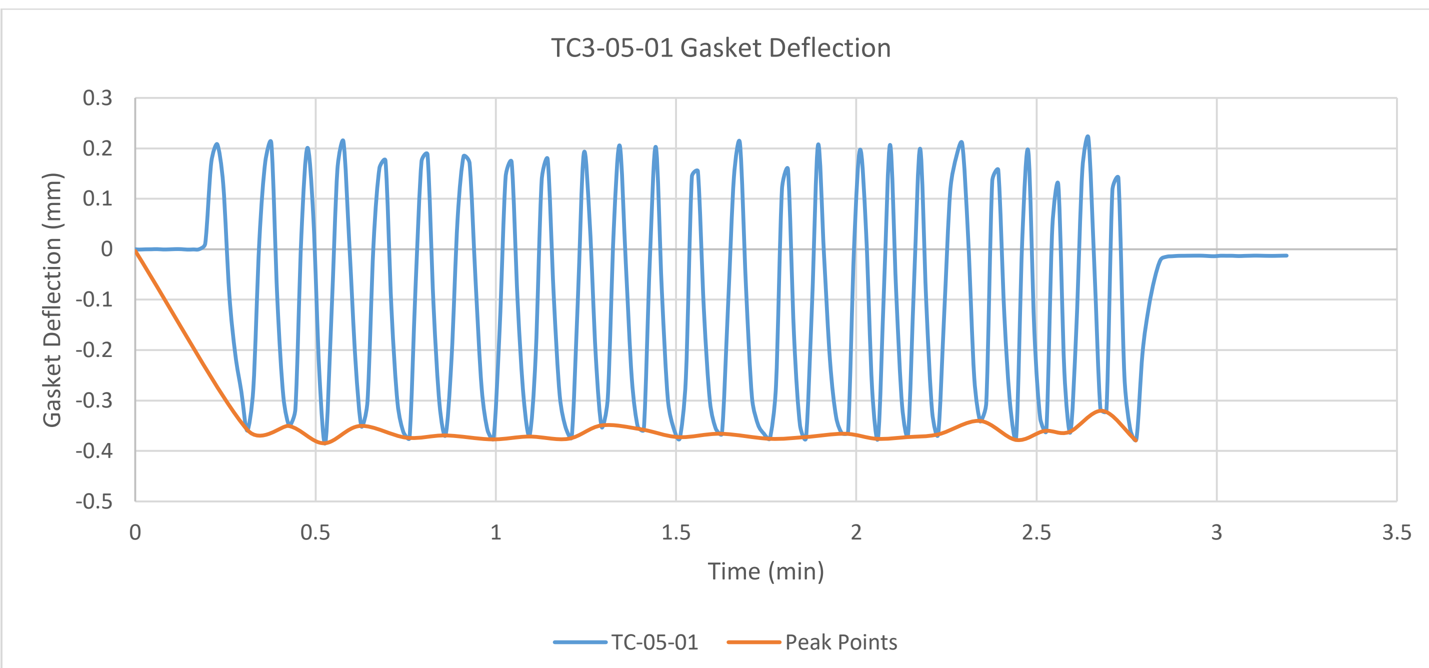

Appendix D-27 TC3-05-01 Test Results

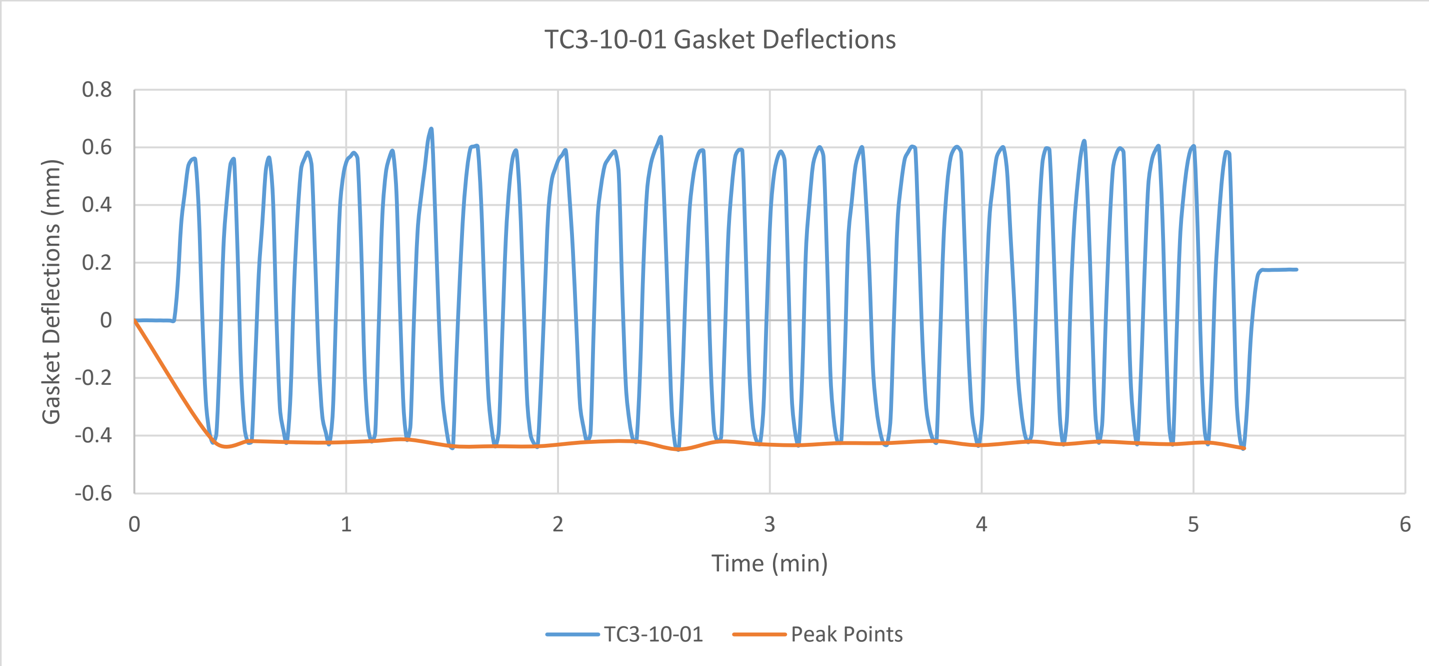

Appendix D-28 TC3-10-01 Test Results

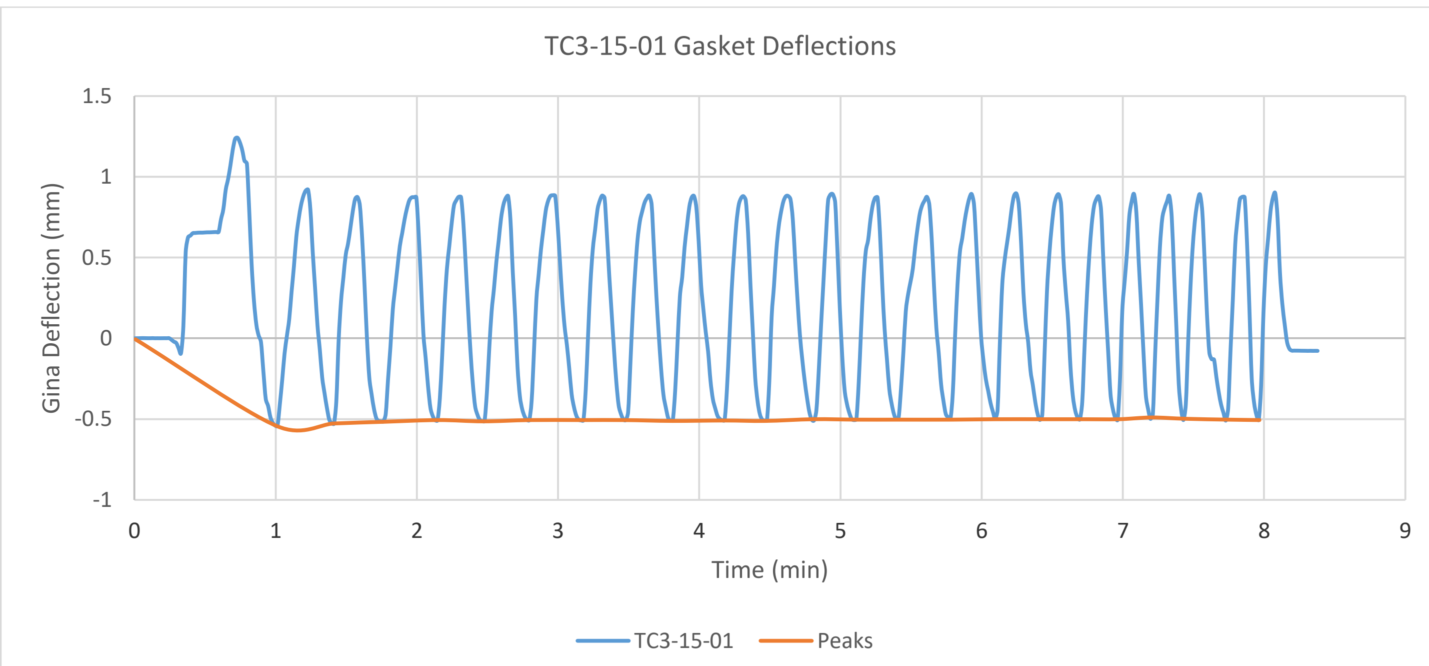

Appendix D-29 TC3-15-01 Test Results

APPENDIX - E : Analyzed Results

E.1.Soil Stress vs Gina Deflection

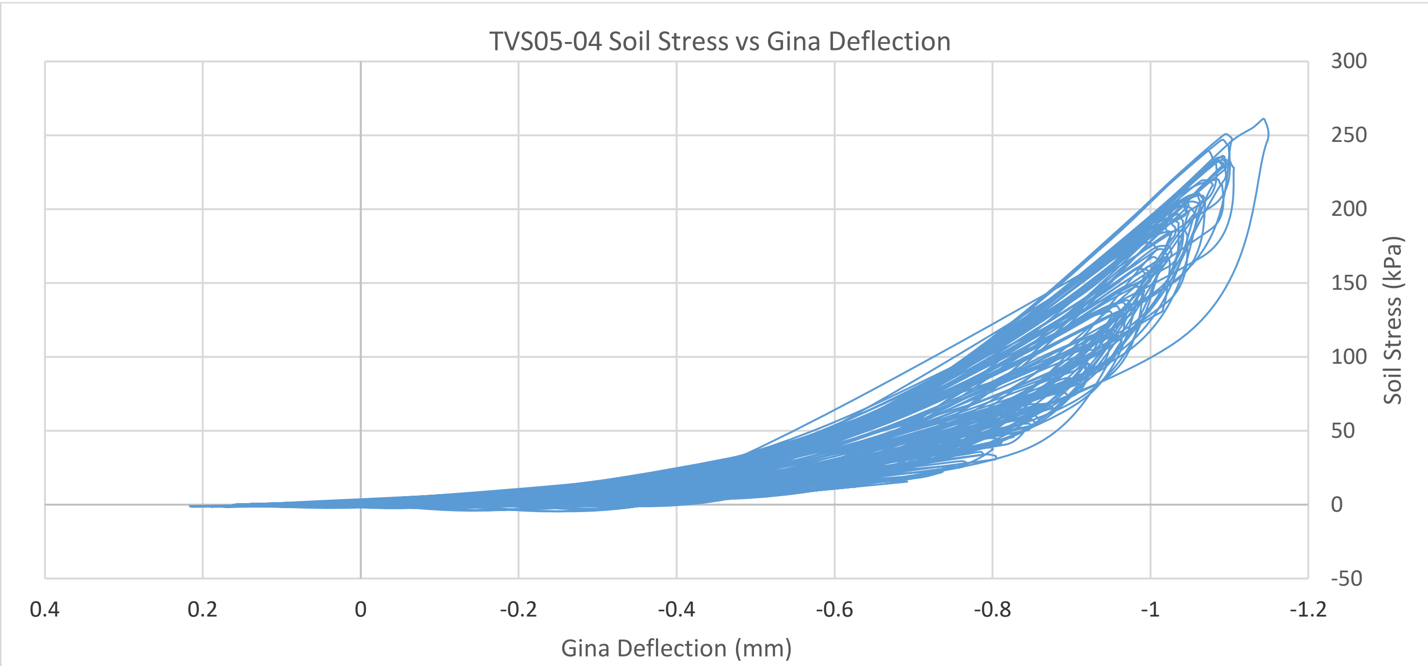

Appendix E-1 TVS05-04 Soil Stress vs Gina Deflection

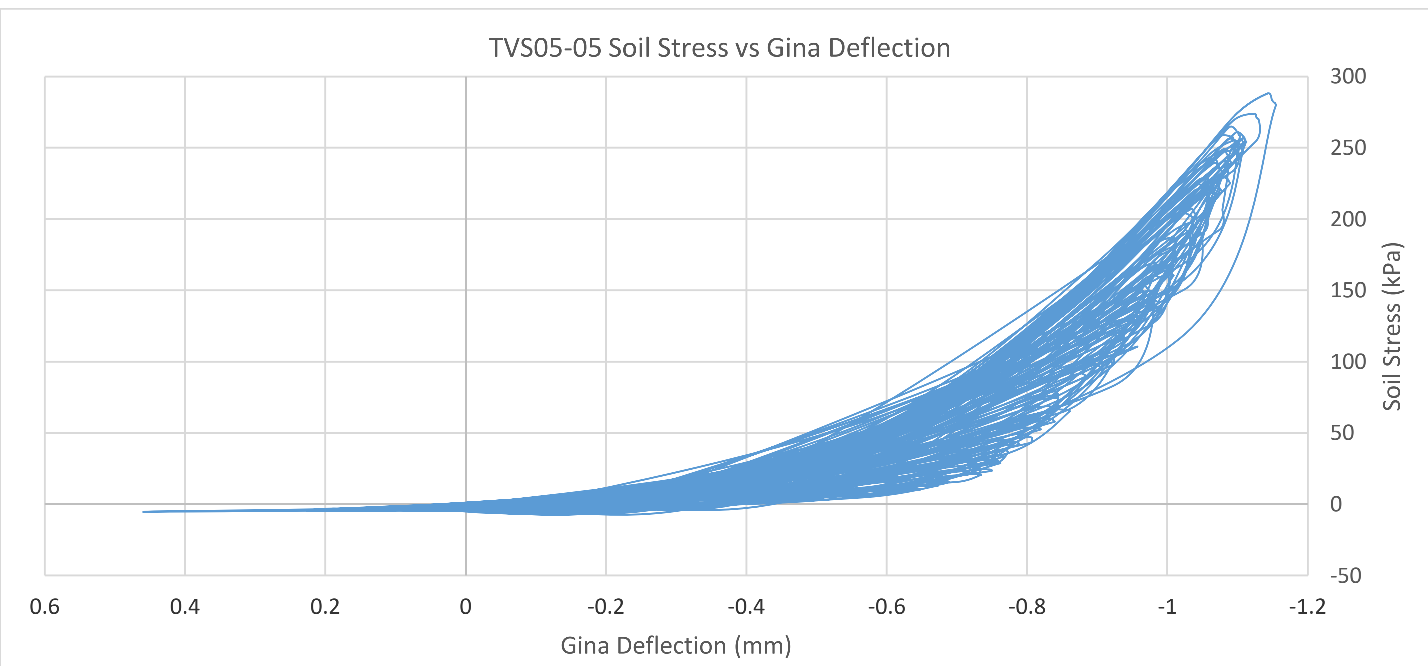

Appendix E-2 TVS05-05 Soil Stress vs Gina Deflection

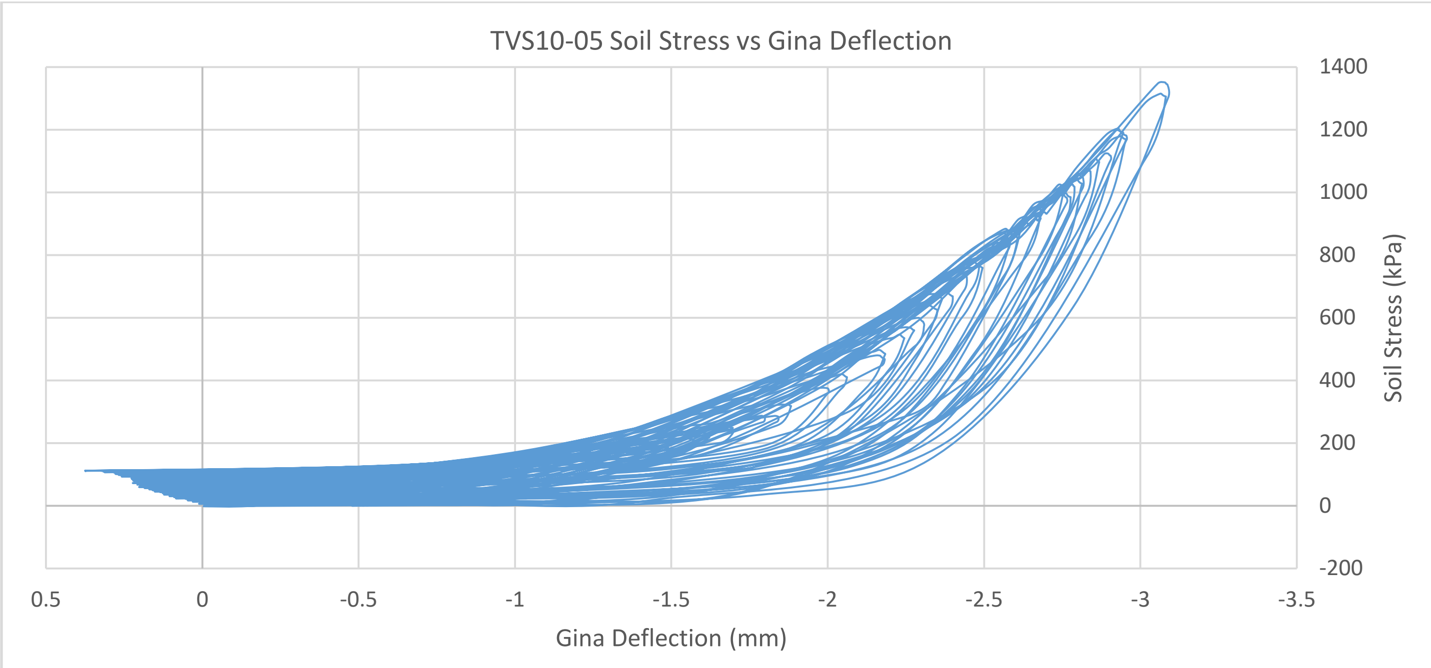

Appendix E-3 TVS10-05 Soil Stress vs Gina Deflection

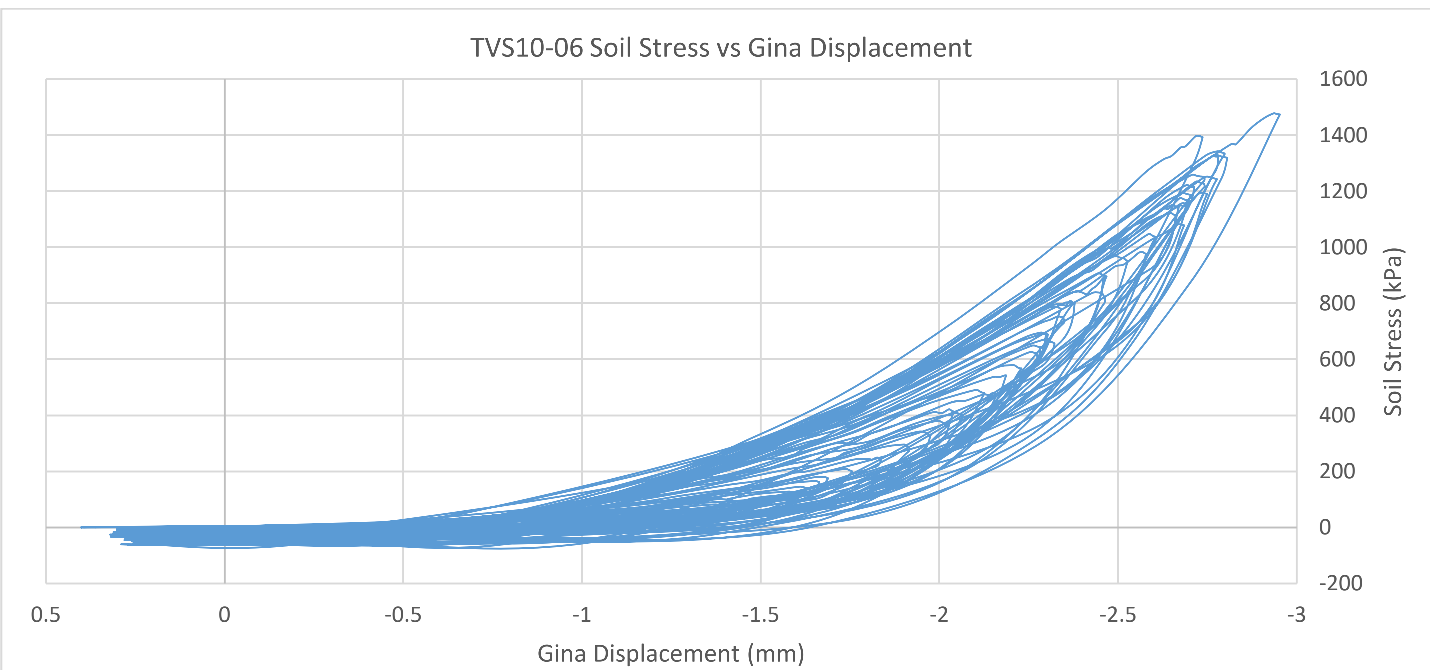

Appendix E-4 TVS10-06 Soil Stress vs Gina Deflection

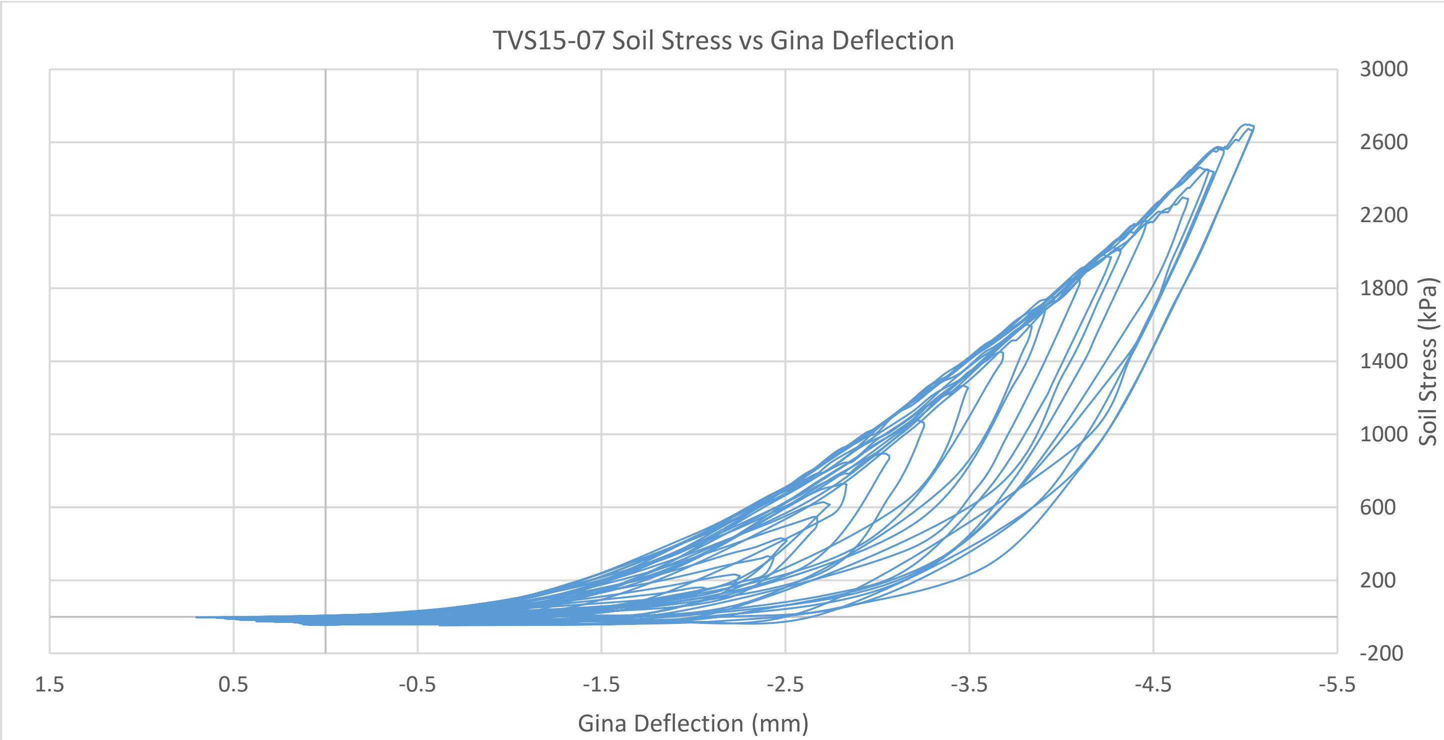

Appendix E-5 TVS15-07 Soil Stress vs Gina Deflection

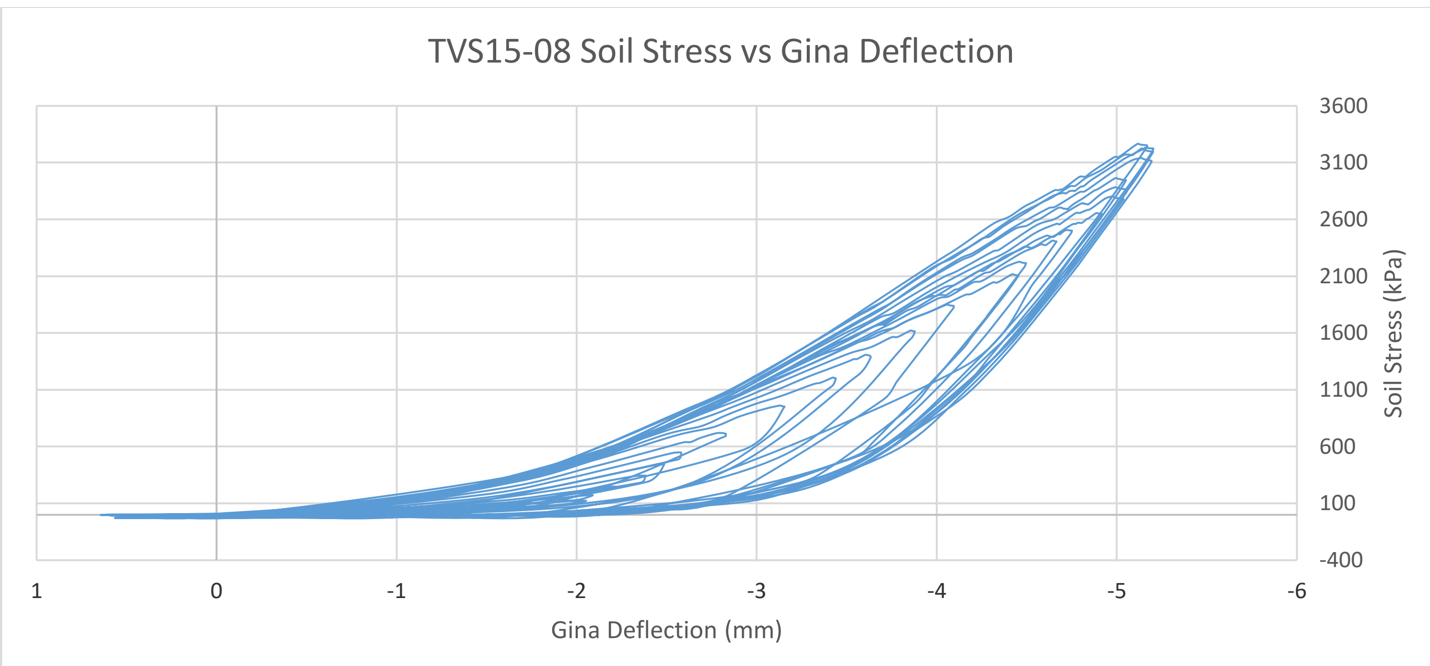

Appendix E-6 TVS15-08 Soil Stress vs Gina Deflection

E.2. Stress Path

The stress path displayed in this section were analyzed before the finite element analysis was finished. Hence this analysis applies the original assumption discussed in section 4.2.2 instead of the adjusted assumptions discussed in section 6.2.2.

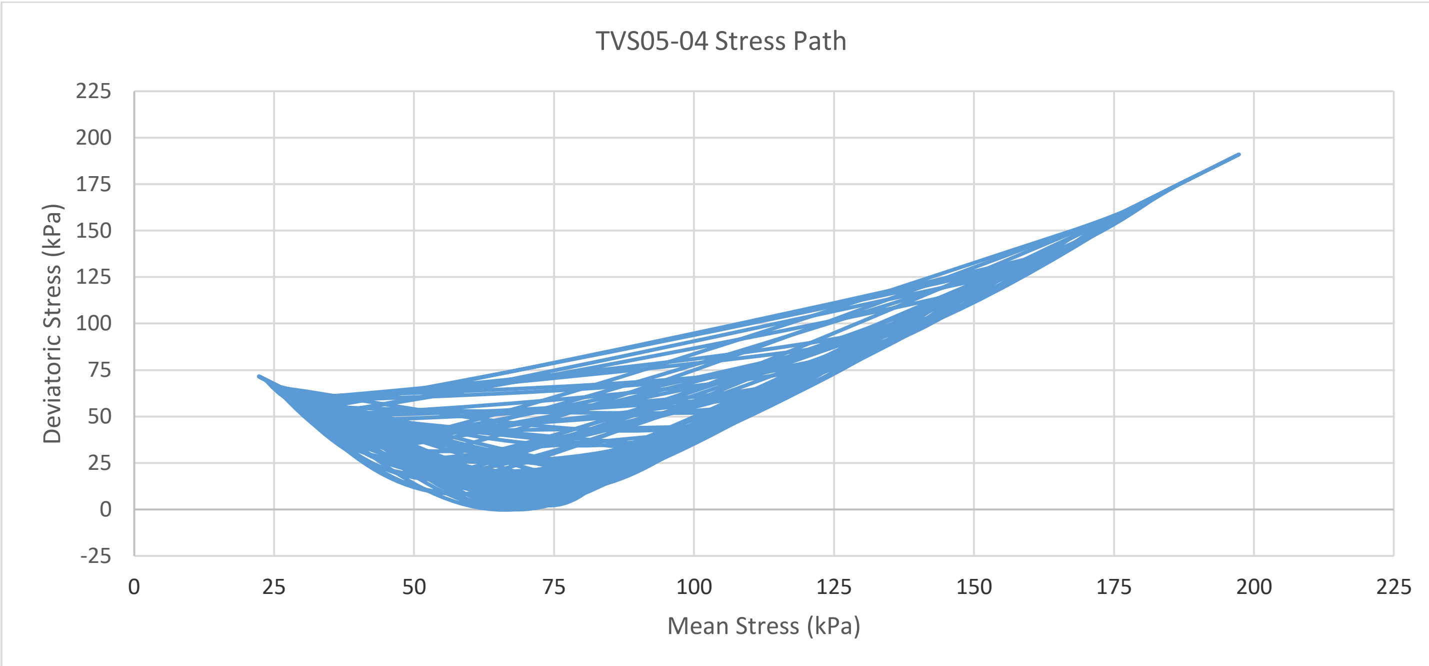

Appendix E-7 TVS05-04 Stress Path

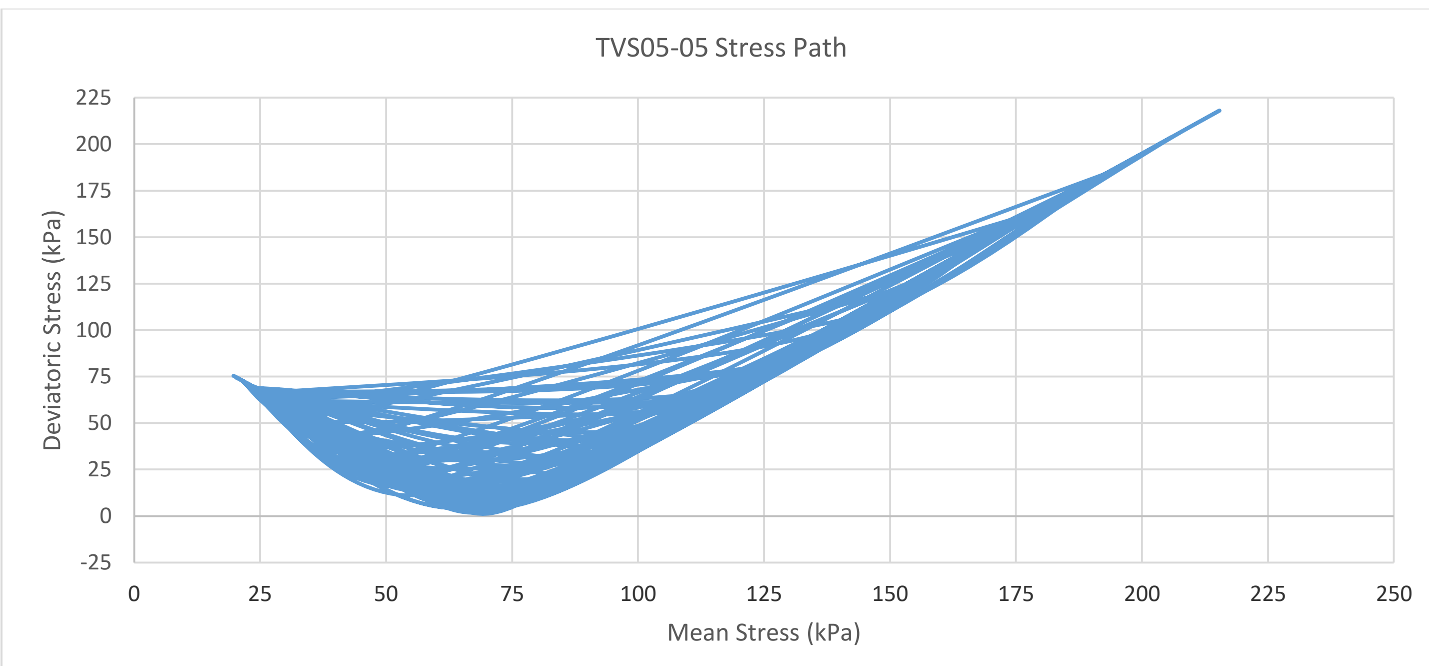

Appendix E-8 TVS05-05 Stress Path

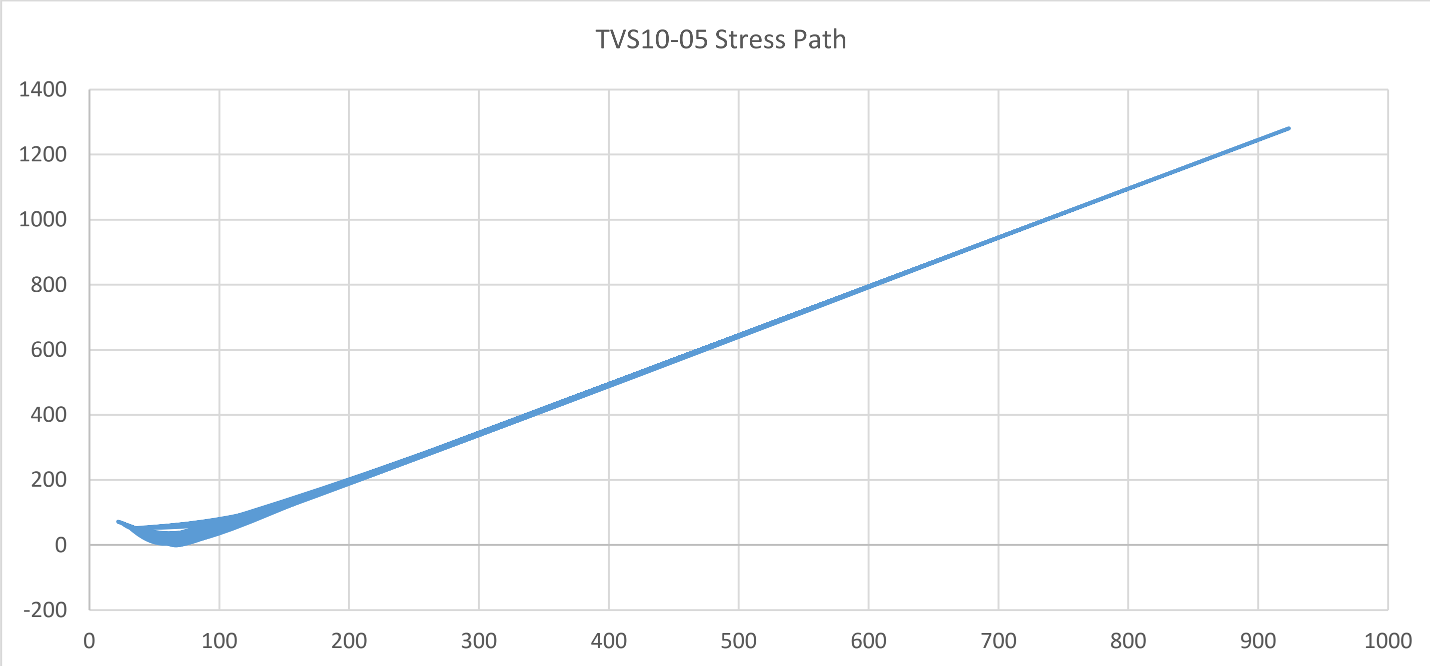

Appendix E-9 TVS10-05 Stress Path

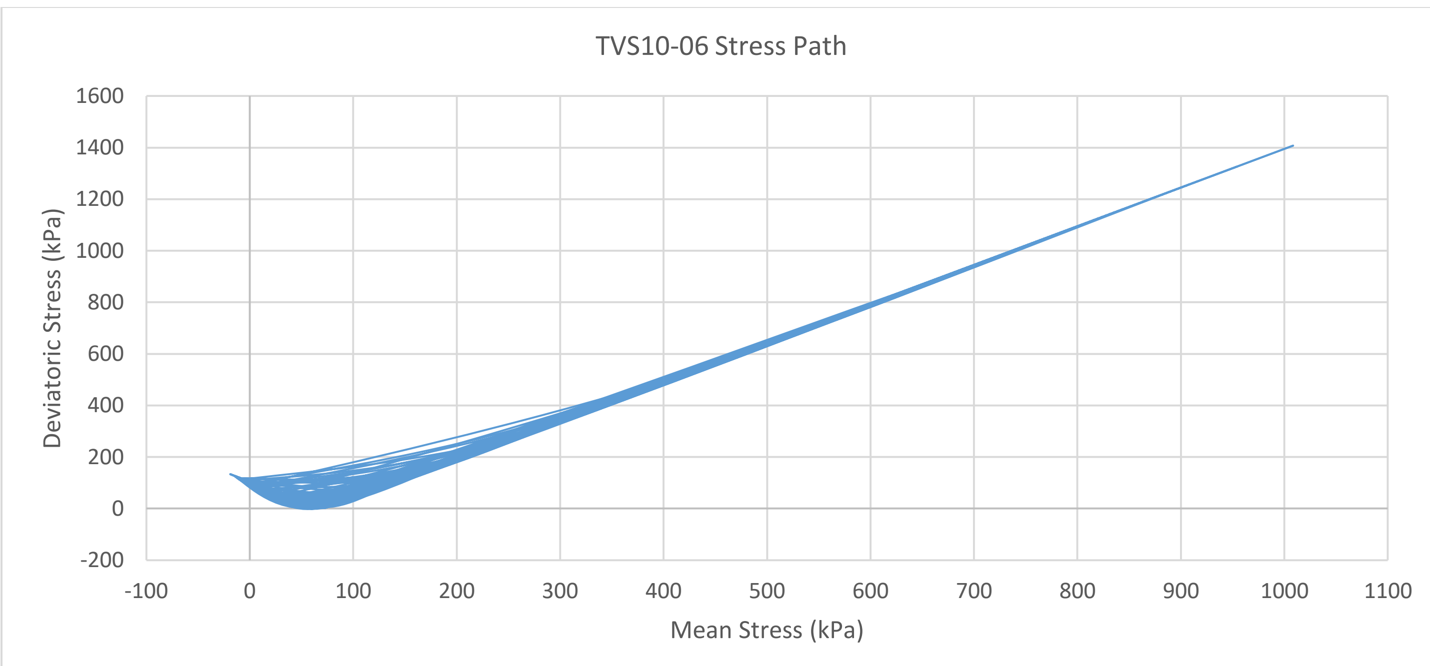

Appendix E-10 TVS10-06 Stress Path

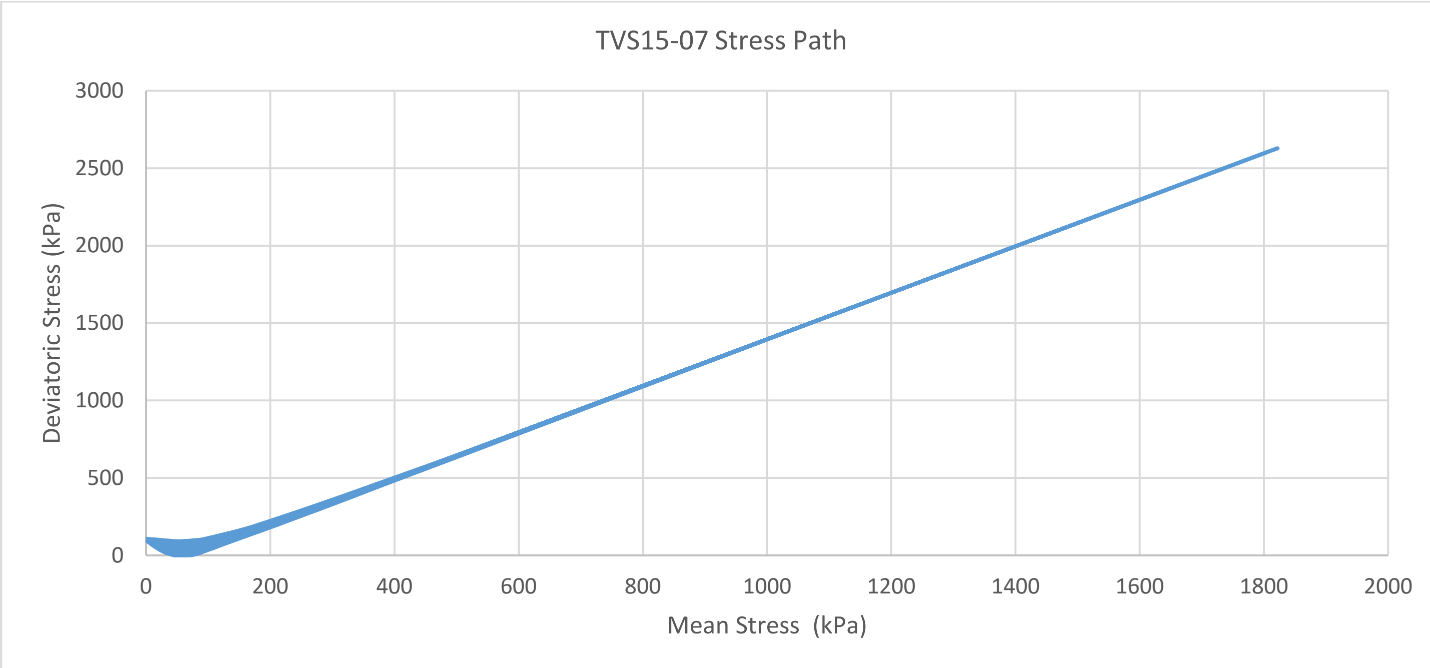

Appendix E-11 TVS15-07 Stress Path

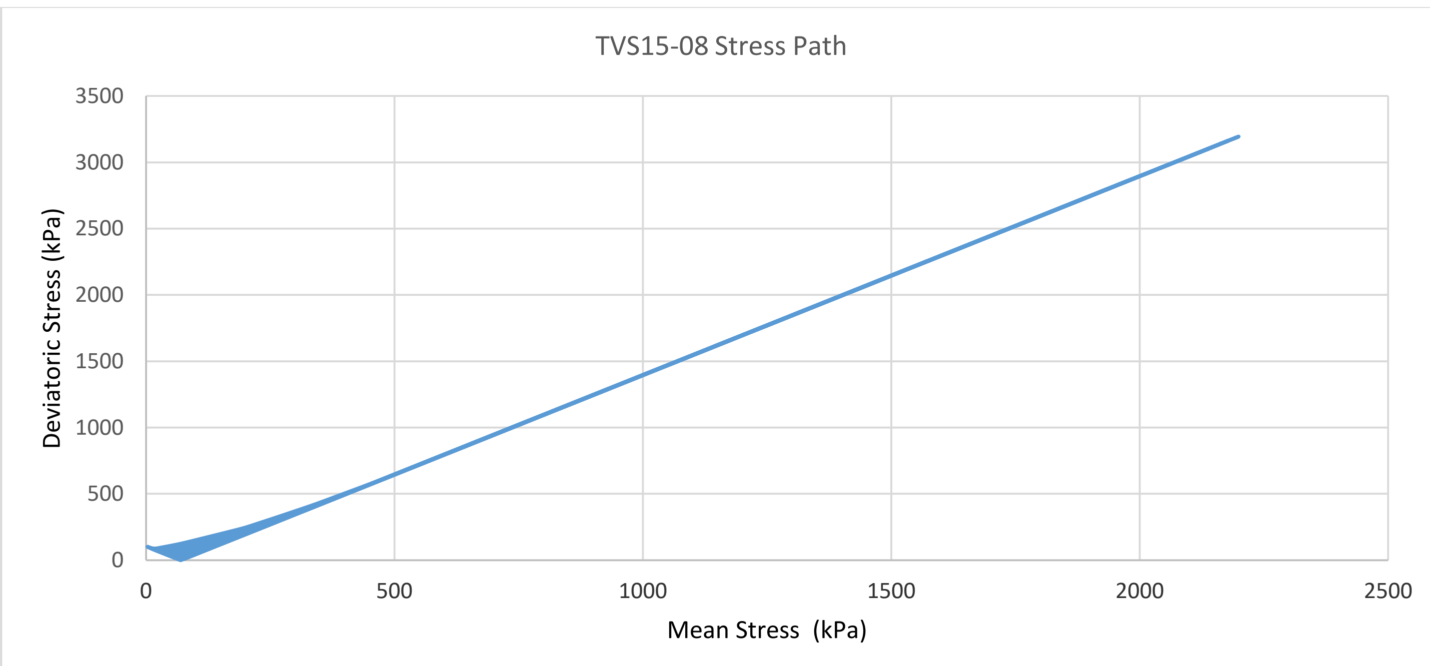

Appendix E-12 TVS15-08 Stress Path

E.3. Peak Points

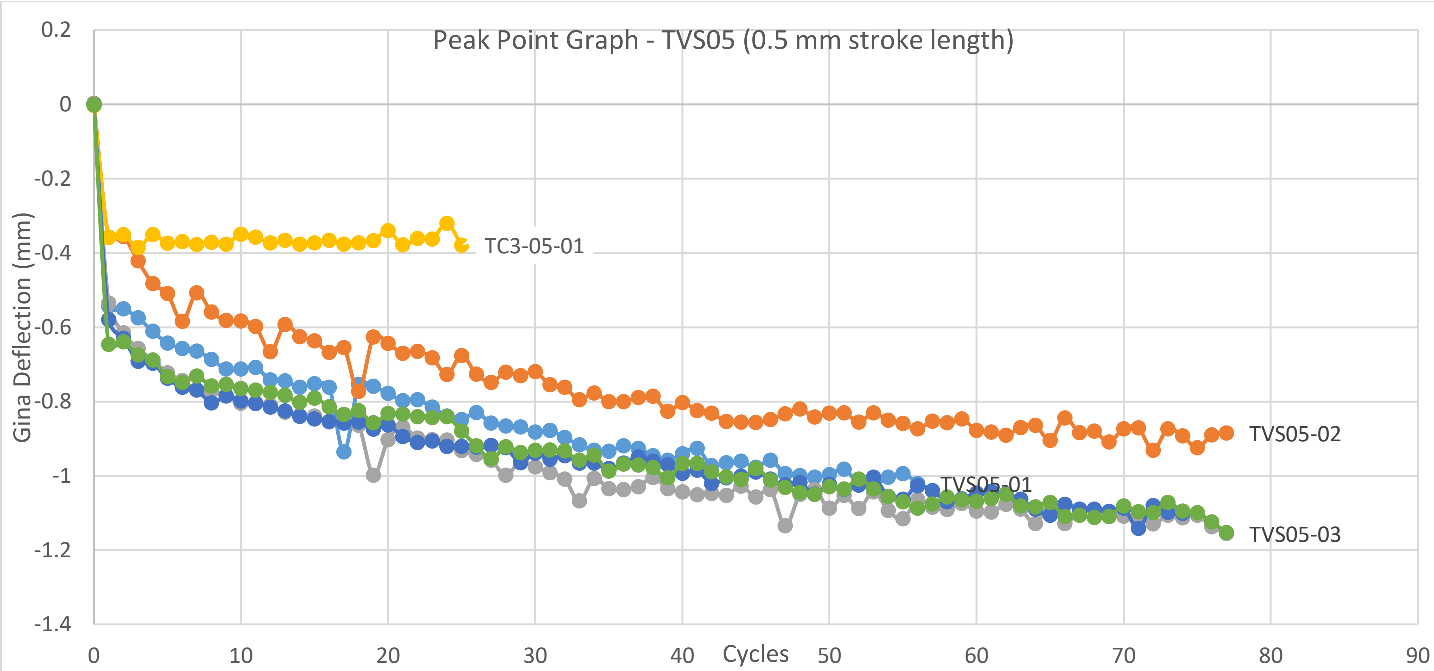

Appendix E-13 TVS05 Peak Points Graph

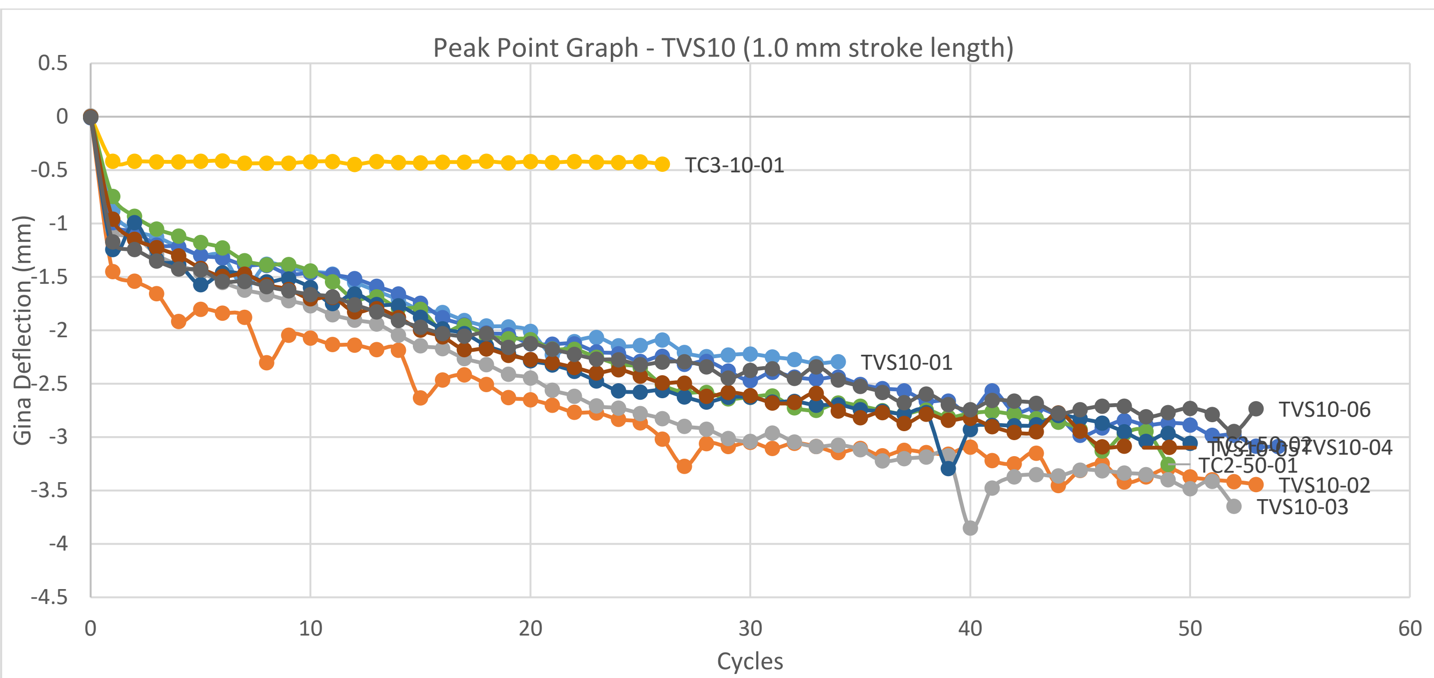

Appendix E-14TVS10 Peak Points Graph

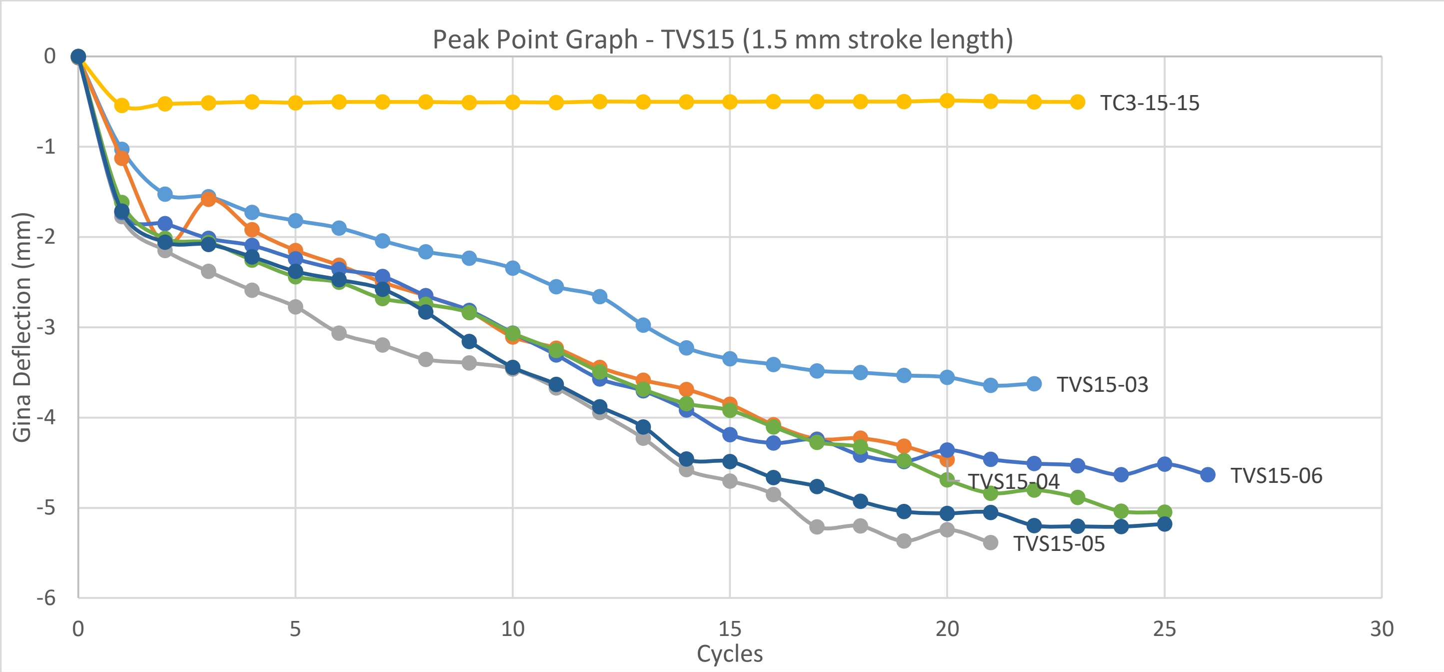

Appendix E-15 TVS15 Peak Points Graph

E.4. Rebound Points

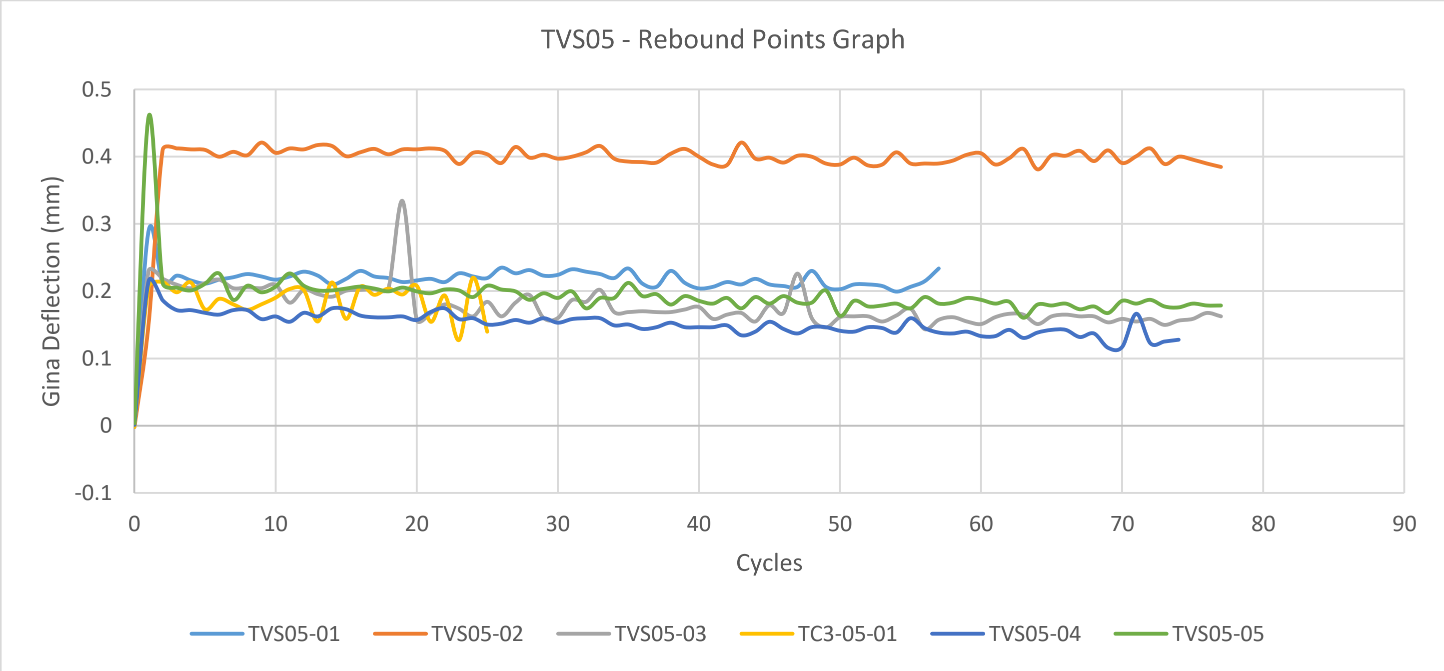

Appendix E-16 TVS05 Rebound Points Graph

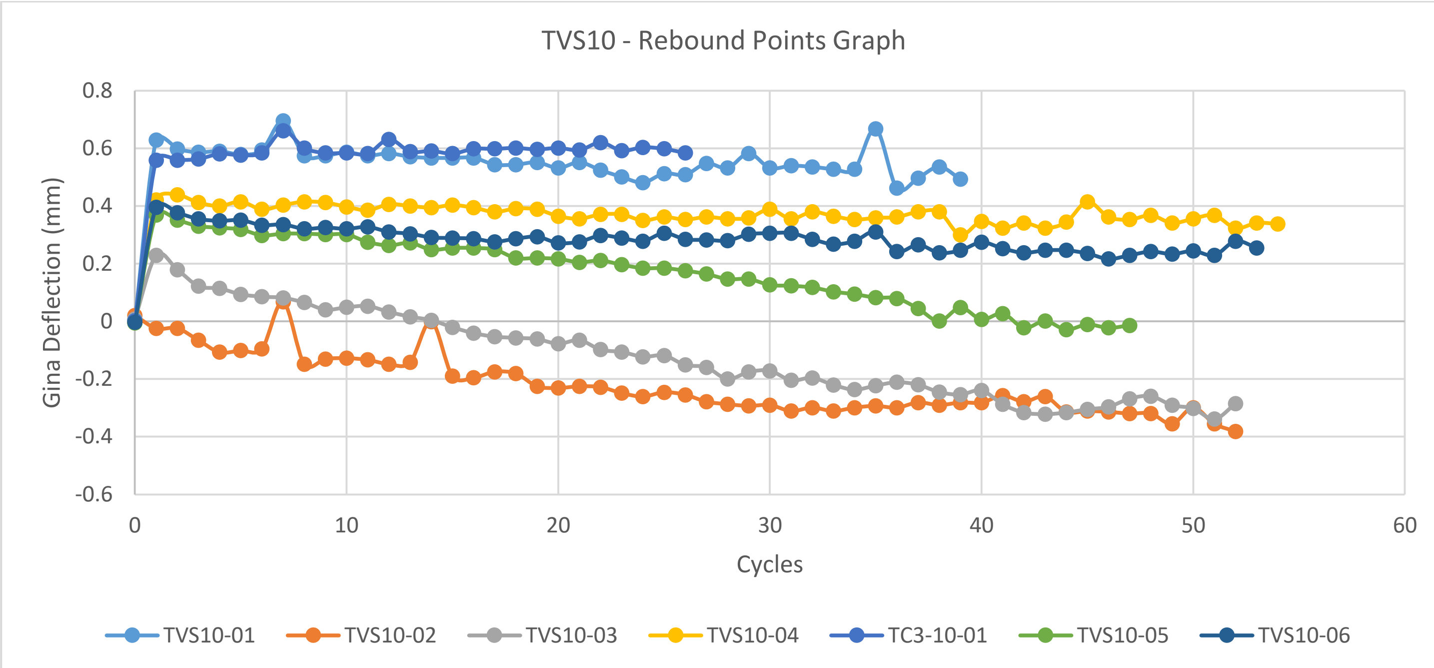

Appendix E-17 TVS10 Rebound Points Graph

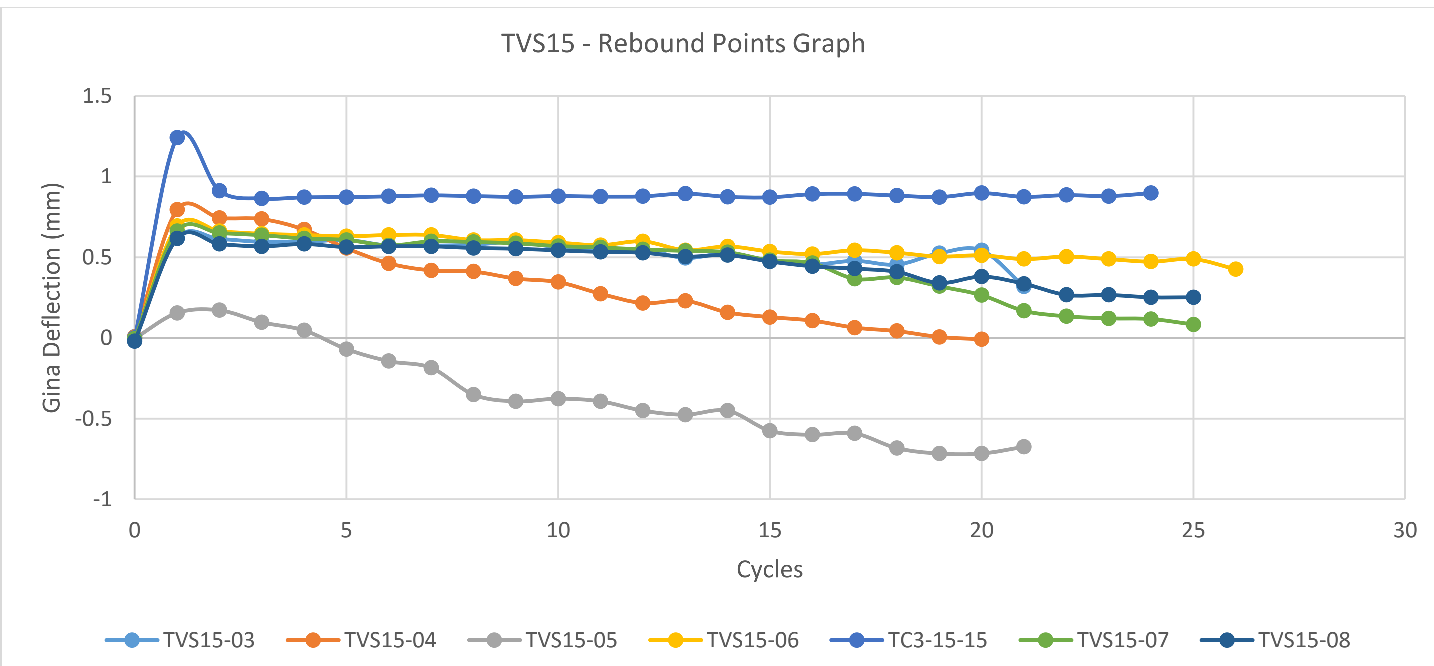

Appendix E-18 TVS15 Rebound Points Graph

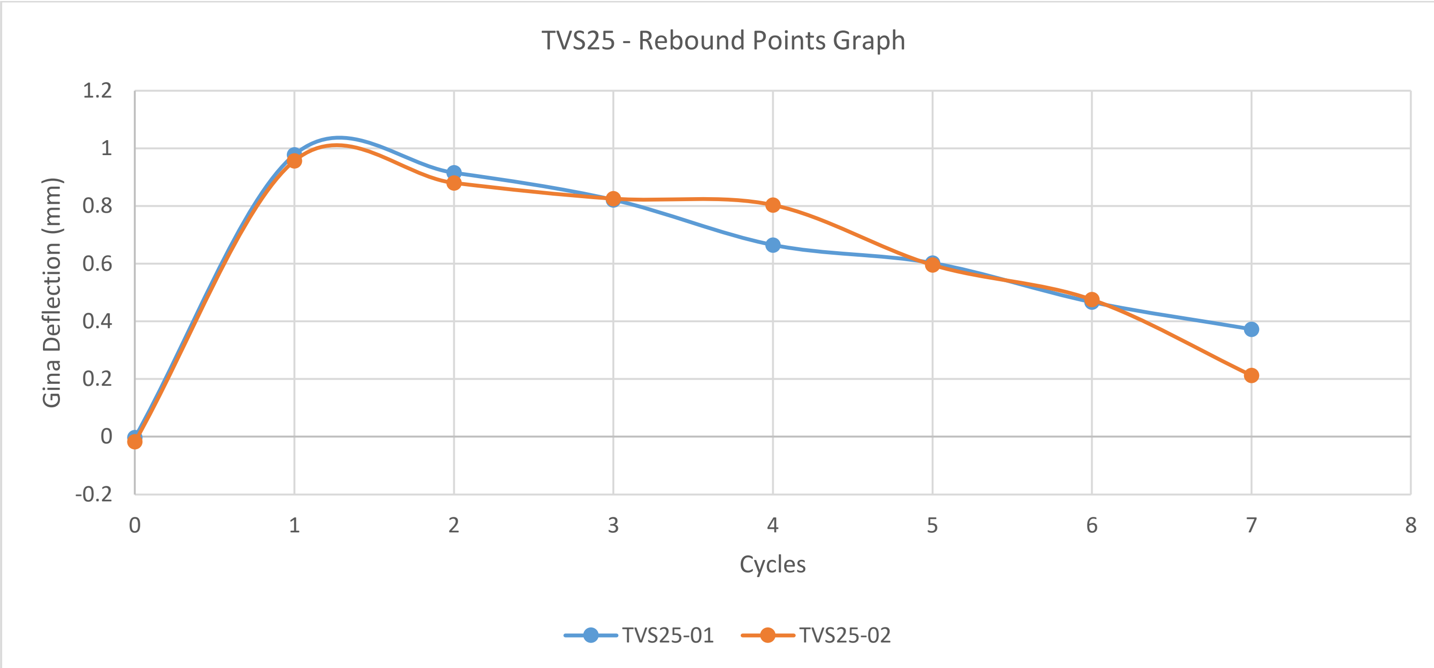

Appendix E-19 TVS25 Rebound Points Graph

APPENDIX - F : Model Joint Gap Stress Analysis

F.1.Normal Condition

The actuator used in the joint gap model has to be able to control the deformation of the joint gap under various test circumstances. Therefore to be able to select the correct actuator, the magnitude of the jacking force must be calculated. The maximum jacking force is calculated as the resistance of compressed soil and the compression force of the Gina gasket.

The dimensions of the joint gap is defined as shown below.

$$L_{lining} := 280mm \qquad w_{soil} := 100mm \qquad w_{gina} := 50mm$$

Soil Pressure

The sand is assumed to have a friction angle of 30 degrees, therefore the coefficient of passive earth pressure is determined to be 3. The maximum depth of the soil cover in the experiment is 4 meters, thus the vertical earth pressure could be calculated.

The lateral earth pressure could subsequently be calculated. The contact area of the force is calculated as the area of the lining plate where the sand is present. The calculation steps to determine the lateral earth pressure and force contact area is as follows:

$$h_{overburden} := 4m \qquad \varphi := 30°$$

$$\sigma_v := \gamma_{soil} \cdot h_{overburden} = 68 \cdot kPa$$

$$K_p := \left(\tan\left(\frac{\pi}{4} + \frac{\varphi}{2}\right)\right)^2 = 3$$

$$\sigma_{hsoil} := K_p \cdot \sigma_v = 204 \cdot kPa$$

$$A_{soil} := w_{soil} \cdot L_{lining} = 0.028\,m^2$$

Gina Pressure

The Gina profile is compressed from its original 53 mm height to the joint gap width of 35 mm. The Young's modulus of the profile is 1.0 MPa, therefore the compression pressure could be determined by using the elastic stress-strain formula. The calculation steps to determine compression stress of the Gina gasket and force contact area is shown below.

$$d_{ginafull} := 53mm \qquad d_{ginacontract} := 35mm \qquad E_{gina} := 1MPa$$

$$\Delta d := d_{ginafull} - d_{ginacontract} = 18 \cdot mm$$

$$\varepsilon_{gina} := \frac{\Delta d}{d_{ginafull}} = 0.34$$

$$\sigma_{hgina} := E_{gina} \cdot \varepsilon_{gina} = 339.623 \cdot kPa$$

$$A_{gina} := L_{lining} \cdot w_{gina} = 1.4 \times 10^4 \cdot mm^2$$

Factors of Safety & Forces

The maximum forces are calculated as the lateral pressure multiplied by the contact area. The soil is assigned higher safety factor to mitigate unpredictable behaviors that might appear due to confinement. The safety factor for the Gina gasket is given in order to accommodate for uncertainties in the gasket materials. The factor of safety for the pressures and total force is stated below.

$$FoS_{soil} := 2 \qquad FoS_{gina} := 1.2 \qquad FoS_{total} := 1.2$$

$$F_{soil} := FoS_{soil} \cdot \sigma_{hsoil} \cdot A_{soil} = 11.424 \cdot kN$$

$$F_{gina} := FoS_{gina} \cdot \sigma_{hgina} \cdot A_{gina} = 5.706 \cdot kN$$

$$F_{total} := FoS_{total} \cdot \left(F_{soil} + F_{gina}\right) = 20.556 \cdot kN$$

According to the calculations, the actuator used must be able to exert approximately 2.6 tons of weight. The pressure diagram is shown in Figure F-1. Note that the soil stress is stated as 408 kPa instead of 204 kPa to take into account the safety factor of 2 for confined spaces.

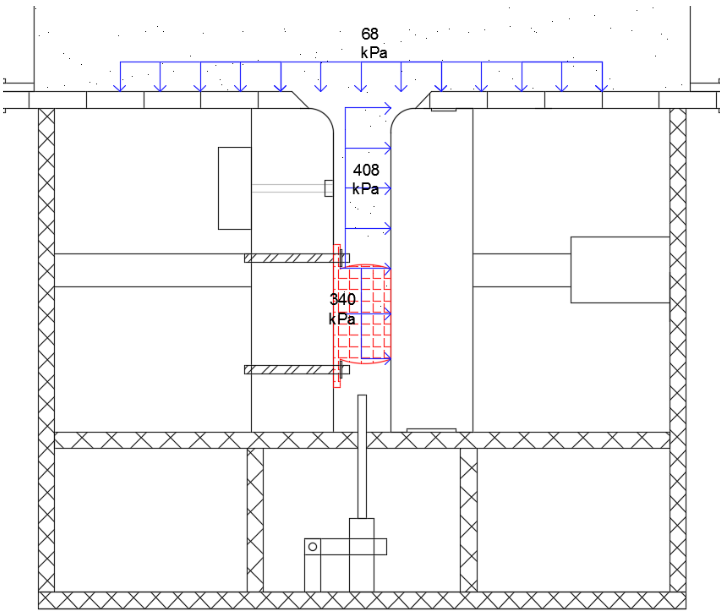

Figure F-1 Pressure Diagram for Calculations (ϕ = 30°). Factor of Safety = 2

F.2. Fully Densified Condition

In the event of a full densification of the sand, where the sand undergoes densification thus increasing its internal friction angle from 30° to 45°, further calculations must be made. The maximum jacking force is still calculated as the resistance of compressed soil and the compression force of the Gina gasket, however the soil compressive resistance is greatly increased.

Soil Pressure

The sand is now assumed to have a friction angle of 45 degrees, therefore the coefficient of passive earth pressure is determined to be 5.828. The maximum depth of the soil cover in the experiment is 4 meters, thus the vertical earth pressure could be calculated. The lateral earth pressure could subsequently be calculated. The contact area of the force is calculated as the area of the lining plate where the sand is present. The calculation steps to determine the lateral earth pressure and force contact area is as follows:

$$h_{overburden} := 4m \qquad \varphi := 45°$$

$$\sigma_v := \gamma_{soil} \cdot h_{overburden} = 68 \cdot kPa$$

$$K_p := \left(\tan\left(\frac{\pi}{4} + \frac{\varphi}{2}\right)\right)^2 = 5.828$$

$$\sigma_{hsoil} := K_p \cdot \sigma_v = 396.333 \cdot kPa$$

$$A_{soil} := w_{soil} \cdot L_{lining} = 0.023\,m^2$$

Gina Pressure

The Gina gasket compressive force is the same as the original calculation, with an elastic modulus of 1 MPa, therefore the gasket forces are similar to the previous calculation

Factors of Safety & Forces

The maximum forces are calculated as the lateral pressure multiplied by the contact area. The soil is still assigned higher safety factor to mitigate unpredictable behaviors that might appear due to confinement. However, due to the ultimate state of load, the safety factor is reduced from 2 to 1.5. The safety factor for the Gina gasket is similar to the original calculation. The factor of safety for the pressures and total force is stated below.

$$FoS_{soil} := 1.5 \quad FoS_{gina} := 1.2 \qquad FoS_{total} := 1.2$$

$$F_{soil} := FoS_{soil} \cdot \sigma_{hsoil} \cdot A_{soil} = 13.816 \cdot kN$$

$$F_{gina} := FoS_{gina} \cdot \sigma_{hgina} \cdot A_{gina} = 5.82 \cdot kN$$

$$F_{total} := FoS_{total} \cdot \left(F_{soil} + F_{gina}\right) = 23.563 \cdot kN$$

According to the calculations, the actuator used must be able to exert approximately 2.3 tons of weight. Note that the soil stress is stated as 595 kPa instead of 397 kPa to take into account the safety factor of 1.5 for ultimate loads.

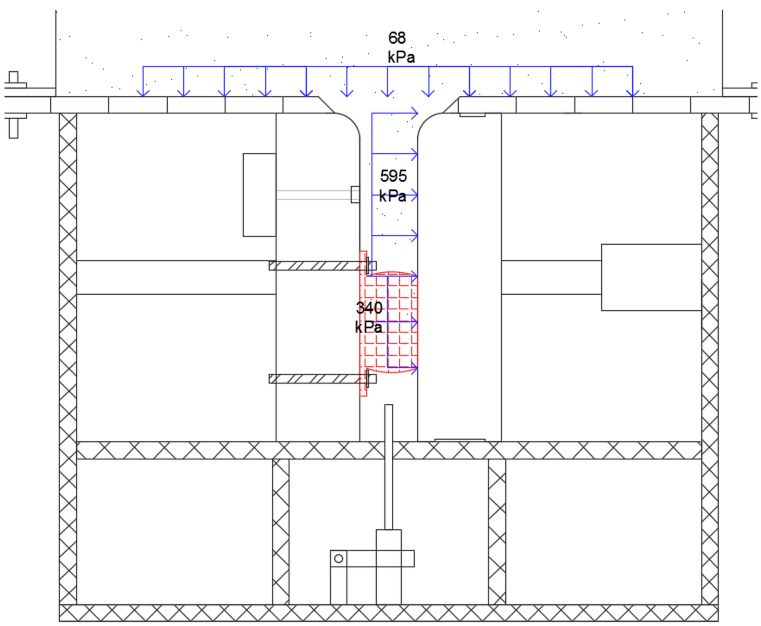

Figure F-2 Pressure Diagram for Calculations (ϕ = 45°). Factor of Safety = 1.5

F.3.Coulomb Lateral Earth Pressure Theory

An alternative method to calculate lateral earth pressure is by utilizing the Coulomb earth pressure theory. Unlike the Rankine theory, the Coulomb lateral earth pressure theory takes into account the friction angle of the interaction between soil and structure, which might yield higher values of K_p. The calculation is similar to the Rankine method save for a different formula for K_p as follows:

$$K_p = \frac{\sin^2(\beta - \phi')}{\sin^2(\beta) * \sin(\beta + \delta') \left[1 - \sqrt{\frac{\sin(\phi' + \delta')\sin(\phi' + \alpha)}{\sin(\beta + \delta')\sin(\beta + \alpha)}}\right]^2}$$

where the value of 2/3 of the friction angle is used for δ' considering the main material of the model lining is steel.

Normal Condition

In normal conditions, the sand is assumed to be deposited loosely, similar to the Rankine calculation method, with an internal friction angle of 30°. The following properties are used.

$$\beta := 90° \qquad \alpha := 0 \qquad \phi := 30° \qquad \delta_w := \frac{2 \cdot \phi}{3} = 20 \cdot °$$

The calculation steps to determine the passive lateral soil pressure are as follows

$$h_{overburden} := 4m$$

$$\sigma_v := \gamma_{soil} \cdot h_{overburden} = 68 \cdot kPa$$

$$K_p := \frac{(\sin(\beta - \phi))^2}{\left[(\sin(\beta))^2 \cdot \sin(\beta + \delta_w)\right] \cdot \left(1 - \sqrt{\frac{\sin(\phi + \delta_w) \cdot \sin(\phi + \alpha)}{\sin(\beta + \delta_w) \cdot \sin(\beta + \alpha)}}\right)^2} = 6.105$$

$$\sigma_{hsoil} := K_p \cdot \sigma_v = 415.164 \cdot kPa$$

$$A_{soil} := w_{soil} \cdot L_{lining} = 0.023\, m^2$$

The calculated actuator forces, along with its factors of safety are as follows:

$$FoS_{soil} := 2 \qquad FoS_{gina} := 1.2 \qquad FoS_{total} := 1.2$$

$$F_{soil} := FoS_{soil} \cdot \sigma_{hsoil} \cdot A_{soil} = 19.297 \cdot kN$$

$$F_{gina} := FoS_{gina} \cdot \sigma_{hgina} \cdot A_{gina} = 5.82 \cdot kN$$

$$F_{total} := FoS_{total} \cdot \left(F_{soil} + F_{gina}\right) = 30.14 \cdot kN$$

Fully Densified Condition

The fully densified sand condition is similar to the fully densified Rankine calculation, which assumes an increase in soil friction angle from 30 degrees to 45 degrees. The calculation steps to determine the lateral soil pressure are as follows.

$$h_{overburden} := 4m$$

$$\sigma_v := \gamma_{soil} \cdot h_{overburden} = 68 \cdot kPa$$

$$K_p := \frac{(\sin(\beta - \phi))^2}{\left[(\sin(\beta))^2 \cdot \sin(\beta + \delta_w)\right] \cdot \left(1 - \sqrt{\frac{\sin(\phi + \delta_w) \cdot \sin(\phi + \alpha)}{\sin(\beta + \delta_w) \cdot \sin(\beta + \alpha)}}\right)^2} = 46.087$$

$$\sigma_{hsoil} := K_p \cdot \sigma_v = 3.134 \times 10^3 \cdot kPa$$

$$A_{soil} := w_{soil} \cdot L_{lining} = 0.023\,m^2$$

The calculated actuator forces, along with its factors of safety are as follows

$$FoS_{soil} := 1.5 \quad FoS_{gina} := 1.2 \qquad FoS_{total} := 1.2$$

$$F_{soil} := FoS_{soil} \cdot \sigma_{hsoil} \cdot A_{soil} = 109.248 \cdot kN$$

$$F_{gina} := FoS_{gina} \cdot \sigma_{hgina} \cdot A_{gina} = 5.82 \cdot kN$$

$$F_{total} := FoS_{total} \cdot \left(F_{soil} + F_{gina}\right) = 138.081 \cdot kN$$

F.4. Elasticity Approach

The final approach to calculating the soil lateral pressure along the model lining is by approximating the soil elastic modulus. The elastic modulus is calculated using the formula developed by Janbu (1963) and Von Soos (1990)

$$\frac{E_{oed}}{p_{ref}} \cong 150\sqrt{\frac{\sigma_y'}{p^{ref}}}\ (loose \,\&\, silty)$$

$$\frac{E_{oed}}{p_{ref}} \cong 500\sqrt{\frac{\sigma_y'}{p^{ref}}}\ (dense \,\&\, clean)$$

(p^{ref} = 100 kPa)

By taking account the Hooke expression, and using a value of 1/3 for the Poisson's ratio of normally consolidated sand, the elasticity could be calculated as:

$$E = 1 + \frac{\nu}{1-\nu} * (1 - 2\nu)E_{oed} \cong \frac{2}{3}E_{oed}$$

Substituting the expression into the Janbu & Von Soos formula yields:

$$E = (100kPa) * \ 150 * \frac{2}{3}\sqrt{\frac{\sigma_y'}{p^{ref}}}\ (loose) \qquad E = (100kPa) * \ 500 * \frac{2}{3}\sqrt{\frac{\sigma_y'}{p^{ref}}}\ (dense)$$

$$E = 15\ MPa * \frac{2}{3}\sqrt{\frac{\sigma_y'}{p^{ref}}}\ (loose) \qquad E = 50\ MPa * \frac{2}{3}\sqrt{\frac{\sigma_y'}{p^{ref}}}\ (dense)$$

Using both expressions for loose and dense sand, the lower and upper limit soil lateral pressure could be calculated.

S

Upper Limit (dense sand)

By assuming the elastic modulus of dense sand, the soil pressure could be calculated as follows:

$$E_{sand2} := 50MPa \cdot \frac{2 \cdot \left(\frac{\sigma_v}{100kPa}\right)^{0.5}}{3} = 27.487 \cdot MPa$$

$$\sigma_{hsoil3} := E_{sand2} \cdot eps = 1.767 \times 10^{3} \cdot kPa$$

The resulting soil pressure is much higher than the other estimates. The results of this calculation will be discussed in the following section.

F.5. Stress State Analysis

The stress state of the soil inside the joint gap could be described by utilizing the Mohr circle scheme, which requires major and minor soil stresses. From the calculations performed in part F.1, the following values were calculated:

- Vertical soil stress = σ_3 = 68 kPa
- Lateral soil stress = σ_1 = 204 kPa

In the case of full densification of the sand, as discussed in part F.2, the following values were obtained:

- Vertical soil stress = σ_3 = 68 kPa
- Lateral soil stress = σ_1 = 397 kPa

The Mohr circle could subsequently be constructed, as shown in the graph displayed in Figure F-3.

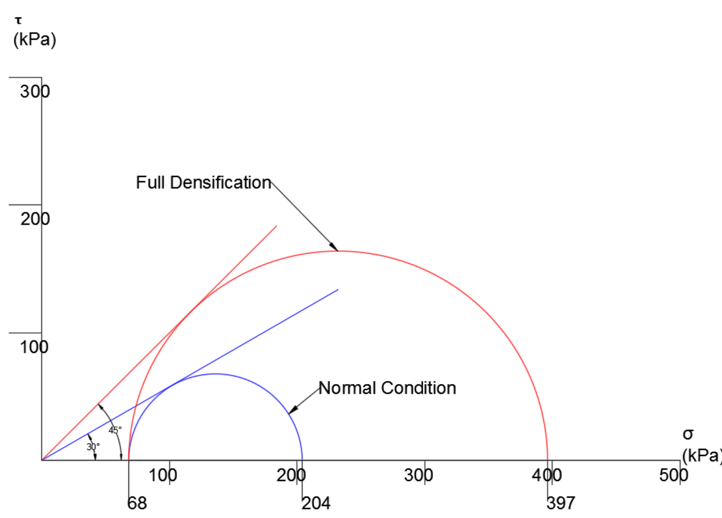

Figure F-3 Mohr-Coulomb Circles for Normal & Fully-Densified Sand

The Coulomb method yields higher lateral earth pressure coefficient, and thus larger lateral pressure. The loose sand configuration yields 416 kPa, while the dense configuration yields 3134 kPa before safety factors. The elastic approach calculation leads to two sets of stresses. The first analysis yields σ_1 value of 531 kPa while the second analysis yields upwards of 1700 kPa. Superimposing the calculation values to the Mohr circle, shown in the graph displayed in Figure F-4, shows that the stresses are past the failure surface of the sand configuration. Therefore the stress states of both these conditions are unlikely unless an increase in σ_3 occurs.

While the normal conditions of the Coulomb analysis yields a realistic result for the lateral earth pressure, the train

The soil elastic strain is produced by the compression and extension of the actuator. The total maximum range of motion of the model lining is 4.5 mm, however the actuator actually moves half-range (2.25 mm) both inwards and outwards. Therefore the strain experienced by the sand is calculated by:

$$\epsilon = \frac{2.25}{35} = 6.429\%$$

Lower Limit (loose sand)

By assuming the elastic modulus of loose sand, the soil pressure could be calculated as follows:

$$E_{sand} := 15MPa \cdot \frac{2 \cdot \left(\frac{\sigma_v}{100kPa}\right)^{0.5}}{3} = 8.246 \cdot MPa$$

$$eps := \frac{2.25}{35} = 6.429 \cdot \%$$

$$\sigma_{hsoil2} := E_{sand} \cdot eps = 530.114 \cdot kPa$$

Subsequently, the maximum forces is calculated as follows:

$$F_{soil2} := FoS_{soil} \cdot \sigma_{hsoil2} \cdot A_{soil} = 18.48 \cdot kN$$

$$F_{total2} := FoS_{total} \cdot \left(F_{soil2} + F_{gina}\right) = 29.159 \cdot kN$$

It was obtained that the maximum force exerted upon the actuator is approximately 2.92 tons.

fully densified condition yields unrealistically high stresses. An argument to these calculations is that the Coulomb calculations make use of the δ value, which is the interface friction angle. Various literatures, such as Das (2011), have suggested the values based on the interface material type. However these values assumes that the field condition of the interface structures are rough, unlike the controlled smoothness of the model tunnel lining. Therefore the actual δ value in the test equipment is expected to be lower. Therefore the results of the fully densified calculation is omitted

As for the elasticity calculations, the loose sand approach yields a more realistic approach where the combination of full densification of the sand, and increase in minor stress due to Gina gasket resistance and soil side friction might just be able to give the calculated major stress. It is important to note that the actuator strength limit is still above this threshold. However in the dense sand approach, the calculated major stress is unrealistically high and would require a tremendous increase in the minor stress to maintain it under the failure envelope. Thus the results of this analysis is omitted.

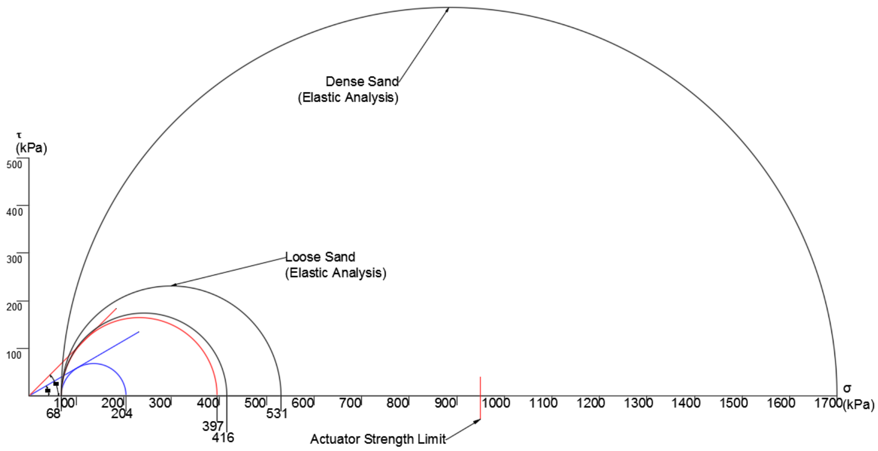

Figure F-4 Mohr Circle of Rankine, Coulomb & Elastic Pressures

APPENDIX - G : Detailed Experiment Procedure

G.1.Main Experiments

The main experiments include the reference configuration as well as all of the variants. The steps following each experiment are similar, with only slight difference in the variables. Hence it is safe to assume a single procedure for each of the main experiments.

Each test begins by resetting the entire equipment, thus also resetting the soil stress state. The test equipment is steadily hoisted by a crane and slowly turned upside down. After the joint gap part is empty of sand, the equipment is again hoisted upwards and flipped right side up. Time estimates for this process is around 30 minutes. Pressure is subsequently applied to the tire to simulate overpressure. The measuring instruments are also checked and readied. Both processes are estimated to take 14 minutes. A pocket penetrometer test is performed prior to loading, with an estimated time of 2 minutes.

The loading process commences with the actuator unwound at half range of the stroke length to obtain the largest joint gap state for that particular configuration. The actuator is subsequently given cyclic loading-unloading motion according to the required number of cycles. The time estimate for this step varies with different test configurations, as shown in Table G-2. The loading process concludes with the actuator pushed back to its null state, where the joint gap is again 35 mm in width.

A second penetrometer test is performed after the loading-unloading cycles had finished, with an estimated time of 2 minutes. The final step is reviewing the data readings obtained from the load cell and LVDT.

A step by step procedure of the reference configuration, and its following estimate of time is shown in Table G-1

Table G-1 Detailed Step-by-Step Procedure & Time Estimate for TVS15-XX Experiment

Reference Configuration		Description	Time Estimate (min)
Code	**TVS15-XX**		
1	Equipment reset		
1.1	Lift+ Check	Model is lifted by crane+ Check gap width	5
1.2	Flip	Model is flipped upside down	10
1.3	Rattle	Rattling the model	2
1.4	Flip	Model is flipped right side up	10
2	Ready Instruments		
2.1	Air pressure	Air pressure applied to tire	5
2.2	Check Manometer	Check manometer pressure	3
2.3	Ready Load Cell	Check load cell for horizontal earth pressure	3
2.4	Ready LVDT	Zero LVDT Reading	3
3	Pocket Penetrometer (Prior)		
3.1	Perform Test	Open flap, insert penetrometer	0.5
3.2	Finish Test	Take out penetrometer, close flap	0.5
3.3	Take reading	Record Penetrometer Reading	1
4	Loading cycle		
4.1	Ready Gap	Crank to half range outwards	1
4.2	Perform loading cycle	Perform a total of 50 cycles	12.5
4.3	Reset Gap	Crank to original position	1
5	Pocket Penetrometer (Post)		
5.1	Perform Test	Open flap, insert penetrometer	0.5
5.2	Finish Test	Take out penetrometer, close flap	0.5
5.3	Take reading	Record Penetrometer Reading	1
6	Instrument Readings		
6.1	Load Cell	Take load cell reading	1
6.2	LVDT	Take LVDT Reading	1
		Total Time	61.5

Each test configuration also share similar estimates in the time that it takes to finish each test. The difference being only in the time it takes to perform the actual loading-unloading cycles. The summary of the estimates of time for each test configuration is shown in Table G-2.

Table G-2 Time Estimates of Each Test Configuration

No.	Test Code	Load Cycle Time (m)	Total Time (m)
1	TVS15-XX	12.5	61.5
2	TVVS05-XX	37.5	86.5
3	TVS10-XX	25	82
4	TVS25-XX	10	59
5	TVS3-XX	7.5	56.5

G.2.Control Experiments

The following set of experiments are the 3 control experiments discussed in part 3.3.3. The experiments have significantly different steps compared to the main experiment.

Zero Cycle Test

The zero cycle test basically omits the loading part and the penetrometer test that follows it from the main configuration. The detailed step-by-step procedure is shown in Table G-3.

Table G-3 Detailed Step-by-Step Procedure & Time Estimate for TC1-XX Experiment

Zero Cycle Test			Description	Time Estimate (min)
Code		TC1-X		
1	Equipment reset			
	1.1	Lift+ Check	Model is lifted by crane+ Check gap width	5
	1.2	Flip	Model is flipped upside down	10
	1.3	Rattle	Rattling the model	2
	1.4	Flip	Model is flipped right side up	10
2	Overpressure			
	2.1	Air pressure	Air pressure applied to tire	5
	2.2	Check Manometer	Check manometer pressure	3
	2.3	Ready Load Cell	Check load cell for horizontal earth pressure	3
	2.4	Ready LVDT	Zero LVDT Reading	3
3	Pocket Penetrometer			
	3.1	Perform Test	Open flap, insert penetrometer	0.5
	3.2	Finish Test	Take out penetrometer, close flap	0.5
	3.3	Take reading	Record Penetrometer Reading	1
4	Instrument Readings			
	4.1	Load Cell	Take load cell reading	5
	4.2	LVDT	Take LVDT Reading	5
Total Time				53

Stepwise Penetrometer Test

The stepwise penetrometer test uses the same test conditions as the reference configuration. However, the penetrometer test is performed every 10 cycles of loading, with each penetrometer test taking approximately 2 minutes. The detailed step-by step procedure is shown in Table G-4.

Table G-4 Detailed Step-by-Step Procedure & Time Estimate for TC2-XX Experiment

Stepwise Penetrometer		Description	Time Estimate (min)
Code	**TC2-X**		
1	Equipment reset		
1.1	Lift+ Check	Model is lifted by crane+ Check gap width	5
1.2	Flip	Model is flipped upside down	10
1.3	Rattle	Rattling the model	2
1.4	Flip	Model is flipped right side up	10
2	Ready Instruments		
2.1	Air pressure	Air pressure applied to tire	5
2.2	Check Manometer	Check manometer pressure	3
2.3	Ready Load Cell	Check load cell for horizontal earth pressure	3
2.4	Ready LVDT	Zero LVDT Reading	3
3	Pocket Penetrometer (Prior)		
3.1	Perform Test	Open flap, insert penetrometer	0.5
3.2	Finish Test	Take out penetrometer, close flap	0.5
3.3	Take reading	Record Penetrometer Reading	1
4	Loading cycle		
4.1	Ready Gap	Crank to half range outwards	1
4.2	Perform loading cycle	Perform a total of 50 cycles	25
4.3	Penetrometer Test	Perform penetrometer test every 10 cycles	8
4.4	Reset Gap	Crank to original position	1
5	Pocket Penetrometer (Post)		
5.1	Perform Test	Open flap, insert penetrometer	0.5
5.2	Finish Test	Take out penetrometer, close flap	0.5
5.3	Take reading	Record Penetrometer Reading	1
6	Instrument Readings		
6.1	Load Cell	Take load cell reading	5
6.2	LVDT	Take LVDT Reading	5
		Total Time	90

Sand-less test

The sand-less test is performed to test the normal deflection of the Gina gasket. Prior to the loading cycle, the drum part of the test equipment must be dismounted along with the sand inside. The modification part of the equipment is estimated to take 30 minutes, however the modification process is only necessary for the first trial out of the three. The detailed steps along with the time estimates are shown in Table G-5.

Table G-5 Detailed Step-by-Step Procedure & Time Estimate for TC3-YY-XX Experiment

Sand-less Test		Description	Time Estimate (min)
Code	**TC3-X**		
1	Equipment reset		
1.1	Take reading	Model is lifted by crane+ Check gap width	5
1.2	Flip	Model is flipped upside down	10
1.3	Rattle	Rattling the model	2
2	Modify Equipment		
2.1	Take Soil Drum Off	Take the soil drum off of the setup	30
3	Loading cycle		
3.1	Ready Gap	Crank to half range outwards	1
3.2	Perform loading cycle	Perform a total of 50 cycles	25
3.3	Reset Gap	Crank to original position	1
4	Instrument Readings		
4.1	LVDT	Take LVDT Reading	5
		Total Time	79

APPENDIX - H Device Pictures

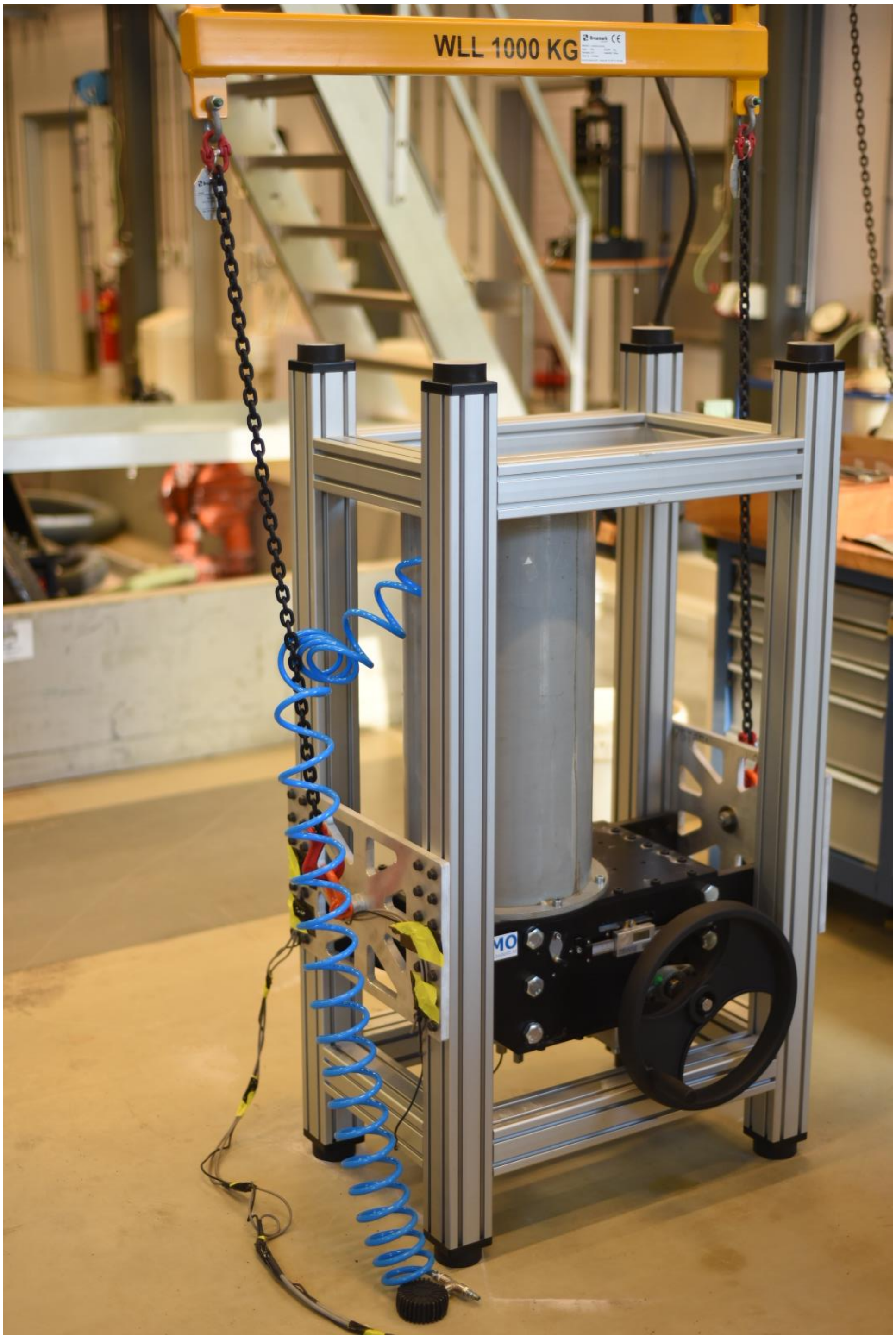

Appendix H-1 Device Photo 1

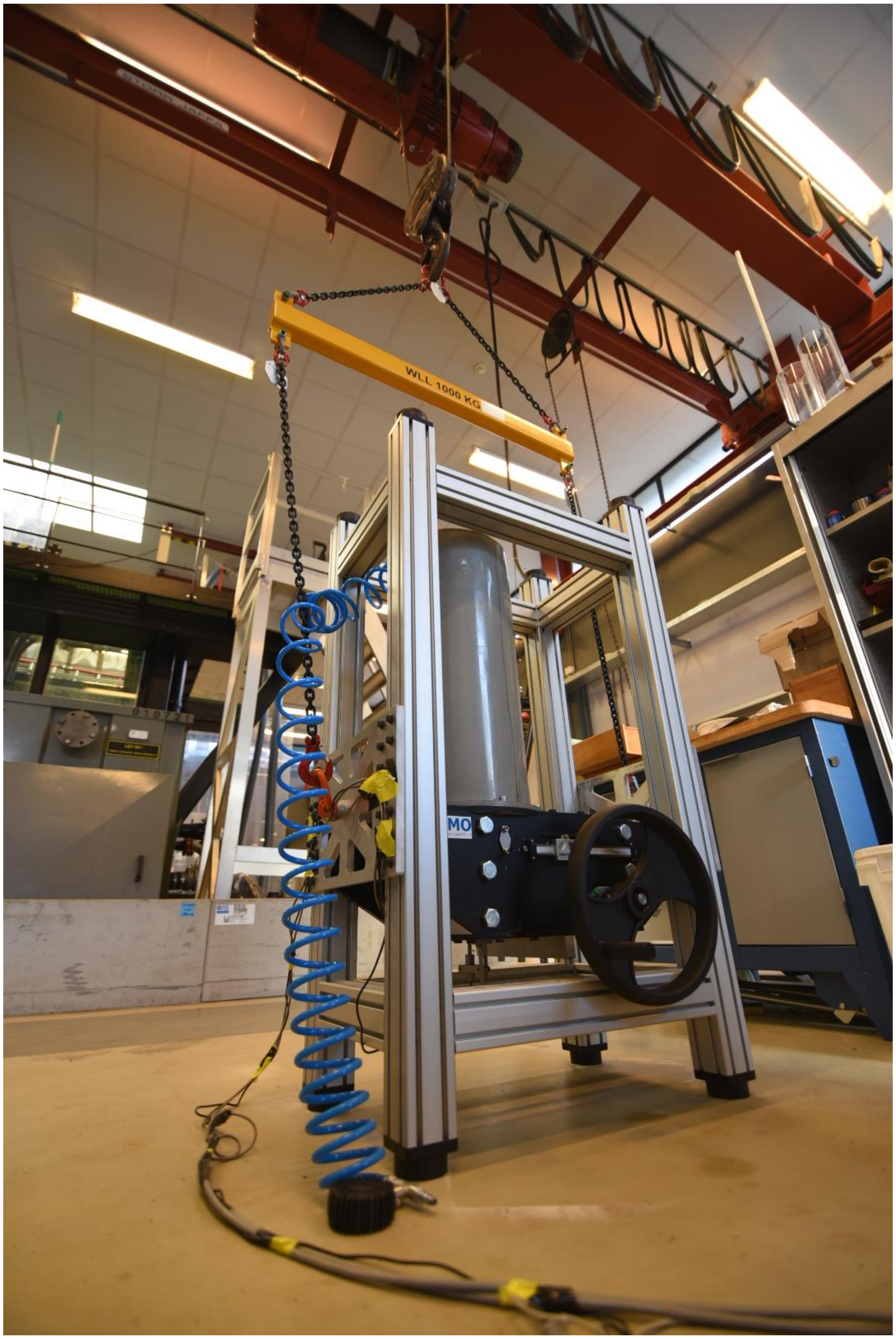

Appendix H-2 Device Photo 2

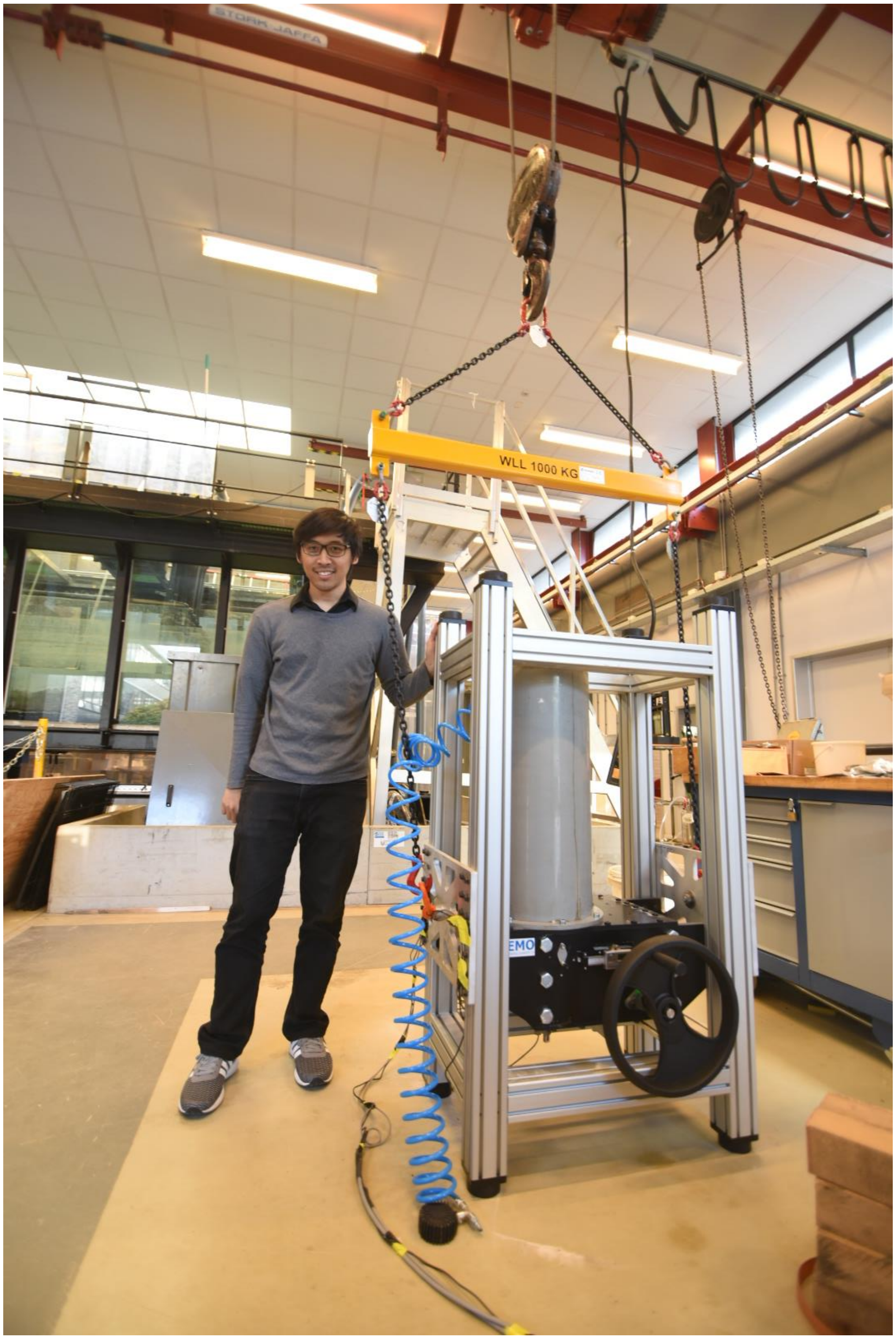

Appendix H-3 Device Photo 3

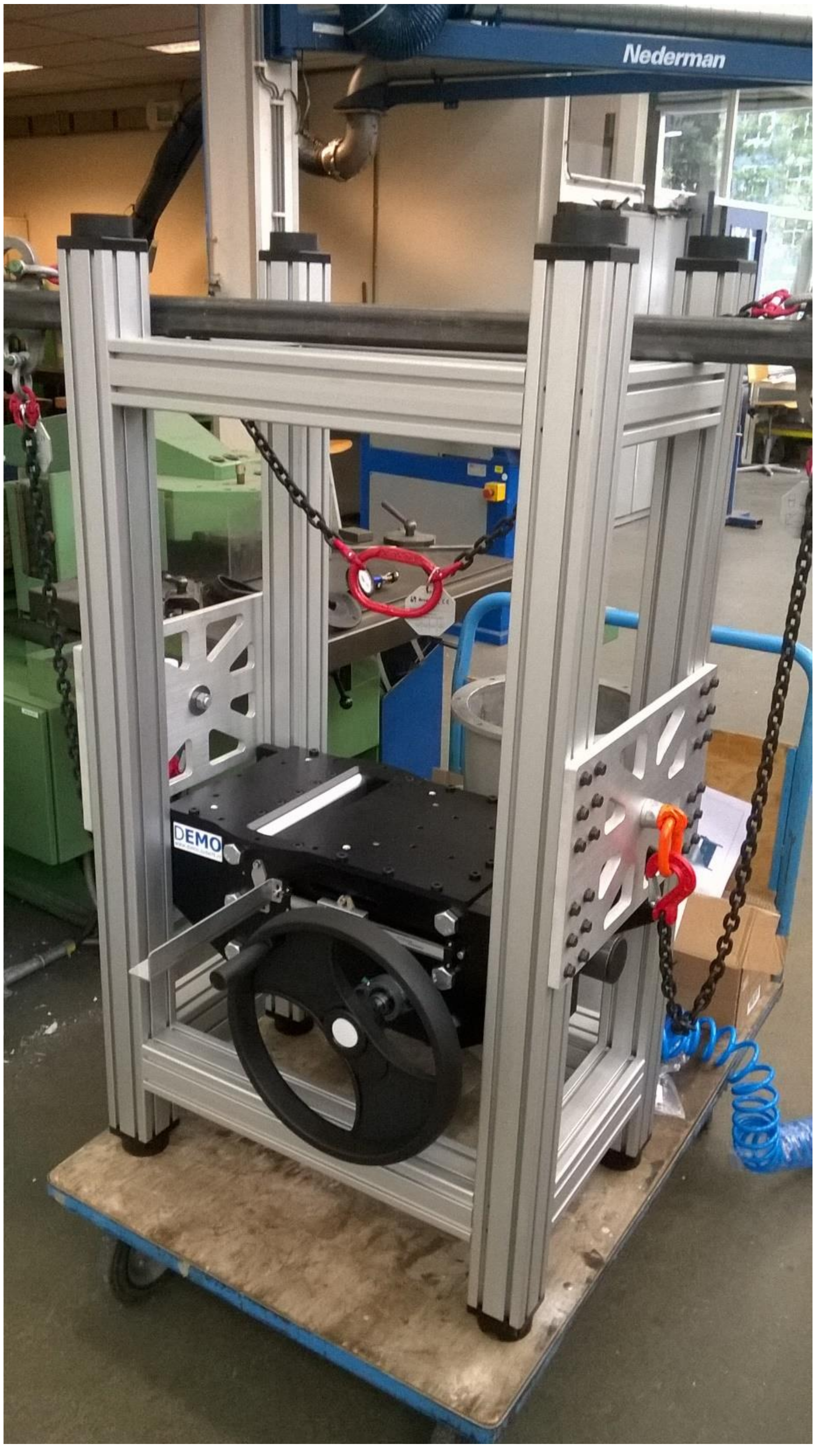

Appendix H-4 Device Photo 4

Appendix H-5 Device Photo 5

APPENDIX - I Estimated Project Plan for Further Research

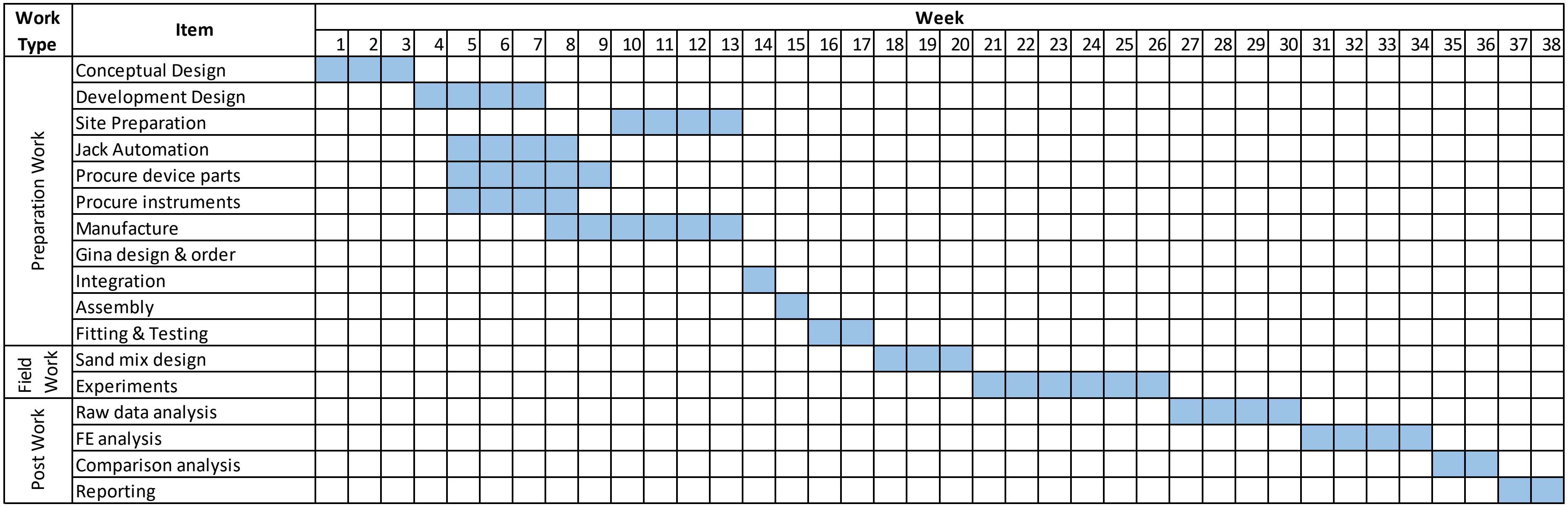

Appendix I-1 Estimated Project Plan for Option 1: Construct a New Device at True Scale

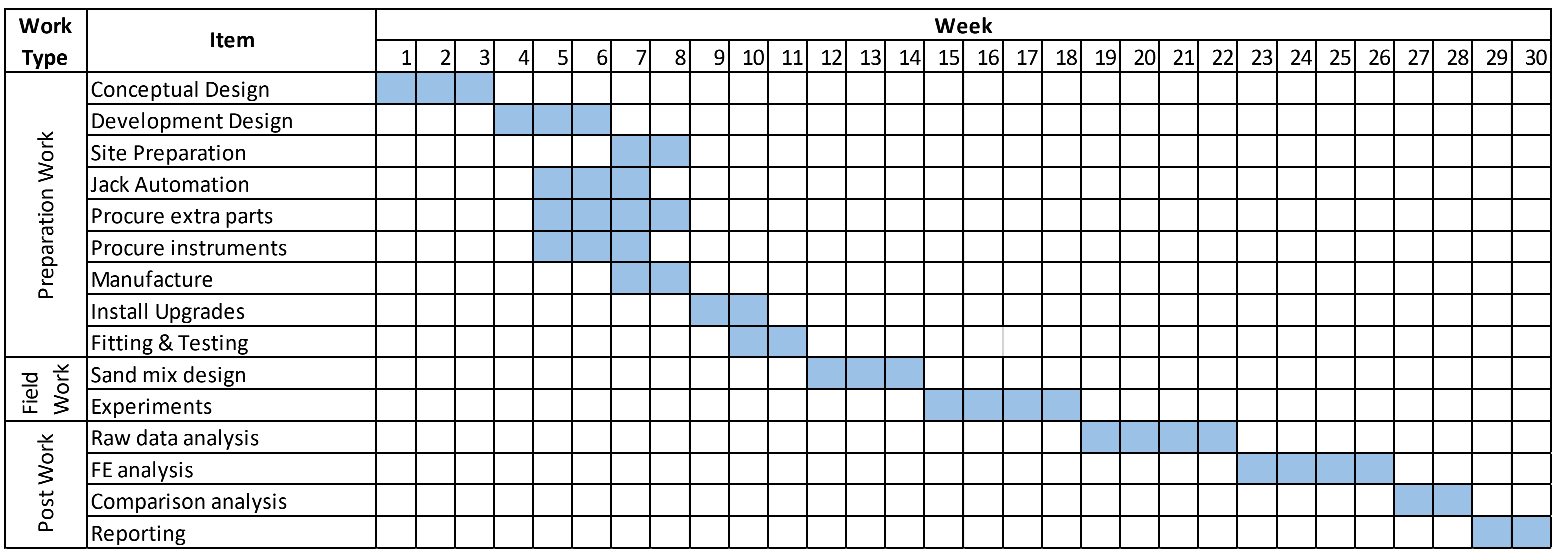

Appendix I-2 Estimated Project Plan for Option 2: Upgrade Existing Design